

## 1. CALCAREOUS NANNOFOSSIL BIOSTRATIGRAPHY OF THE CALIFORNIA MARGIN<sup>1</sup>

Eliana Fornaciari<sup>2</sup>

### ABSTRACT

Selected calcareous nannofossils were investigated by means of quantitative and semiquantitative methods in middle Miocene to Pleistocene sediments from the California margin (Pacific Ocean) recovered during Ocean Drilling Program Leg 167. The goal of the work was to provide detailed dating and correlations of the successions recovered that span a wide latitudinal transect (from 29°N to 40°N) affected by strongly variable ecological conditions. The standard zonations are not easily applied in these sediments; hence, additional biohorizons have been adopted that are useful in the area. Specifically, the reliability of 50 biohorizons has been evaluated by considering their mode of occurrence, ranking, and spacing.

For the Pleistocene interval, the following six biohorizons are considered reliable: last occurrence (LO) of *Pseudoemiliana lacunosa*, first occurrence (FO) of *Gephyrocapsa* sp. 3, LO and FO of large *Gephyrocapsa*, FO of *Gephyrocapsa oceanica* s.l., and LO of *Reticulofenestra asanoi*. The acme end (AE) of small *Gephyrocapsa* spp. and the LOs of *Helicosphaera sellii* and *Calcidiscus macintyreii* do not seem to be reliable in the study area.

For the Pliocene interval, the following nine biohorizons are considered reliable: LO of *Discoaster pentaradiatus*, LO of *Discoaster surculus*, LO of *Discoaster tamalis*, LO and first common and continuous occurrence (FCO) of *Discoaster asymmetricus*, paracme beginning (PB) and paracme end (PE) of *Discoaster pentaradiatus*, LO of *Reticulofenestra pseudumbilicus*, and LO of *Amaurolithus delicatus*. The LOs of *Discoaster brouweri* and *Discoaster triradiatus* and the FCO of *P. lacunosa* seem to be moderately reliable.

For the late Miocene interval, the following eight biohorizons are considered reliable: LO of *Discoaster quinquerramus*, PB and PE of *R. pseudumbilicus*, FO of *Amaurolithus primus*, FO and LO of *Minylitha convallis*, LO of *Catinaster calyculus*, and FO of *Catinaster* spp.

Sediments of middle Miocene age were recovered only at low-latitude Site 1010. Therefore, the reliability of the six biohorizons identified (*Discoaster kugleri* FO and LO, *Calcidiscus macintyreii* FO, *Cyclicargolithus floridanus* last common and continuous occurrence [LCO], *Calcidiscus premacintyreii* LO, and *Sphenolithus heteromorphus* LO) cannot be fully evaluated.

These events have been correlated with the global chronostratigraphic scale and calibrated to the geomagnetic polarity time scale. This integrated time frame has been used for dating the successions recovered during Leg 167. The biozones proposed for the Pleistocene seem to be valid globally, and they are proposed as an alternative to the standard zonation.

### INTRODUCTION AND GOALS

Ocean Drilling Program (ODP) Leg 167 represents the first deep drilling since 1978 to study ocean history in the North American Pacific margin. During Leg 167, more than 7000 m of middle Miocene to Holocene sediments were recovered at 13 sites (Sites 1010 to 1022) in the California margin of the northwest Pacific Ocean (Fig. 1; Table 1). The primary objective of this leg was to collect sediments to study the links between the evolution of North Pacific climate and the evolution of the California Current system, with respect to both long-term climate history and high-frequency climatic variability.

One of the basic requirements for this purpose is the availability of an accurate chronology. Biostratigraphy remains a necessary step in establishing such a chronology (Shackleton et al., 1995). Because the onboard calcareous nannofossil biostratigraphy was based only on analyses of core-catcher samples, it was deemed necessary to study supplementary samples, particularly at those sites where detailed paleoclimatic and paleoceanographic studies were being conducted.

The first goal of the present study is, therefore, to present a more complete data set on the calcareous nannofossil biostratigraphy for Leg 167 to supplement the *Initial Reports* volume (Lyle, Koizumi, Richter, et al., 1997).

The study area covers a large latitudinal transect (from 29°N to 40°N) and is strongly affected by the California Current system;

therefore, the environmental conditions are highly variable. Subtropical and subarctic flora and fauna mix along this zone, and, as noted by Wise (1973) and Bukry (1981), the calcareous nannofossil “standard” zonal schemes of Martini (1971) and Okada and Bukry (1980; Fig. 2) cannot be easily applied. Hence, to get intersite correlations and age estimates, the reliability of the biohorizons used in the standard zonations and proposed in the existing literature is evaluated. As a result of this analysis, a regional biostratigraphic scheme is proposed that is correlated with the global chronostratigraphic scale (GCS) and, to a large extent, is calibrated to the geomagnetic polarity time scale (GPTS). This integrated time frame has been used for the dating and correlation of Leg 167 sites.

### STRATEGY

The reliability of biostratigraphic events (biohorizons) is a much-discussed topic (e.g., Gradstein et al., 1985; Hills and Thierstein, 1989; Rio, Fornaciari, et al., 1990; Rio, Raffi, et al., 1990; Bralower et al., 1989). In this paper, an event is considered as reliable when it is easily reproducible among different researchers and when it keeps the same ranking and spacing in different successions (Gradstein et al., 1985). The reliability of a biohorizon is dependent upon

1. The clear taxonomy of species that defines the event (index species),
2. The relative abundance of the species in the proximity of the event that the species defines,
3. The mode of occurrence (subtle, abrupt, etc.) of the change in distribution pattern of the index species, and

<sup>1</sup>Lyle, M., Koizumi, I., Richter, C., and Moore, T.C., Jr. (Eds.), 2000. *Proc. ODP, Sci. Results, 167*: College Station TX (Ocean Drilling Program).

<sup>2</sup>Dipartimento di Geologia, Paleontologia e Geofisica, Università di Padova, Via Giotto 1, 35137 Padova, Italy. eliana@dmp.unipd.it

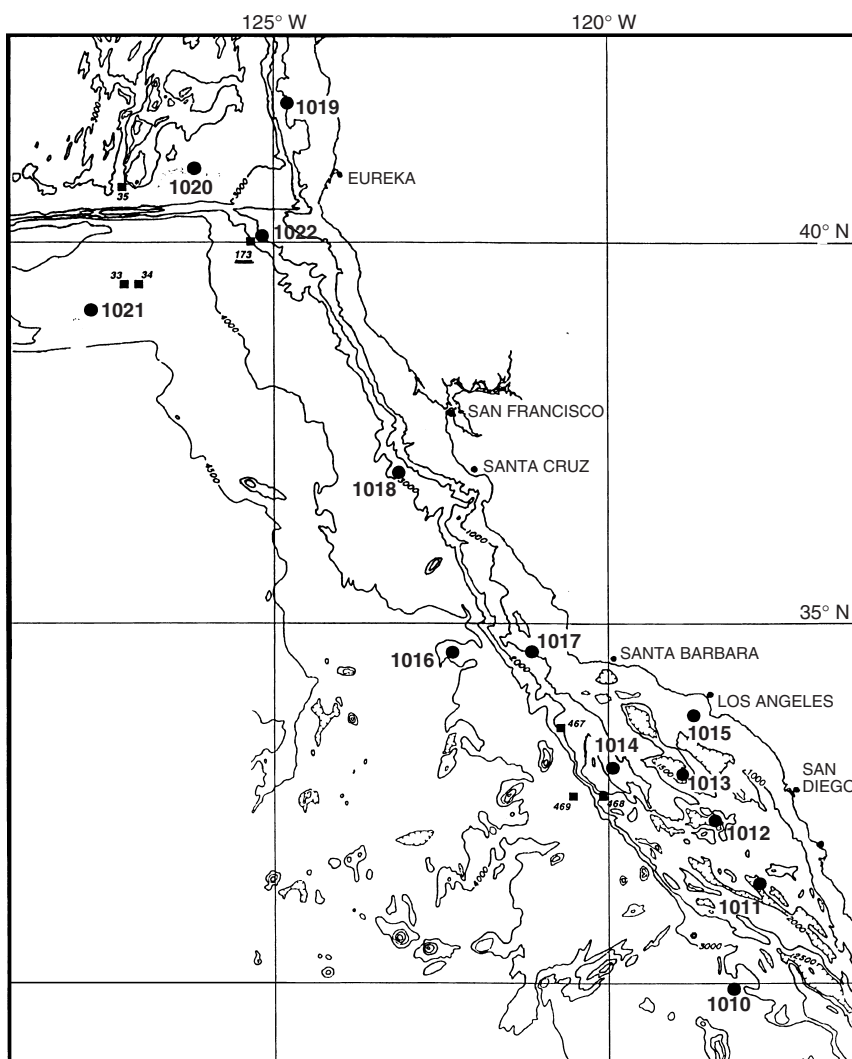


Figure 1. Location map of Leg 167 sites in the California margin.

Table 1. Summary of Leg 167 holes studied.

Hole	Latitude	Longitude	Water depth (m)	Remarks	Number of studied samples	Average sampling per m.y.	
1010B, 1010C	29°57.905'N, 29°57.905'N	118°06.047'W, 118°06.044'W	3465	Within the core of the southern California Current	156	100	
1011B	31°16.817'N	117°38.008'W	2033	Inshore of the California Current, in an area of coastal upwelling	91	100	
1012A	32°16.970'N	118°23.024'W	1783		106	50	
1013A	32°48.040'N	118°53.922'W	1575	Close to DSDP Leg 5, Site 35, at the transition between the California Current and the subtropical gyre	50	50	
1014	32°49'N	119°58'W	1177		620	3.1-6.2	
1015	33°42.92'N	118°49'W	912	Close to DSDP Leg 18, Site 173, beneath the California Current	88	100-300	
1016A	34°32.415'N	122°16.594'W	3846		49	40	
1017B	34°32.091'N	121°6.415'W	967	Close to DSDP Leg 18, Site 173, beneath the California Current	49	36	
1018A	36°59.300'N	123°16.653'W	2467		94	36	
1019C	41°40.972'N	124°55.975'W	989	Northern region of the California Current in an area of moderate upwelling	49	11-50	
1020B	41°0.051'N	126°26.064'W	3050		342	10	
1021B	39°5.248'N	127°46.993'W	4215	Close to DSDP Leg 18, Site 173, beneath the California Current	215	50	
1022A	40°4.850'N	125°20.559'W	1927		43	180	
					Total:	1903	

Chronostratigraphy	Series Epoch Stage Age	Calcareous nannofossil Biostratigraphy												
		GPTS		Low latitude		North California Margin	South California Margin	Mediterranean		California Margin		Additional biohorizons		
		Chron	Polarity	Okada & Bukry (1980) Bukry (1991)		Wise (1973)		Bukry (1981)		Rio, Raffi et al. (1990) Fornaciari et al. (1996)			This work	
				Zone	Definition	Zone	Definition	Zone	Definition	Zone	Definition		Zone	Definition
Pleistocene Pliocene early mid- late Messinian Tortonian Serravallian Langhian middle	Ma 1n 1r 2n 2r 3 2An 4 2Ar 3n CN10 3r 3An 3Ar 3Bn 3Br 4n 4r 4An 4Ar 5n 5r 5An 5Ar 5AA 5AB 5AC 5ADn 5ADr 5Bn 5Br	CN15 CN14 CN13 CN12 CN11 CN10 CN9 CN8 CN7 CN6 CN5 CN4	<i>E. huxleyi</i> FO <i>E. ovata</i> LO <i>C. oceanica</i> FO <i>C. caribbeana</i> FO <i>D. brouweri</i> LO <i>D. pentaradiatus</i> LO <i>D. surculus</i> LO <i>D. tamalis</i> LO <i>Sphenolithus</i> spp. LO <i>R. pseudoumbilicus</i> LO <i>D. asymmetricus</i> FCO <i>A. tricorniculatus</i> LO <i>A. primus</i> LO <i>C. rugosus</i> FO <i>C. acutus</i> FO <i>D. quinquaramus</i> LO <i>A. primus</i> FO <i>D. berggrenii</i> FO <i>D. loeblichii</i> FO <i>D. neorectus</i> FO <i>D. hamatus</i> LO <i>C. calyculus</i> FO <i>D. hamatus</i> FO <i>C. coalitus</i> FO <i>D. kugleri</i> FO <i>S. heteromorphus</i> LO <i>H. ampliaptera</i> LO	<i>Emiliania huxleyi</i> FO <i>Cephyrocapsa</i> → <i>P. lacunosa</i> <i>Emiliania annula</i> <i>C. doronicoides</i> → <i>Cephyrocapsa</i> FO <i>D. brouweri</i> LO <i>Discoaster brouweri</i> <i>P. lacunosa</i> FO <i>Reticulofenestra pseudoumbilicus</i> → <i>A. tricorniculatus</i> LO <i>Ceratolithus rugosus</i> → <i>C. rugosus</i> FO <i>Amaurolithus tricorniculatus</i> <i>Discoaster mendomobensis</i> → <i>A. tricorniculatus</i> FO <i>Dictyocha aspera</i> <i>Reticulofenestra pseudoumbilicus</i> → <i>C. triacantha</i> LO <i>C. triacantha</i> <i>R. pseudoumbilicus</i> → <i>C. floridanus</i> LO <i>Cyclocargolithus floridanus</i> <i>H. ampliaptera</i> LO	CN15 CN14 CN13 CN12 CN11 CN10 CN9 CN8 CN7 CN6 CN5 CN4	<i>E. huxleyi</i> FO <i>P. lacunosa</i> LO <i>C. oceanica</i> FO <i>C. caribbeana</i> FO <i>D. brouweri</i> LO <i>D. pentaradiatus</i> LO <i>D. surculus</i> LO <i>D. tamalis</i> LO <i>R. pseudoumbilicus</i> LO <i>D. asymmetricus</i> AB <i>Amaurolithus</i> spp. LO <i>D. asymmetricus</i> FCO <i>C. rugosus</i> FO <i>C. acutus</i> FO <i>D. quinquaramus</i> LO <i>A. primus</i> FO <i>D. berggrenii</i> FO <i>D. loeblichii</i> FO <i>D. hamatus</i> LO <i>D. hamatus</i> FO <i>C. coalitus</i> FO <i>D. kugleri</i> FO <i>S. heteromorphus</i> LO <i>H. ampliaptera</i> LO	MNN21 MNN20 MNN19f MNN19e MNN19d MNN19c MNN19b MNN19a MNN18 MNN16b-17 MNN16a MNN14-15 MNN13 MNN12 BARREN INTERZONE MNN11 MNN10 MNN9 MNN8 MNN7 MNN6 MNN5 MNN4b	<i>E. huxleyi</i> FO <i>P. lacunosa</i> LO <i>Cephyrocapsa</i> sp.3 FO <i>Cephyrocapsa</i> sp.3 FO <i>Large Cephyrocapsa</i> LO <i>C. macintyreii</i> LO <i>C. oceanica</i> s.l. FO <i>D. brouweri</i> LO <i>D. pentaradiatus</i> LO <i>D. surculus</i> LO <i>D. tamalis</i> LO <i>R. pseudoumbilicus</i> LO <i>D. asymmetricus</i> FCO <i>H. sellii</i> FO <i>A. primus</i> LO <i>A. tricorniculatus</i> LO <i>A. primus</i> FO <i>D. berggrenii</i> FO <i>D. loeblichii</i> FO <i>D. hamatus</i> LO <i>D. bellus</i> FO <i>H. stalis</i> FCO <i>H. walbersdorfensis</i> LO <i>C. premacintyreii</i> LCO <i>R. pseudoumbilicus</i> FCO <i>S. heteromorphus</i> LO <i>H. walbersdorfensis</i> FCO <i>S. heteromorphus</i> PE	CN15 CN14 CN13bC CN13bE CN13bA CN13a CN12 CN11b CN11a CN10 CN9 *CN8b *CN8a *CN7 + *CN6 CN5 CN4	<i>E. huxleyi</i> FO <i>P. lacunosa</i> LO <i>Cephyrocapsa</i> sp.3 FO <i>Large Cephyrocapsa</i> LO <i>Large Cephyrocapsa</i> FO <i>G. oceanica</i> s.l. FO <i>D. brouweri</i> LO <i>D. pentaradiatus</i> LO <i>D. surculus</i> LO <i>D. tamalis</i> LO <i>R. pseudoumbilicus</i> LO <i>D. asymmetricus</i> FCO <i>D. quinquaramus</i> LO <i>R. pseudoumbilicus</i> PE <i>A. primus</i> FO <i>M. convallis</i> LO <i>R. pseudoumbilicus</i> PB <i>M. convallis</i> FO <i>Catinaster</i> spp. FO <i>D. kugleri</i> FO <i>S. heteromorphus</i> LO <i>H. ampliaptera</i> LO	<i>R. asanoi</i> LO <i>H. sellii</i> LO <i>C. macintyreii</i> LO <i>D. pentaradiatus</i> PE <i>A. delicatus</i> LO <i>D. pentaradiatus</i> PB <i>P. lacunosa</i> FCO <i>D. hamatus</i> LO <i>D. kugleri</i> LCO <i>D. kugleri</i> FCO <i>C. macintyreii</i> FO <i>C. premacintyreii</i> LCO <i>C. floridanus</i> LCO			

Figure 2. Adopted time framework–Pleistocene–Pliocene calcareous nannofossil events and zonations proposed for the California margin compared with standard zonation of Okada and Bukry (1980) and Bukry (1991) and Mediterranean zonations (Rio, Raffi, et al., 1990; Fornaciari et al., 1996). At left: geomagnetic polarity time scale (GPTS) after Cande and Kent (1995). CN = Neogene coccolith, MNN = Mediterranean Neogene Nannoplankton. \* = emended zones and subzones. FO = first occurrence, LO = last occurrence, FCO = first common and continuous occurrence, LCO = last common and continuous occurrence. AB = acme beginning, PB = paracme beginning, PE = paracme end.

4. The preservation potential of the species defining the event.

Therefore, the rank of biostratigraphic reliability of an index species is evaluated on the following basis:

1. Unambiguous taxonomy,
2. Mode of occurrence of the event (= morphology of the event),
3. Consistency of the relative position with respect to the other biohorizons, and
4. Position of the events vs. the chronomagnetostratigraphy.

To this purpose, the presence and abundance of those species that have been proposed as biostratigraphically useful were monitored, establishing their distribution patterns with the quantitative and semi-quantitative counting methods outlined below. On the basis of such distribution patterns, the morphology of the various biohorizons was evaluated, thus obtaining the first fundamental information on their reliability. Afterward, the ranking of the various biohorizons was checked within the study area and with respect to other regions. When available, magnetostratigraphy was used for constructing age-depth plots and inferring age estimates to be compared with the ages reported in the literature.

## MATERIAL

The sites drilled during Leg 167 can be subdivided into five different transects (Fig. 1):

1. The Gorda Transect, up to 40°N, which includes Sites 1019, 1022, 1020, and 1021, drilled in a region of strong summer upwelling;
2. The Conception Transect, at 35°N (Sites 1017 and 1016), is influenced by year-round upwelling of fairly cool surface waters;
3. The north-south Coastal Transect from 31°N to 42°N, is composed of Sites 1019, 1022, 1018, 1017, 1014, 1013, 1012, and 1011, which spans 1000–2500 m water depth;
4. The Northern Depth Transect from 37°N to 42°N (Sites 1019, 1022, 1018, 1020, and 1021), which spans 1000–4200 m water depth; and
5. The Southern Depth Transect from 30°N to 35°N (Sites 1015, 1017, 1013, 1014, 1012, 1011, 1010, and 1016), which spans 475–3850 m water depth.

The sites studied are located along the California margin (Fig. 1) and are listed in Table 1, where the sampling resolution for each site is reported. The temporal extension of the various sections is summarized in Figure 3, where the available magnetostratigraphic records are shown.

Approximately 1900 samples were analyzed.

## METHODS

The samples were prepared from unprocessed material as smear slides and were examined under a light microscope at 1250× magnification. First, all samples were examined with qualitative methods. Successively, the presence or absence of index species in the stratigraphic intervals critical for detecting the various biohorizons were checked by using the quantitative and semiquantitative counting methods suggested by Thierstein et al. (1977), Backman and Shackleton (1983), Rio, Fornaciari, et al. (1990), and Rio, Raffi, et al. (1990). Semiquantitative data have been collected by counting the index species in 1-mm<sup>2</sup> squares (i.e., *Amaurolithus*, *Ceratolithus*, *Sphenolithus*, *Gephyrocapsa*, and *Pseudoemiliana lacunosa*). The quantitative data have been collected by counting the index species relative to a prefixed number of taxonomically related forms (species of

helicoliths relative to 10–50 helicoliths; *Reticulofenestra pseudumbilicus*, *Cyclicargolithus floridanus*, and *P. lacunosa* relative to 50–100 reticulofenestrids; species of *Calcidiscus* relative to 10–50 *Calcidiscus*; *Coccolithus miopelagicus* relative to 10–100 *Coccolithus*; species of *Discoaster* relative to 30–200 discoasterids; and species of *Gephyrocapsa* relative to 100–300 *Gephyrocapsa*).

The considered taxa are reported in alphabetic order and by generic epithets in Appendix A. Bibliographic references for the species are given in Loeblich and Tappan (1966, 1968, 1969, 1970a, 1970b, 1971, 1973), Aubry (1984, 1988, 1989, 1990), and Perch-Nielsen (1985). The adopted taxonomic concepts are those of Rio, Fornaciari, et al. (1990); Rio, Raffi, et al. (1990); Fornaciari et al. (1990); and Raffi et al. (1993) and are summarized in the taxonomic notes.

## RESULTS

Calcareous nannofossils are generally well represented in the studied material. Abundance, preservation, and assemblage composition vary with water depth, latitude, and stratigraphic interval. Miocene and Pleistocene assemblages are better preserved and more diversified than the Pliocene ones.

The distribution patterns of 30 middle Miocene to Pleistocene calcareous nannofossil index species, established by different counting methods, are shown in Figures 4–21. Together these species define 50 biohorizons, which are listed and discussed in Tables 2–5. Their stratigraphic position at each site is reported in Appendix B. Following the strategy outlined above, on the basis of the established distribution patterns and available magnetostratigraphy (Figs. 22–25), the reliability of the 50 biohorizons is evaluated below and the results are summarized in Tables 2–5. Then, on the basis of the regionally reliable biohorizons, a biostratigraphic scheme integrated with the GPTS and GCS is proposed (Fig. 2), upon which the age assignments at single sites are based. In the following section the data obtained for the Pleistocene, Pliocene, and Miocene time intervals are discussed.

### Pleistocene

The Pleistocene Series was formally defined in 1983 by the Global Stratotype Section and Point (GSSP) of the Vrica section in southern Italy (Aguirre and Pasini, 1985), just below the top of the Olduvai Subchron (C2n Subchron in the terminology of Cande and Kent, 1995), with an age of 1.806 Ma (Lourens et al., 1996). In this work, the base of the Pleistocene is approximated with magnetostratigraphy when available, or by means of the first occurrence (FO) of *Gephyrocapsa oceanica* s.l., which occurs some 80 k.y. above the Vrica GSSP (Raffi et al., 1993; Rio, Raffi, et al., 1997). A subdivision of the Pleistocene Series has not been attempted because it is controversial (Van Eysinga, 1975; Ruggeri and Sprovieri, 1977, 1979; Rio, 1982; Berggren and Van Couvering, 1974; Haq et al., 1987; Ruggeri et al., 1984; Haq and Van Eysinga, 1986; Rio et al., 1991; Berggren et al., 1985; Berggren, Hilgen, et al., 1995; and Van Couvering, 1997), and the subdivisions proposed up to now cannot be recognized by means of the calcareous nannofossils.

Sediments belonging to the Pleistocene Series are well represented at all sites of Leg 167 (Fig. 3), and in some cases (i.e., Sites 1017, 1018, 1019, and 1020) the Pleistocene sequence is expanded.

The classification of Pleistocene sediments by means of calcareous nannofossils in the light microscope is based on the eight biohorizons reported in Table 2. Two additional biohorizons in the late Pleistocene, the FO and the acme beginning (AB) of *Emiliana huxleyi*, are not discussed in this paper because they cannot be confidently recognized with the light microscope technique used in this study.

### Biohorizons Based on *Gephyrocapsids*

The *gephyrocapsids* are a major component of the Pleistocene calcareous nannofossil assemblage, both in the California margin area

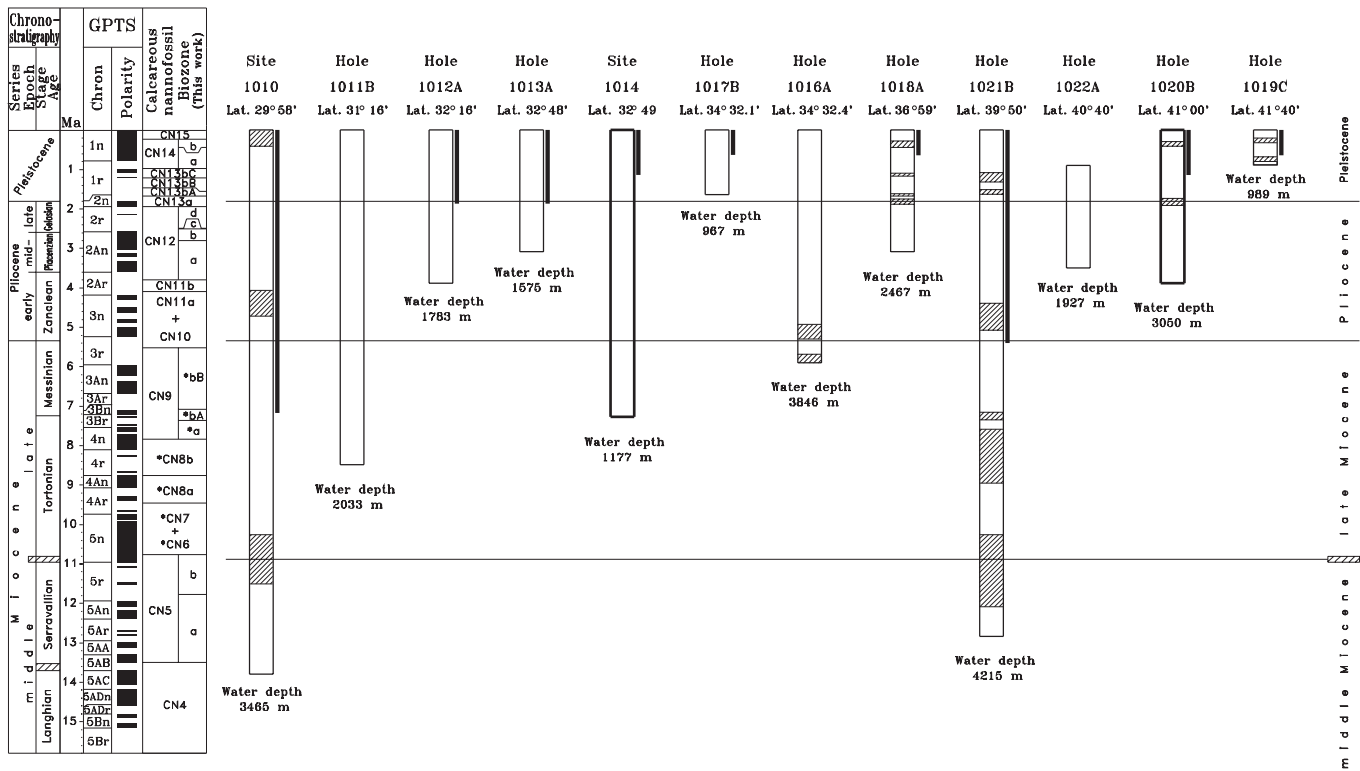


Figure 3. Position of investigated sections relative to integrated biomagnetostratigraphy. Black columns at right of sites/holes denote sections where magnetostratigraphy was measured. Striped areas in the site/holes columns indicate barren intervals. Bold lines show sites/holes sampled at high resolution.

and worldwide. They provide at least five globally useful biohorizons (P2, P3, P5, P6, and P8 in Table 2). Taxonomy and nomenclature of gephyrocapsids are complex and contradictory. For the present study, the biometric subdivision proposed by Rio (1982) and Raffi et al. (1993) has been followed.

The gephyrocapsids appeared in the late Miocene (Bonci and Pirini Radrizzani, 1992; Pujos, 1987) with small forms (<4 μm; “small *Gephyrocapsa* spp.”). They remained a secondary component of the calcareous nannofossil assemblages into the late Pliocene, when their abundance increased and they underwent a gradual size increase from ~4 to ~7 μm (Rio, 1982). Based on this progressive size increase, it is possible to define at least two different biohorizons: the FO of *Gephyrocapsa oceanica* s.l. (defined as gephyrocapsids >4 μm, with an open central area) and the FO of large *Gephyrocapsa* spp. (gephyrocapsids >5.5 μm; Rio, 1982; Raffi et al., 1993). These two bioevents have been referred to differently in the literature. The FO of *G. oceanica* s.l. corresponds to the FOs of medium-sized *Gephyrocapsa* spp. of Raffi et al. (1993) and *Gephyrocapsa* spp. A-B of Wei (1993), whereas the FO of large *Gephyrocapsa* of Rio (1982) and Raffi et al. (1993) corresponds to the FO of *Gephyrocapsa* spp. A-B >5.5 μm of Wei (1993).

Following the early Pleistocene rapid size increase, gephyrocapsids underwent a major evolutionary change with the virtual disappearance of medium- and large-sized forms and the onset of an interval characterized by the dominance of small *Gephyrocapsa* spp. (Gartner, 1977; Rio, 1982; Raffi et al., 1993). This major paleontologic change is referred to in the literature as the LO of large *Gephyrocapsa* spp. by Rio, Raffi, et al. (1990) and Raffi et al. (1993) and as the LO of *Gephyrocapsa* spp. A-B of Wei (1993)

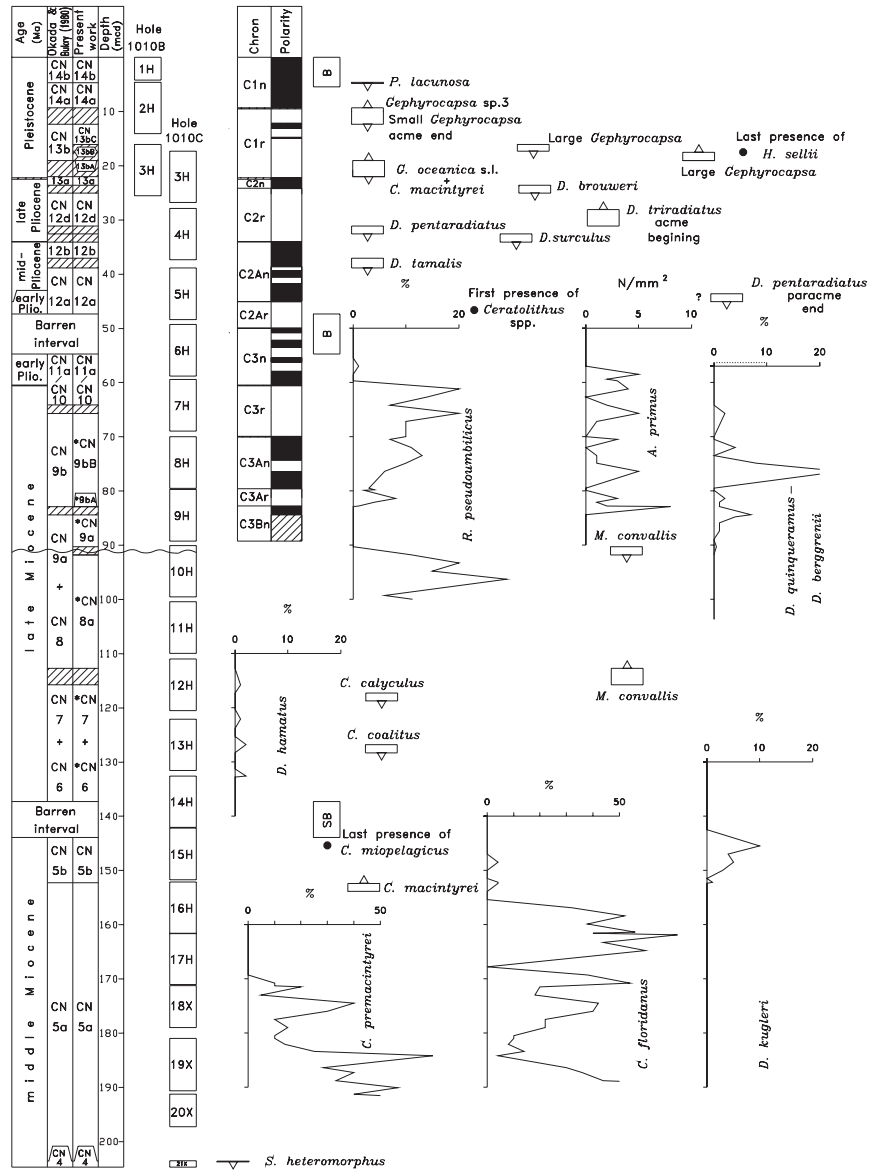
The end of the interval of dominance of the small *Gephyrocapsa* spp. was referred to as the acme end (AE) of small *Gephyrocapsa* spp. by Gartner (1977) and thereafter used as a zonal boundary definition in the early Pleistocene. This bioevent is marked by the reentrance (RE) of normal-sized gephyrocapsids (size between 4.0 and

5.5 μm), among which there is a form characterized by having the bridge in the central area parallel to the short axis of the placolith. This form is missing in the underlying interval. Following Rio (1982), such specimens have been labelled *Gephyrocapsa* sp. 3. Gartner’s AE of small *Gephyrocapsa* spp. has been referred to as *Gephyrocapsa* spp. C-D by Wei (1993) and as the RE of *Gephyrocapsa* spp. by Raffi et al. (1993).

In the California margin, all these biohorizons based on gephyrocapsids can be recognized across the entire Leg 167 latitudinal transect, as discussed below.

1. The FO of *G. oceanica* s.l., considered as a synchronous event occurring at the transition between marine isotope Stages (MIS) 59 and 60, with an age of 1.69 Ma (Table 2), has been recorded at all sites. It occurs just above the Olduvai (C2n) Subchron at Sites 1010 (Figs. 4, 5), 1012 (Fig. 8), 1013 (Fig. 9), and 1021 (Figs. 18, 19). Age-depth plots at low-latitude Site 1010 (Fig. 22; Table 2) and at mid-latitude Site 1021 (Fig. 25; Table 2) suggest an interpolated age of  $1.635 \pm 0.115$  Ma and  $1.765 \pm 0.045$  Ma, respectively, in agreement with previous evaluations (Table 2). The event, therefore, appears to be reliable and useful in this area.
2. The FO of large *Gephyrocapsa* spp., considered a slightly diachronous event (Raffi et al., 1993; Wei, 1993; Lourens et al., 1996; Table 2), has been observed at all sites. At low-latitude Site 1010 the estimated age for this event is  $1.46 \pm 0.06$  Ma (Fig. 22; Table 2), in agreement with the ages inferred in low-latitude areas (Raffi et al., 1993; Wei, 1993). The FO of large *Gephyrocapsa* spp. appears to be a useful and reliable event in the California margin.
3. The LO of large *Gephyrocapsa* spp. is considered a globally synchronous event occurring within MIS 37 with an age of 1.24 Ma (Raffi et al., 1993; Table 2). This biohorizon has been detected at Sites 1010, 1012, 1014, 1017, 1018, and 1020

Figure 4. Chronostratigraphy and calcareous nannofossil biostratigraphy at Site 1010. Magnetostratigraphy from A. Hayashida (unpubl. data). In the zonal columns, striped intervals at boundaries represent uncertainties (due to sample spacing) within which biohorizons occur. Striped areas in the chronostratigraphy columns represent intervals within which chronostratigraphic boundaries occur. \* = emended zones and subzones. Wavy line = gap. B = barren interval, SB = sub-barren interval. mcd = meters composite depth. N/mm<sup>2</sup> = number of specimens per square millimeter. See text for other counting methods.



- (Figs. 4, 5, 8, 10, 11, 13, 14, 16, 17). The age inferred for the large *Gephyrocapsa* spp. LO at Site 1020 is 1.23 Ma (Fig. 24; Table 2), in agreement with previous evaluations (Table 2). At Site 1010, the age-depth plot instead suggests a slightly older age (Fig. 22; Table 2), probably as a result of the low-resolution sampling (Table 1).
- The FO of *Gephyrocapsa* sp. 3 has been shown to be slightly diachronous by Wei (1993) and Raffi et al. (1993), occurring within MIS 27 (~1.00 Ma) at low latitudes and within MIS 25 (~0.96 Ma) in middle to high latitudes (Raffi et al., 1993; Table 2). *Gephyrocapsa* sp. 3 occurs discontinuously in the California margin, where it is also very rare. However, at Sites 1010, 1014, 1020, and 1021 (Figs. 4, 5, 10, 11, 16–19), its first appearance could be placed slightly above the Jaramillo Subchron, with an inferred age of 0.88/0.99 Ma (Figs. 22–25; Table 2) that compares well with previous evaluations. Hence, despite the low abundance and the discontinuous occurrence, the FO of *Gephyrocapsa* sp. 3 has been considered useful for correlations within the area.
  - The AE of small *Gephyrocapsa* spp. (FO of *Gephyrocapsa* spp. C-D of Wei [1993] and RE of *Gephyrocapsa* spp. of Raffi

et al. [1993]) occurs close to the top of the Jaramillo Subchron at Sites 1010, 1012, 1013, 1014, and 1021 (Figs. 4, 5, 8, 9, 10, 11, 18, 19) and well within the Brunhes Chron at Sites 1017, 1018, 1019, and 1020 (Figs. 13–17). In particular, at Site 1020 the age-depth plot suggests an age of 0.625 ± 0.005 Ma (Fig. 24; Table 2), comparable to that obtained by Wei (1993) for mid-southern latitude Site 593. Because of this diachrony, the AE of small *Gephyrocapsa* spp. has been considered a poorly reliable event in the studied area.

**Other Reliable Pleistocene Biohorizons**

The LO of *Reticulofenestra asanoi* (a >6.5-µm circular reticulofenestrid) has been evidenced as a useful event by Takayama and Sato (1987). Wei (1993) proved this event globally synchronous at an age of ~0.88 Ma. In the California margin, *R. asanoi* has been analyzed quantitatively only at Site 1014 (Figs. 10, 11), where the species is well represented and its extinction is a clear event occurring in the middle part of Chron 1r (Fig. 11). The age-depth plot suggests an age of 0.88 Ma (Fig. 23; Table 2), in agreement with previous evaluations (Takayama and Sato [1987], 0.83 Ma; Matsuoka and Okada

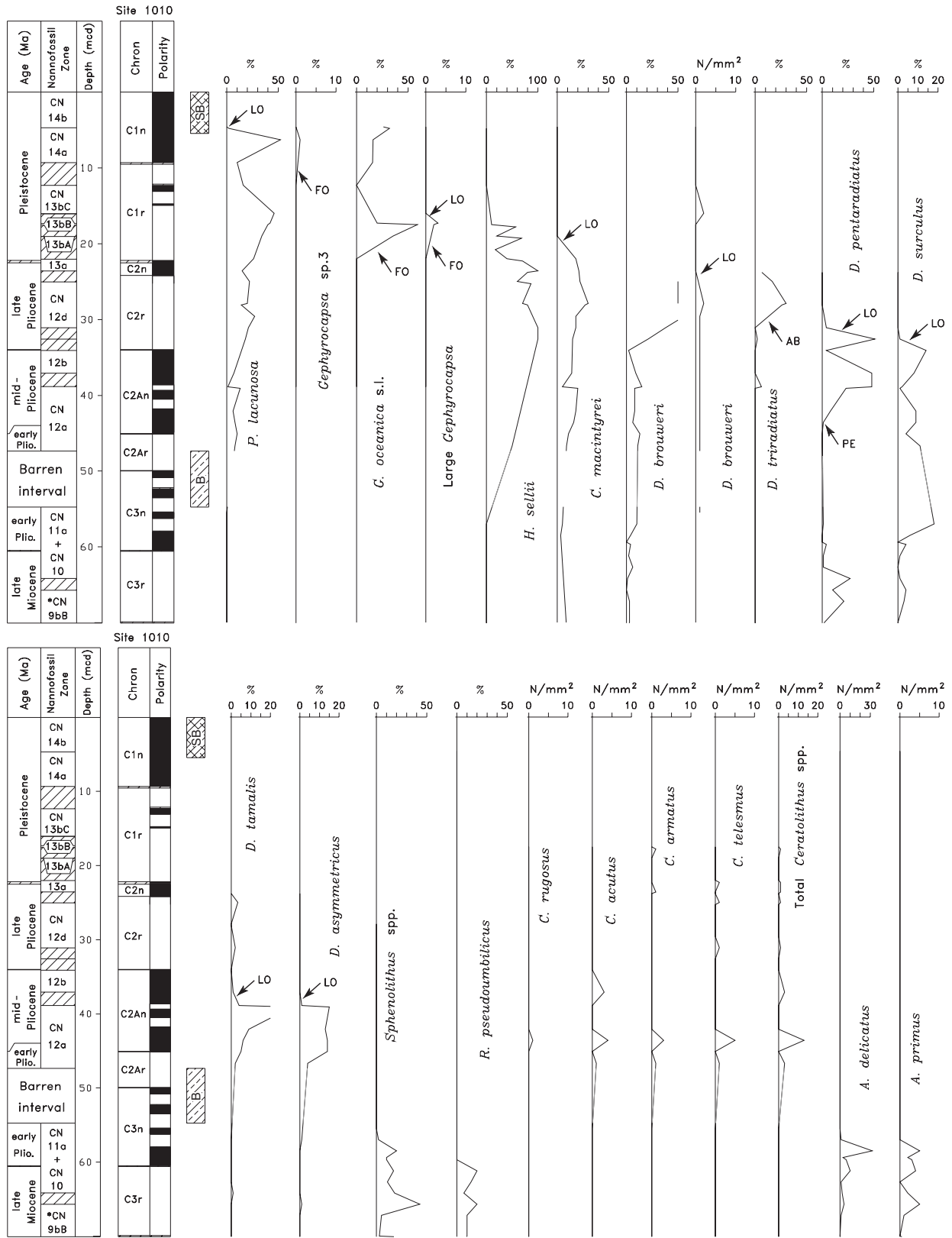


Figure 5. Abundance patterns of selected late Miocene to Pleistocene calcareous nannofossils at Site 1010. See Figures 2 and 4 for symbol and abbreviation definitions.

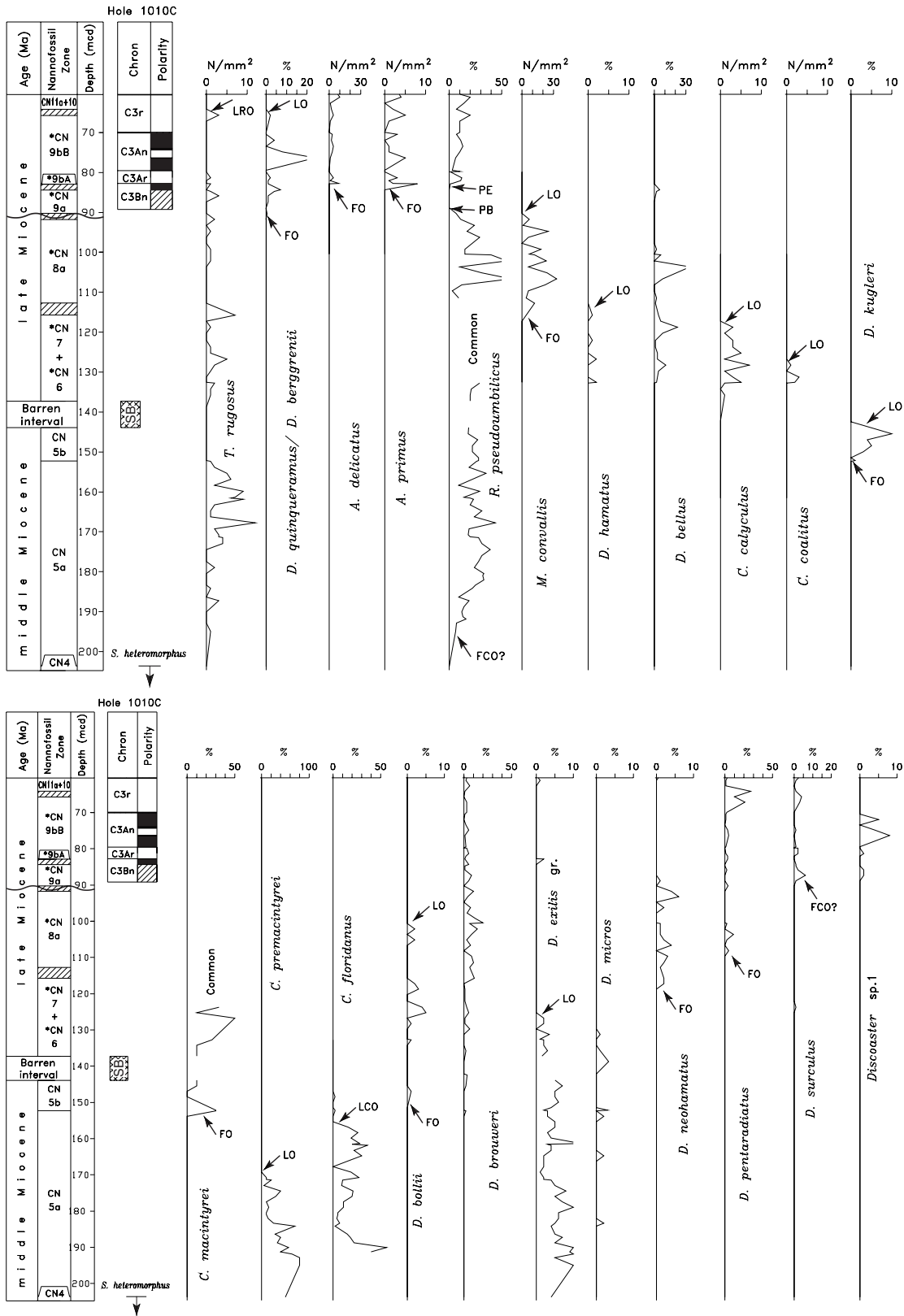


Figure 6. Abundance patterns of selected middle Miocene to late Miocene calcareous nannofossils at Site 1010. See Figures 2 and 4 for symbol and abbreviation definitions.

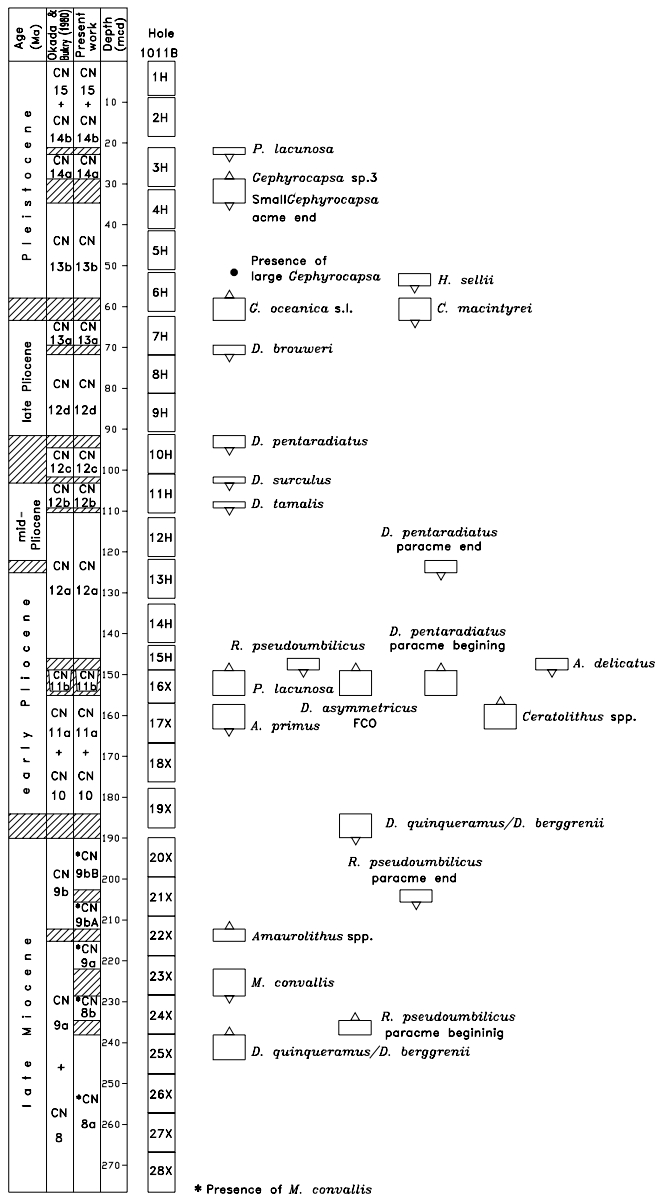


Figure 7. Chronostratigraphy and calcareous nannofossil biostratigraphy at Hole 1011B. See Figure 4 for symbol and abbreviation definitions.

[1989], 0.81 Ma; Wei [1993], 0.88 Ma; Bassinot et al. [1994], 0.88 Ma). The LO of *R. asanoi* is a useful and reliable biohorizon within the mid-Pleistocene in this area.

Another reliable biohorizon observed in the California margin is the LO of *P. lacunosa*. The species is well represented, and its extinction is easily determined at all sites studied with detailed quantitative counting (Figs. 5, 11, 17, 19). However, it must be noted that at all sites, except Site 1014, the event appears to be abrupt, most probably because of the low-resolution sampling. In fact, at Site 1014, where the time spacing between samples is ~6 k.y., *P. lacunosa* shows strong abundance fluctuations before its extinction (Figs. 10, 11), in agreement with the findings by Thierstein et al. (1977).

**Other Pleistocene Biohorizons**

The LO of *H. sellii* has been proposed by Gartner (1977) as a useful early Pleistocene event. However, it has been proved to be time transgressive over various water masses by Backman and Shackleton

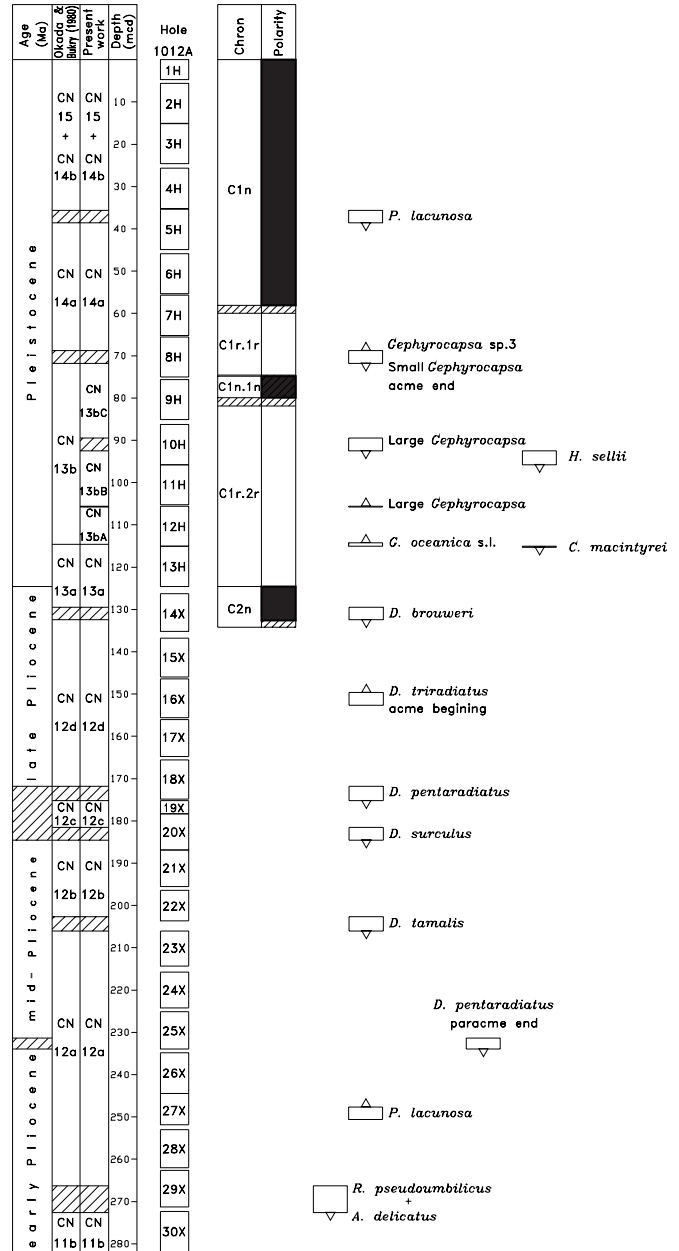


Figure 8. Chronostratigraphy and calcareous nannofossil biostratigraphy at Hole 1012A. Magnetostratigraphy from A. Hayashida (unpubl. data). See Figure 4 for symbol and abbreviation definitions.

(1983), Wei (1993), and Raffi et al. (1993). In the studied area helicoliths occur discontinuously (e.g., Site 1010, Fig. 5), making it difficult to pinpoint the LO of *H. sellii*. However, at Sites 1011, 1012, 1016, 1017, and 1018 the event is associated with or just below the LO of large *Gephyrocapsa* spp. (Figs. 7, 8, 12–14). Therefore, it is found in a stratigraphic position comparable to that observed in the Mediterranean (Rio, Raffi, et al., 1990) and middle North Atlantic Ocean successions (Raffi et al., 1993). The LO of *H. sellii* in the California margin has been considered as an unreliable event because the species is too rare in the early Pleistocene.

The LO of *C. macintyreii* has been proposed as an early Pleistocene biohorizon by Gartner (1977), but it has been proved to be time transgressive (Raffi et al., 1993; Wei, 1993; Table 2). Specifici-

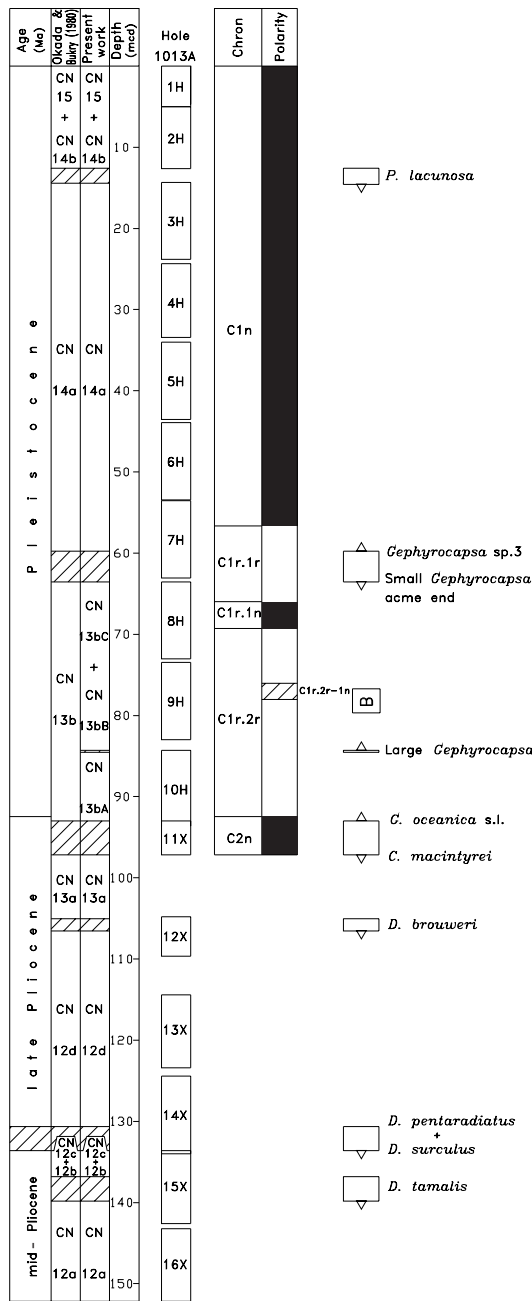


Figure 9. Chronostratigraphy and calcareous nannofossil biostratigraphy at Hole 1013A. Magnetostratigraphy from site chapter in Lyle, Koizumi, Richter, et al. (1997). See Figure 4 for symbol and abbreviation definitions.

cally, the event normally occurs slightly above the FO of *G. oceanica* s.l. (Rio, Raffi, et al., 1990; Raffi et al., 1993; Wei, 1993; Gartner, 1977), but it has been associated with the MIS 57/58 transition (1.67 Ma) in some areas, and with the MIS 55 (1.6 Ma) in others (Raffi et al., 1993; Wei, 1993; Table 2). *Calcidiscus macintyreii* is generally well represented in the California margin. However, it occurs discontinuously and is rare in its final range (see Site 1014 in Fig. 11, Site 1020 in Fig. 17, and Site 1021 in Figs. 18–19). With reference to those sites where the sampling resolution was sufficiently high, the LO of *C. macintyreii* has been observed in its “right” position only at low-latitude Site 1014 (Figs. 10, 11). At mid-latitude Site 1020, the event is definitively below the FO of *G. oceanica* s.l., and at Site 1021, studied in low resolution, the event seems to be associated with

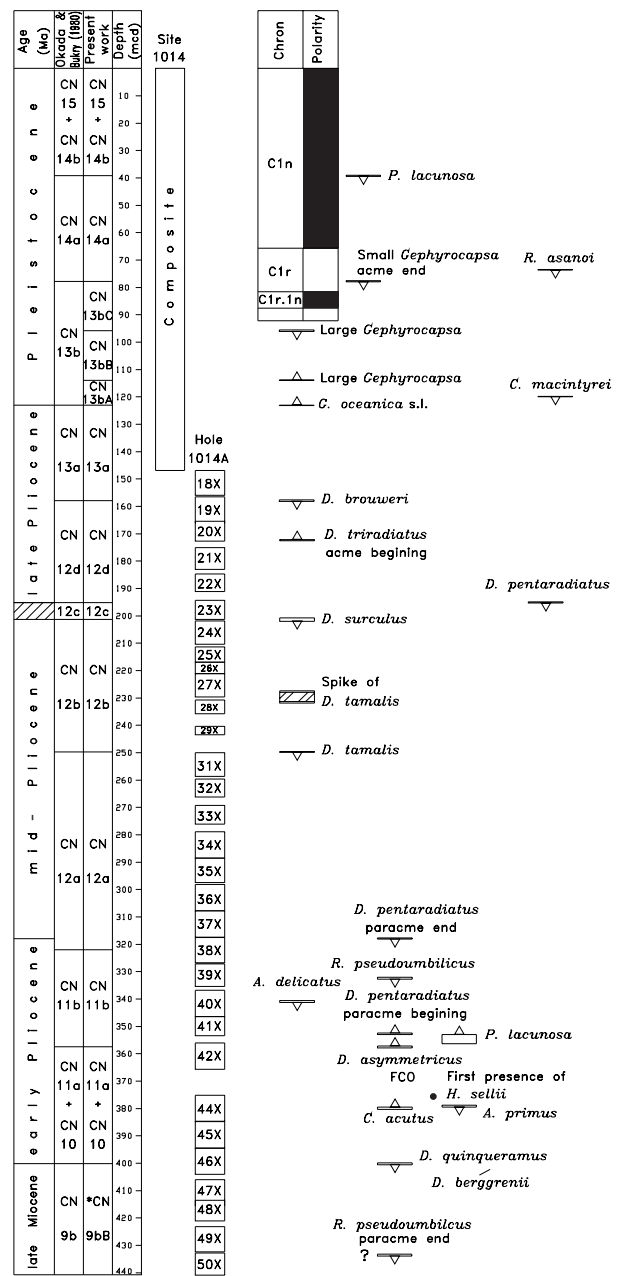


Figure 10. Chronostratigraphy and calcareous nannofossil biostratigraphy at Site 1014. Magnetostratigraphy from Lyle, Koizumi, Richter, et al., 1997. See Figure 4 for symbol and abbreviation definitions.

the Olduvai (C2n) Subchron, with an estimated age of  $1.915 \pm 0.015$  Ma (Fig. 25; Table 2). These data seem to indicate that the LO of *C. macintyreii* in the California margin is more time transgressive than previously thought, and hence a poorly reliable event.

**Emendation of the Pleistocene Zonation of Okada and Bukry (1980)**

The biostratigraphic resolution provided by the standard zonations of Okada and Bukry (1980) for the Pleistocene is limited (Fig. 2), and normally workers refer to additional biohorizons for a finer subdivision. The set of biohorizons discussed above makes it possible to propose a better resolved and more reliable zonation for the Pleistocene that can be applied to the California margin area and in

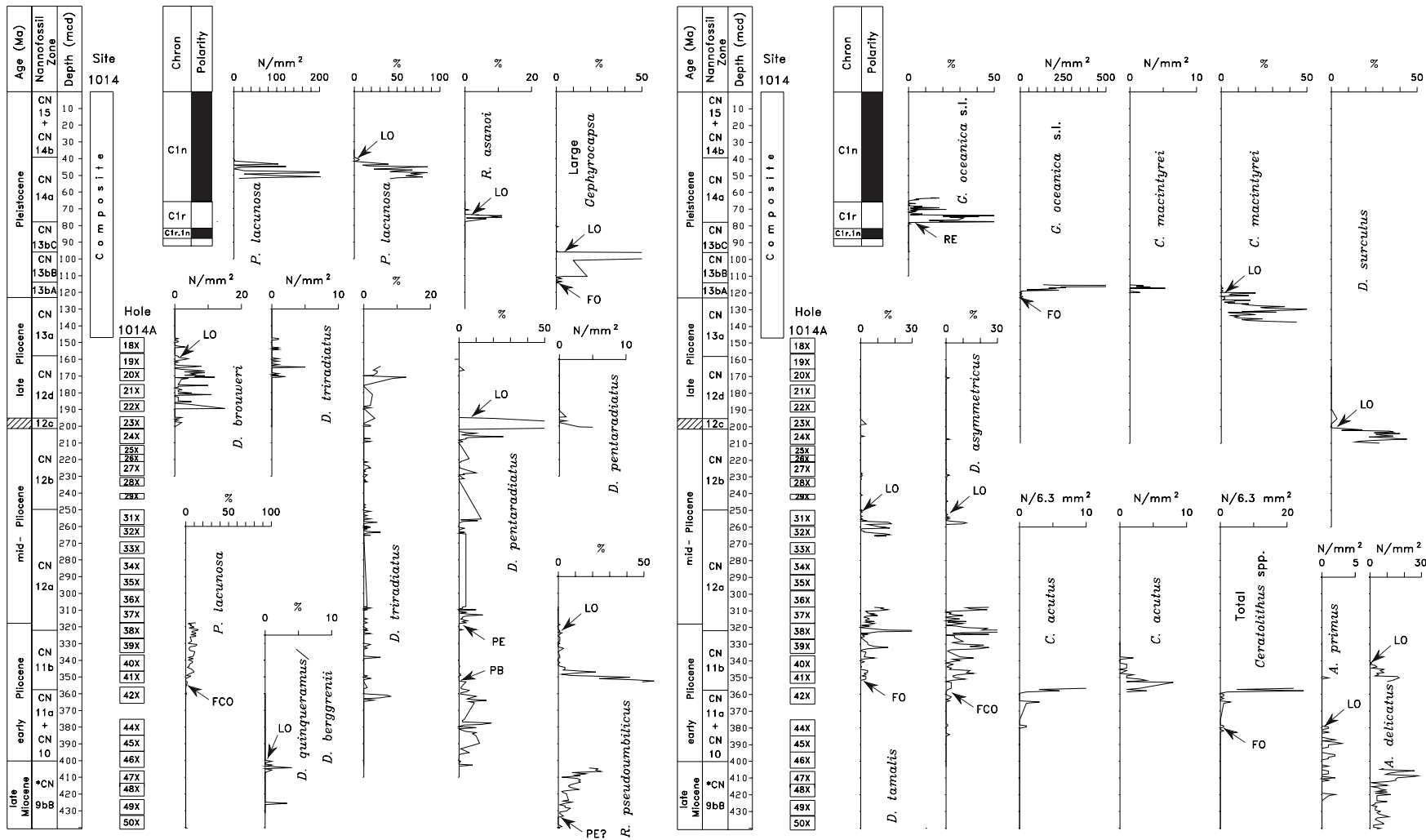


Figure 11. Abundance patterns of selected late Miocene to Pleistocene calcareous nannofossils at Site 1014. See Figures 2 and 4 for symbol and abbreviation definitions.

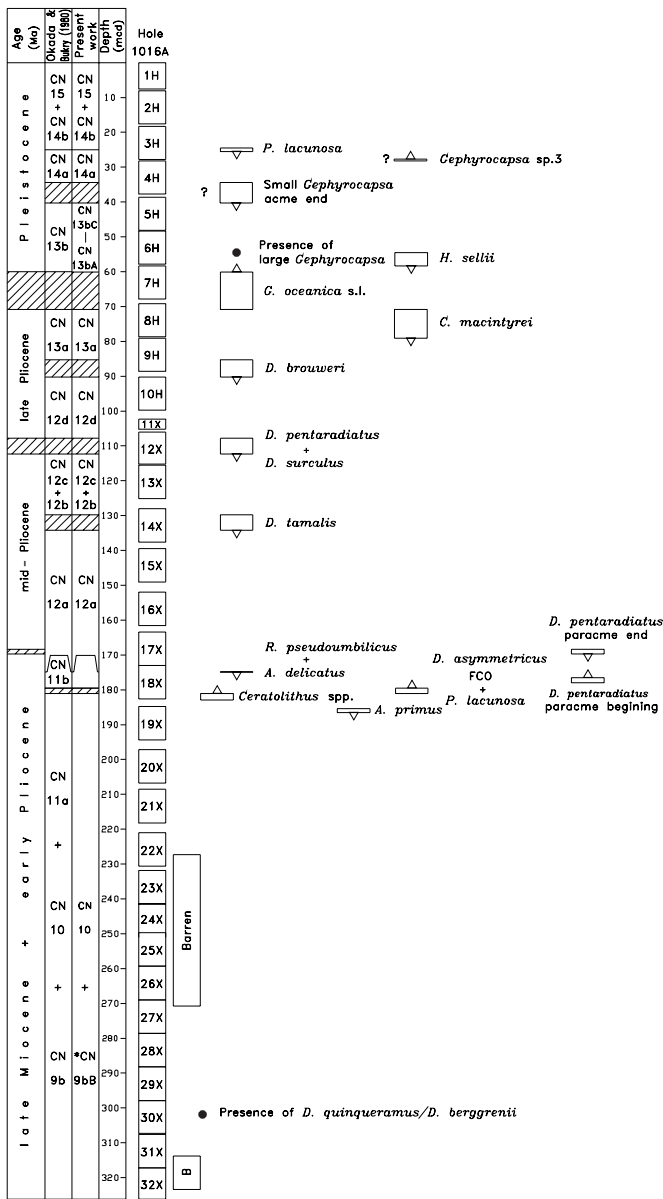


Figure 12. Chronostratigraphy and calcareous nannofossil biostratigraphy at Hole 1016A. See Figure 4 for symbol and abbreviation definitions.

most of the low- to high-latitude areas. Therefore, the following emendation of the early to mid-Pleistocene zonation of Bukry (1973) as coded by Okada and Bukry (1980) is proposed:

- CN13bA: from the FO of *G. oceanica* s.l. to the FO of large *Gephyrocapsa* spp.;
- CN13bB: from the FO to the LO of large *Gephyrocapsa* spp.;
- CN13bC: from the LO of large *Gephyrocapsa* spp. to the FO of *Gephyrocapsa* sp. 3; and
- CN14a: from the FO of *Gephyrocapsa* sp. 3 to the LO of *Pseudemiliana lacunosa*.

Bukry (1973) and Okada and Bukry (1980) considered these biostratigraphic intervals as subzones. Because they are widely recognizable over various water masses as demonstrated by the extensive literature available, it has been proposed to rank them at zone level. The definitions and occurrences of these four new biostratigraphic units are given in Appendix C in addition to any related remarks.

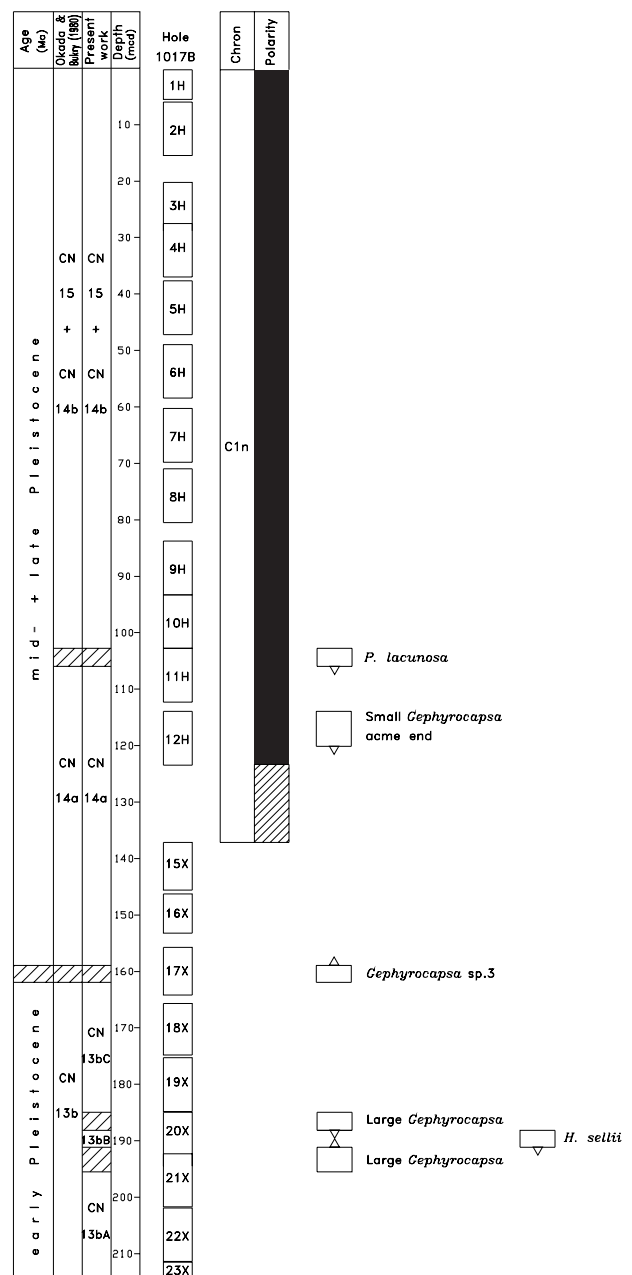


Figure 13. Chronostratigraphy and calcareous nannofossil biostratigraphy at Hole 1017B. Magnetostratigraphy from Lyle, Koizumi, Richter, et al., 1997. See Figure 4 for symbol and abbreviation definitions.

### Pliocene

The Pliocene/Miocene boundary has not been formally defined yet, but following a common practice, in this paper it is equated with the reestablishment of the open marine conditions in the Mediterranean, namely at the base of the Mediterranean Zanclean Stage (Rio et al., 1991; Hilgen and Langereis, 1988). The recognition of the Miocene/Pliocene boundary is generally considered difficult at a global scale (e.g., Benson et al., 1991; Benson and Hoddell, 1994; Benson and Rakic-El Bied, 1996; and Suc et al., 1997). Recently, however, it has been shown that the base of the Zanclean is associated with the upper part of Chron C3r, some 80 k.y. below the Thevra (C3n.4n) Subchron (Zijderveld et al., 1986; Channell et al., 1988; Hilgen and Langereis, 1988), at an age of 5.33 Ma (Lourens et al., 1996). This

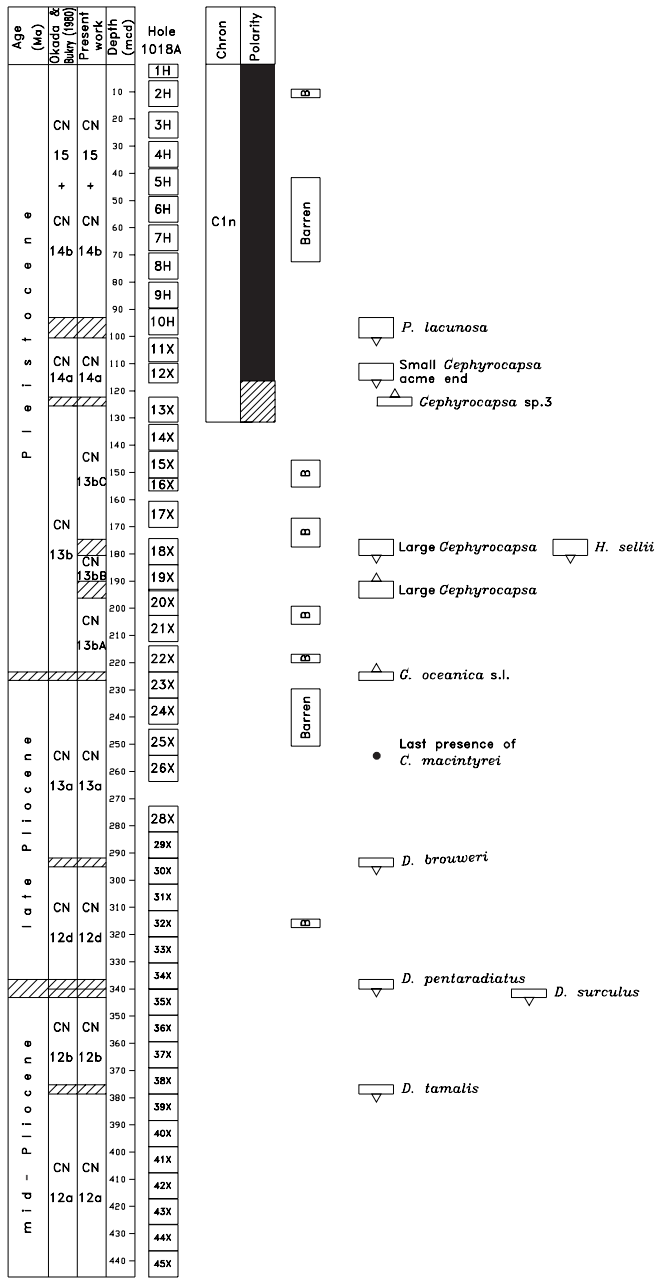


Figure 14. Chronostratigraphy and calcareous nannofossil biostratigraphy at Hole 1018A. Magnetostratigraphy from Lyle, Koizumi, Richter, et al., 1997. See Figure 4 for symbol and abbreviation definitions.

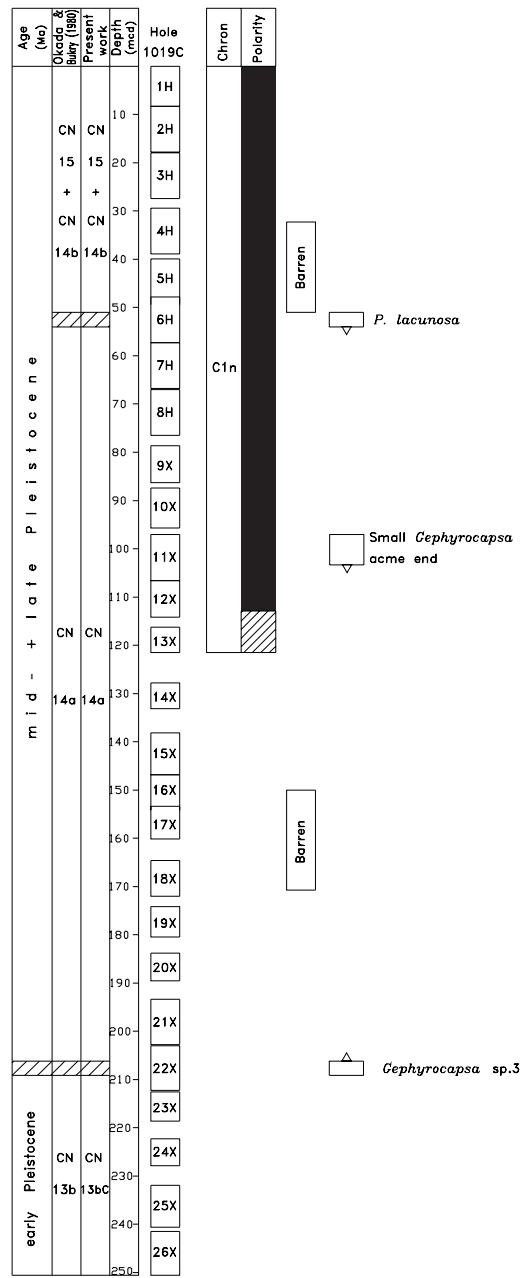


Figure 15. Chronostratigraphy and calcareous nannofossil biostratigraphy at Hole 1019C. Magnetostratigraphy from Lyle, Koizumi, Richter, et al., 1997. See Figure 4 for symbol and abbreviation definitions.

chronological information allows us to approximate the Miocene/Pliocene boundary by the LO of *Discoaster quinqueramus* (5.54 Ma according to Backman and Raffi, 1997) and the FO of *Ceratolithus acutus* (5.37 Ma according to Backman and Raffi, 1997). It must be noted that the practice of recognizing the Miocene/Pliocene boundary by means of these biohorizons is well established among nannofossil paleontologists (Bukry, 1973; Rio, Fornaciari, et al., 1990; Raffi and Flores, 1995). Because of the unreliability of the FO of *C. acutus* in the California margin area (see below), magnetostratigraphy and/or the LO of *D. quinqueramus* are used for approximating the Miocene/Pliocene boundary.

The Pliocene Series has been subdivided into three intervals (early, mid-, and late Pliocene) following a recent formal decision of the In-

ternational Commission on Stratigraphy (Rio et al., 1998; Castradori et al., 1998). The early Pliocene corresponds to the Zanclean Stage, the mid-Pliocene to the Piacenzian Stage, and the late Pliocene to the Gelasian Stage (Rio et al., 1998; Castradori et al., 1998). This three-fold subdivision of the Pliocene Series is easily recognizable by means of calcareous nannofossil biostratigraphy. The early Pliocene (Zanclean)/mid-Pliocene (Piacenzian) boundary, defined in Sicily by a lithologic level corresponding to the Gilbert/Gauss boundary, at an age of 3.66 Ma, is approximated by the LO of *Sphenolithus* spp. (3.7 Ma according to Lourens et al., 1996) and the LO of *R. pseudumbilicus* (3.82 Ma according to Shackleton et al., 1995). In the California margin area, the LO of *Sphenolithus* spp. is not reliable. The early/mid-Pliocene boundary has been placed by using magnetostratigra-

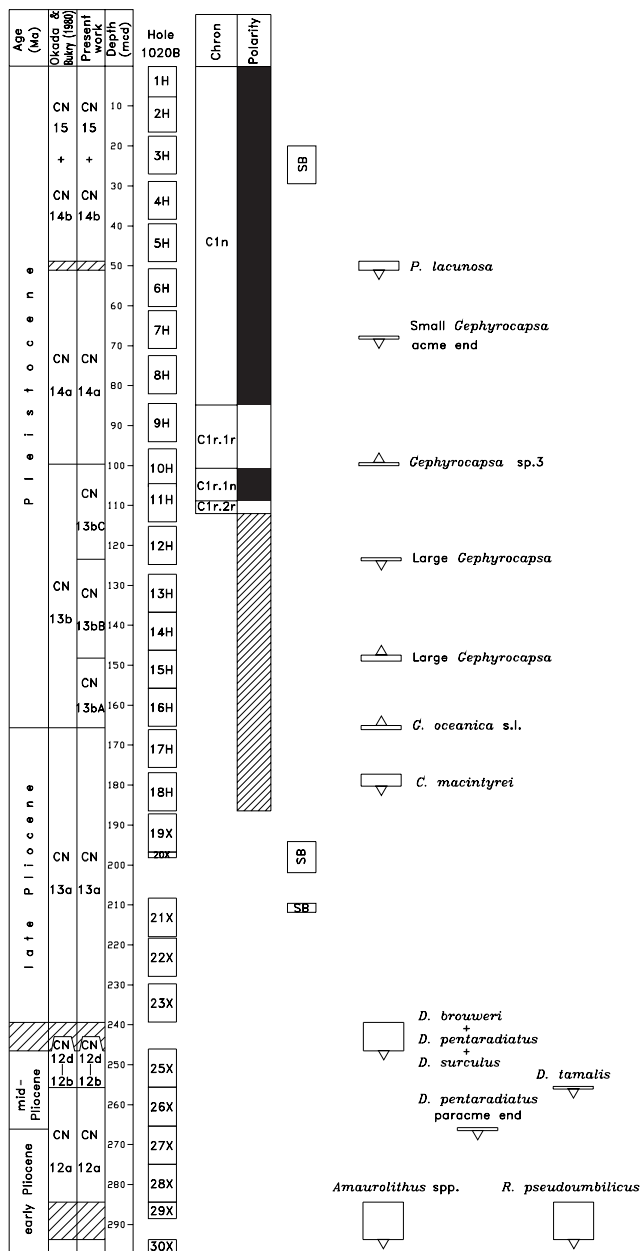


Figure 16. Chronostratigraphy and calcareous nannofossil biostratigraphy at Hole 1020B. Magnetostratigraphy from Lyle, Koizumi, Richter, et al., 1997. See Figure 4 for symbol and abbreviation definitions.

phy, when available, or the paracme end (PE) of *Discoaster pentaradiatus*, which is closely associated with the Gilbert/Gauss boundary in this area (see discussion below). The mid-Pliocene (Piacenzian)/late Pliocene (Gelasian) boundary is defined in Sicily by a lithic level close to the Gauss/Matuyama boundary, at an age of 2.55 Ma (Rio et al., 1998). In the California margin area it is well approximated by the closely spaced successive extinctions of *Discoaster surculus* (~2.53 Ma) and *D. pentaradiatus* (~2.52 Ma).

The Pliocene Series is well represented at all Leg 167 sites (Fig. 3) with a thickness of as much as 270 m at Site 1014 (Fig. 10).

The Pliocene calcareous nannofossil assemblage is generally poorly diversified and badly preserved, especially in the lower Pliocene sections where barren intervals are present (Fig. 3). The 16 biohorizons that have been proposed as useful for the correlation and

classification of the ~3.52-m.y.-long Pliocene Series have been reported in Table 3. In the following section the reliability of all these biohorizons in the California margin is discussed.

### Biohorizons Based on Discoasterids

Discoasterids provide at least eight biohorizons for subdividing the Pliocene Series (PI5, PI7, PI10, and PI12–PI16 in Table 3). They are known to be missing in sediments underlying high latitudes and high-nutrient water masses (Chepstow-Lusty et al., 1989, 1991, 1992; Chepstow-Lusty and Chapman, 1995). The vastly different latitudinal and ecological conditions represented in Leg 167 sites make it difficult to evaluate the reliability of the discoasterid biohorizons in the entire area.

The simultaneous LOs of *Discoaster brouweri* and *Discoaster triradiatus* (the last representative of the discoasterids; Ericson et al., 1963), generally used in all low- and middle-latitude zonation (Table 3; Fig. 2), have been detected at Sites 1010 (Figs. 4, 5), 1011 (Fig. 7), 1012 (Fig. 8), 1013 (Fig. 9), 1014 (Figs. 10, 11), 1016 (Fig. 12), 1018 (Fig. 14), 1020 (Figs. 16, 17), 1021 (Figs. 18, 19), and 1022 (Fig. 21). At the low-latitude Sites 1010 and 1012 and at mid-latitude Site 1021 the *D. brouweri* and *D. triradiatus* LOs occur slightly above the base of the Olduvai Subchron (Figs. 4, 8, and 18), in agreement with the previous evaluations of Raffi et al. (1993), Wei (1993), and Channell et al. (1990). However, at mid-latitude Sites 1020 and 1022 (Figs. 16, 17, and 21), located near the core of the Northern California Current (Lyle, Koizumi, Richter, et al., 1997), the LOs of *D. brouweri* and *D. triradiatus* are associated with the LOs of *Discoaster pentaradiatus* and *Discoaster surculus*, at a lower stratigraphic level with respect to previous sites. Wise (1973), who studied Site 173 located 16 km from Site 1022, observed as well an early LO of *D. brouweri* in this area of cold and probably high-productivity water masses. The LOs of *D. brouweri* and *D. triradiatus* are diachronous events in the California margin, useless for long-distance correlation in the area. Bukry (1973) used the LO of *D. brouweri* as a zonal boundary. Because the LO of *D. brouweri* is of limited geographic applicability, it would be better utilized as a subzonal boundary definition.

Due to the high abundance of *D. triradiatus* in the upper part of the range of *D. brouweri* (Takayama, 1970), Backman and Shackleton (1983) defined the AB of *D. triradiatus* as a late Pliocene biohorizon. In the investigated area, *D. triradiatus* is well represented only at the low-latitudes Sites 1010 (Figs. 4, 5), 1012 (Fig. 8), and 1014 (Figs. 10, 11), whereas it is rare or absent at other mid-latitude sites. At Site 1010, the AB of *D. triradiatus* occurs in the basal part of the Matuyama (C2r) Chron (Fig. 4) at an interpolated age of  $2.29 \pm 0.1$  Ma (Fig. 22; Table 3). This age estimate is within the range of previous evaluations (from 2.15 to 2.25 Ma according to Berggren, Hilgen, et al., 1995). However, the AB of *D. triradiatus* seems to be of limited utility in the California margin, because the species is too rare.

Close to the Gauss/Matuyama boundary, concomitantly with the enhancement of Northern Hemisphere glaciation, the productivity of discoasterids decreased drastically, and all species except *D. brouweri* and *D. triradiatus* became extinct (Backman and Pestiaux, 1987). This major turnover in the calcareous nannofossil assemblage occurred in ~300–400 k.y. and the successive shortly spaced LOs of *D. tamalis*, *D. surculus*, and *D. pentaradiatus* are generally used for biostratigraphic purposes (Fig. 2; Table 3). These three biohorizons have been recognized at all sites (Site 1010, Figs. 4, 5; Site 1011, Fig. 7; Site 1012, Fig. 8; Site 1013, Fig. 9; Site 1014, Figs. 10, 11; Site 1016, Fig. 12; Site 1018, Fig. 14; Site 1020, Figs. 16, 17; Site 1021, Figs. 18, 19; and Site 1022, Fig. 21). Quantitative and semiquantitative distribution patterns around extinctions are provided for Sites 1010 (Fig. 5), 1014 (Fig. 11), 1020 (Fig. 17), and 1021 (Fig. 19).

*D. pentaradiatus* shows variable abundance close to its extinction, but its LO datum has been detected at all sites. At both Sites 1010 (low-latitude) and 1021 (mid-latitude; Figs. 4 and 18) the LO of

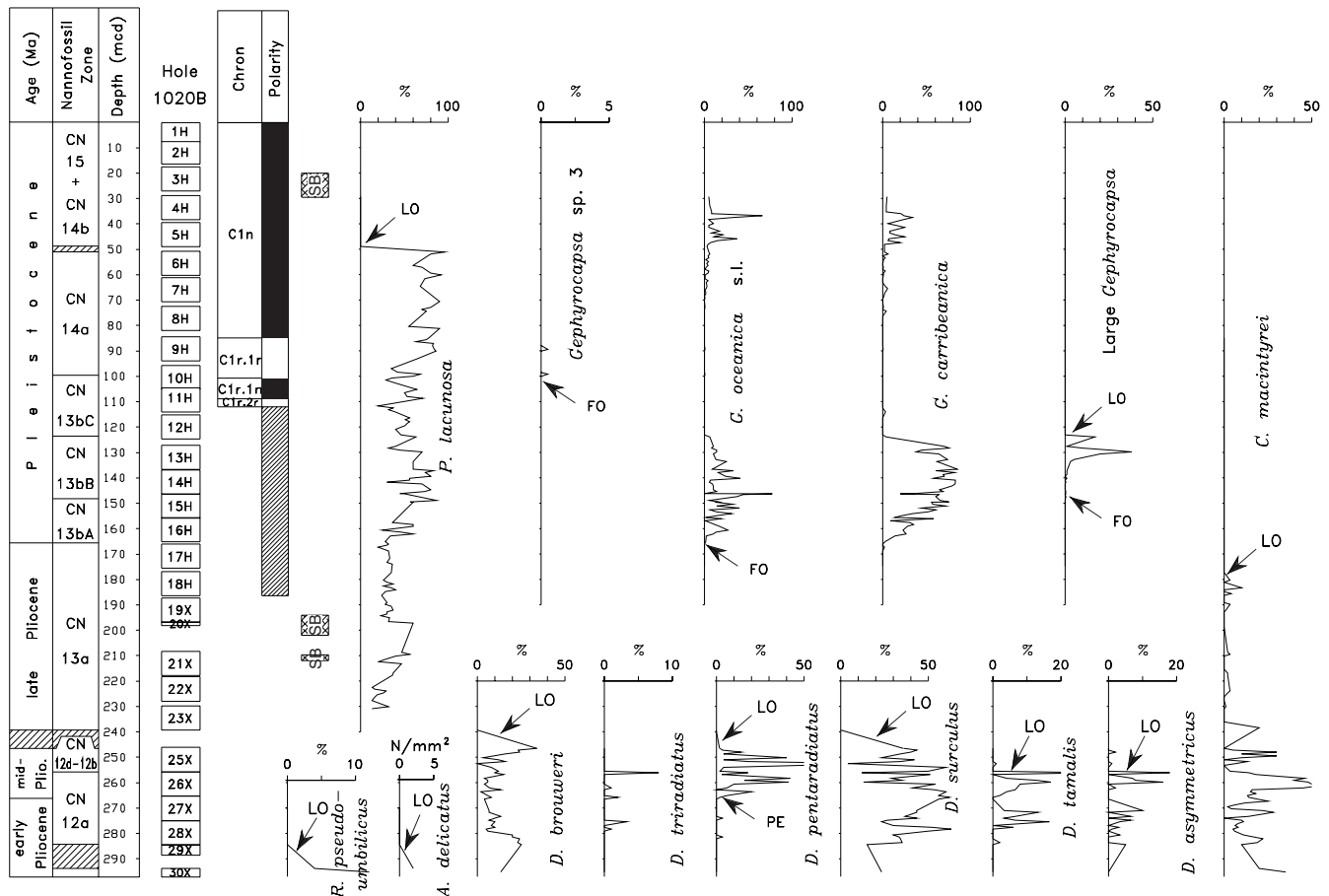


Figure 17. Abundance patterns of selected mid-Pliocene to Pleistocene calcareous nannofossils at Hole 1020B. See Figures 2 and 4 for symbol and abbreviation definitions.

*D. pentaradiatus* is associated with the lowermost part of the Matuyama Chron (C2r.2r). The age-depth plots of Sites 1010 (Fig. 22) and 1021 (Fig. 25) suggest an age of  $2.44 \pm 0.05$  Ma and an age of up to 2.51 Ma (Table 3), respectively. There are contradictions in the literature concerning the synchronicity of the LO of *D. pentaradiatus* (compare Wei, 1993 and Berggren, Hilgen, et al., 1995). Previous age evaluations range from 2.52 Ma (Tiedeman et al., 1994) and 2.51 Ma (Lourens et al., 1996), to 2.36/2.51 Ma (Wei, 1993). These ages compare well with the evaluation at Sites 1010 and 1021, and suggest that the LO of *D. pentaradiatus* can be considered as a fairly good event even if the species is sometimes rare and scattered.

The LO of *Discoaster surculus* has been recognized at all sites and occurs either together or slightly below the LO of *D. pentaradiatus* as observed by all previous authors (Müller, 1978; Ellis, 1979; Raffi and Rio, 1979; Rio, Raffi, et al., 1990). Quantitative or semi-quantitative distribution patterns established at Sites 1010 (Fig. 5), 1014 (Fig. 11), 1020 (Fig. 17), and 1021 (Fig. 19) indicate that the species is common to abundant around its extinction, which appears to be abrupt. At Sites 1010 (low latitude) and 1021 (mid-latitude) the LO of *D. surculus* is associated with the lowermost part of the Matuyama Chron (C2r.2r), with an interpolated age of up to 2.55 Ma (Figs. 22, 25; Table 3) in fairly good agreement with previously reported evaluations (Lourens et al., 1996; Wei., 1993; Berggren, Hilgen, et al., 1995; Table 3). The LO of *D. surculus* appears to be a reliable event in the California margin, and, probably, the easiest detected Pliocene discoasterid event in the area.

The final range of *Discoaster tamalis* has been established in detail at Sites 1014 (Fig. 11) and 1020 (Fig. 17). The species shows an

abrupt decline followed by a few spikes of occurrence that are probably related to a tail of low productivity of the species also known from other areas (Rio, Raffi, et al., 1990). The LO of *D. tamalis* is defined as the drop of abundance that is easily detected at all sites. At Sites 1010 (low latitude) and 1021 (mid-latitude), the LO of *D. tamalis* is associated with the late Gauss Chron (lower part of Chron C2An.1n; Figs. 4, 18), with an interpolated age of  $\sim 2.97$  Ma (Figs. 22, 25; Table 3). This age evaluation is not in strong contrast with previous estimates (2.83 Ma; Table 3), considering that it is based on an interpolation from sediment accumulation rates. Therefore the LO of *D. tamalis* is a fairly useful event in the California margin area.

In the early Pliocene the only biohorizon used from the zonal scheme of Okada and Bukry (1980) is the first common and continuous occurrence (FCO) of *Discoaster asymmetricus* (Fig. 2; Table 3). This event has been detected at Sites 1011 (Fig. 7), 1014 (Figs. 10, 11), 1016 (Fig. 12), and 1021 (Figs. 18, 19) and it can easily be recognized in the California margin, where *D. asymmetricus* is fairly well represented (Figs. 11, 19). At Site 1021 (sampled in low resolution; Table 1), the FCO of *D. asymmetricus* is associated with Chron 2Ar at an age of  $3.925 \pm 0.065$  Ma (Fig. 25). Previously, this event has been associated with the top of the Cochiti (C3n.1n) Subchron with an estimated age of 4.2 Ma (Berggren, Hilgen, et al., 1995; Table 3) and with Subchron C2Ar with an estimated age of 4.12 Ma (Lourens et al., 1996). Despite the possible diachroneity with respect to other areas, the FCO of *D. asymmetricus* has been considered a regionally useful biohorizon.

Within the early Pliocene discoasterid assemblages of the California margin, a peculiar distribution pattern of *Discoaster pentaradia-*

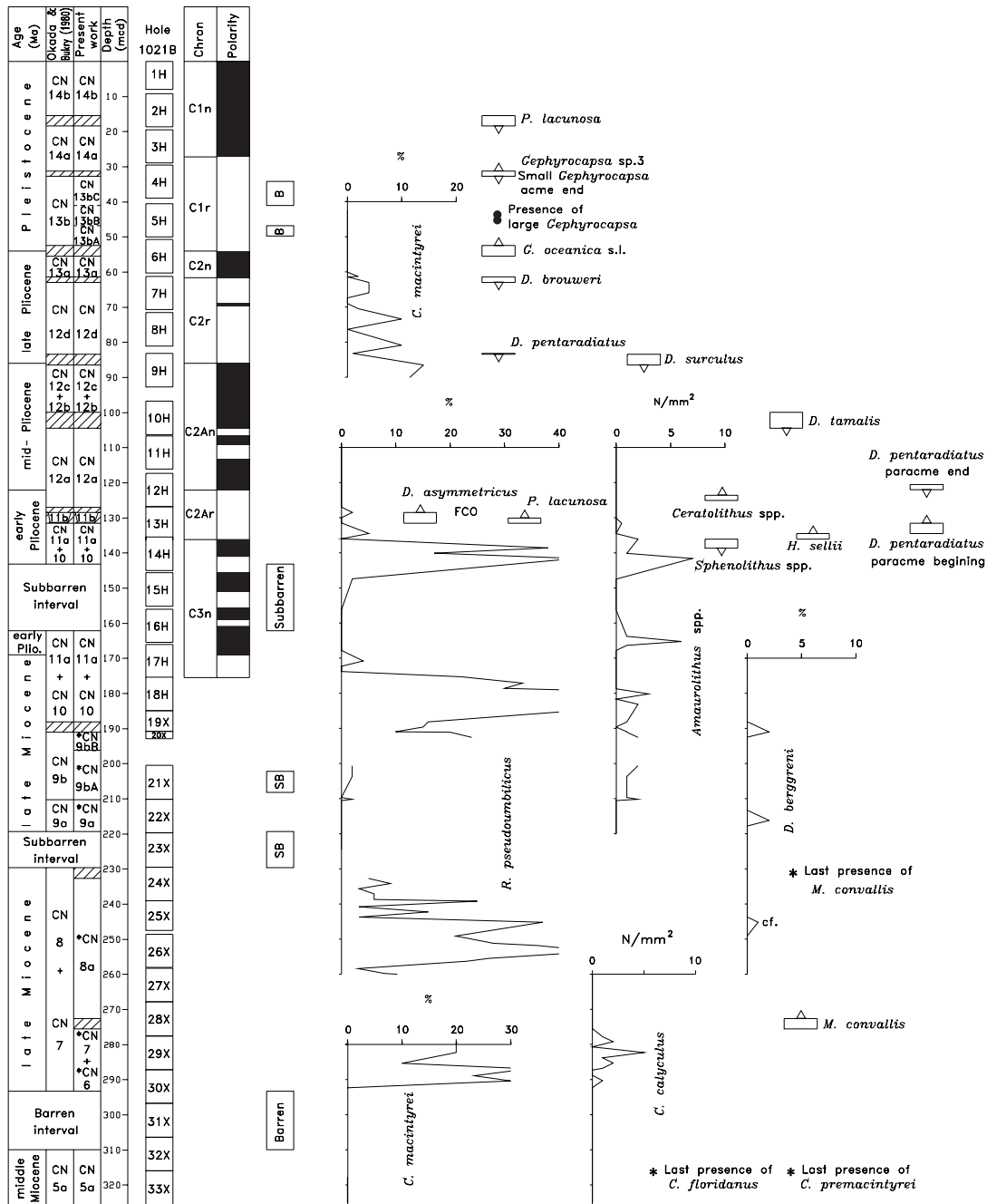


Figure 18. Chronostratigraphy and calcareous nannofossil biostratigraphy at Hole 1021B. Magnetostratigraphy from C. Richter (unpubl. data). See Figure 4 for symbol and abbreviation definitions.

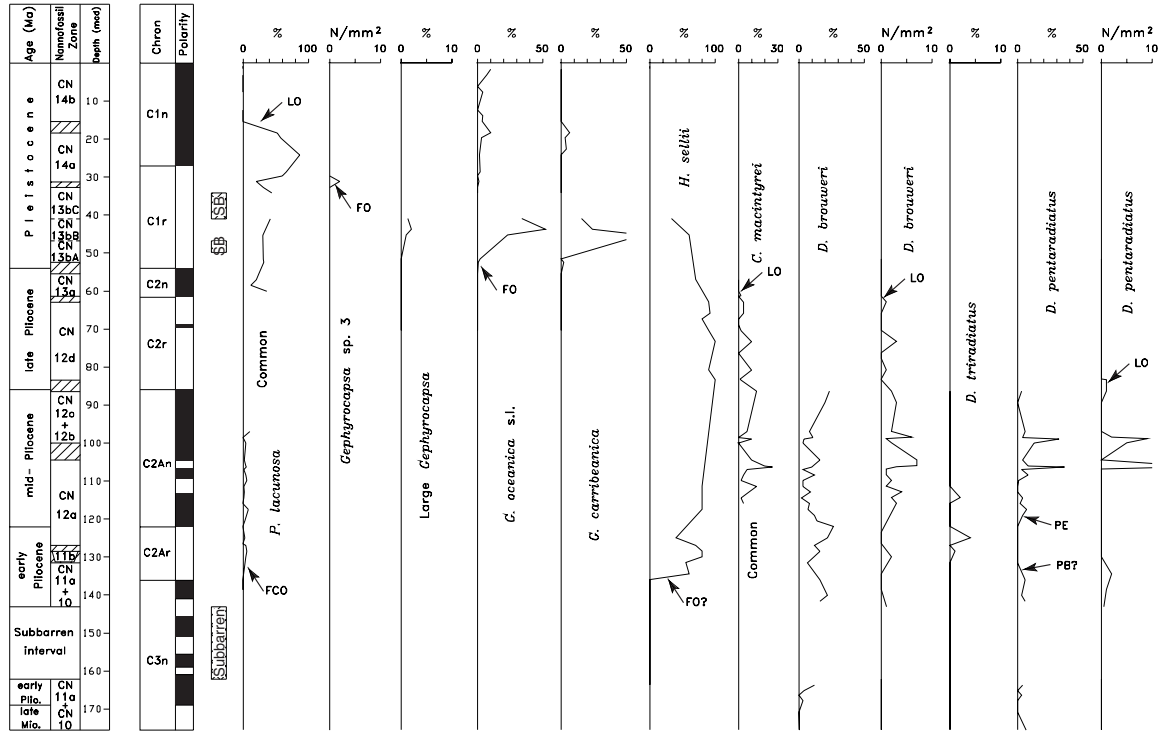
*tus* has been detected: this species is virtually missing in a short interval close to the Gilbert/Gauss boundary at Site 1021 (Figs. 18, 19) and in a similar stratigraphic position at Site 1014 (Figs. 10, 11). An analogous absence interval (paracme) of *D. pentaradiatus* had been observed by Driever (1981, 1988) and Rio, Raffi, et al. (1990) in the Mediterranean area. These authors proposed two biohorizons, the paracme beginning (PB) and PE of *D. pentaradiatus*, that are very useful in the Mediterranean area, where they are associated with the Gilbert/Gauss transition as well. Specifically, Lourens et al. (1996) estimated ages of 3.93 and 3.61 Ma for the PB and PE of *D. pentaradiatus* respectively. Note that the PB of *D. pentaradiatus* has been recognized at Sites 1011 (Fig. 7) and 1016 (Fig. 12), and the PE of *D.*

*pentaradiatus* has been observed at Sites 1010 (Figs. 4, 5), 1011 (Fig. 7), 1012 (Fig. 8), 1016 (Fig. 12), and 1020 (Figs. 16, 17). The PB and PE of *D. pentaradiatus* are considered reliable in the California margin area and basically correlatable with the events observed in the Mediterranean.

**Biohorizons Based on Ceratoliths and Triquetrorhabduliids**

The early Pliocene zonal scheme of Okada and Bukry (1980) is largely based on biohorizons defined by ceratoliths (FO of *Ceratolithus acutus*, FO of *Ceratolithus rugosus*, and LOs of *Amaurolithus primus* and *Amaurolithus tricorniculatus*; Fig. 2). In addition,

Hole 1021B



Hole 1021B

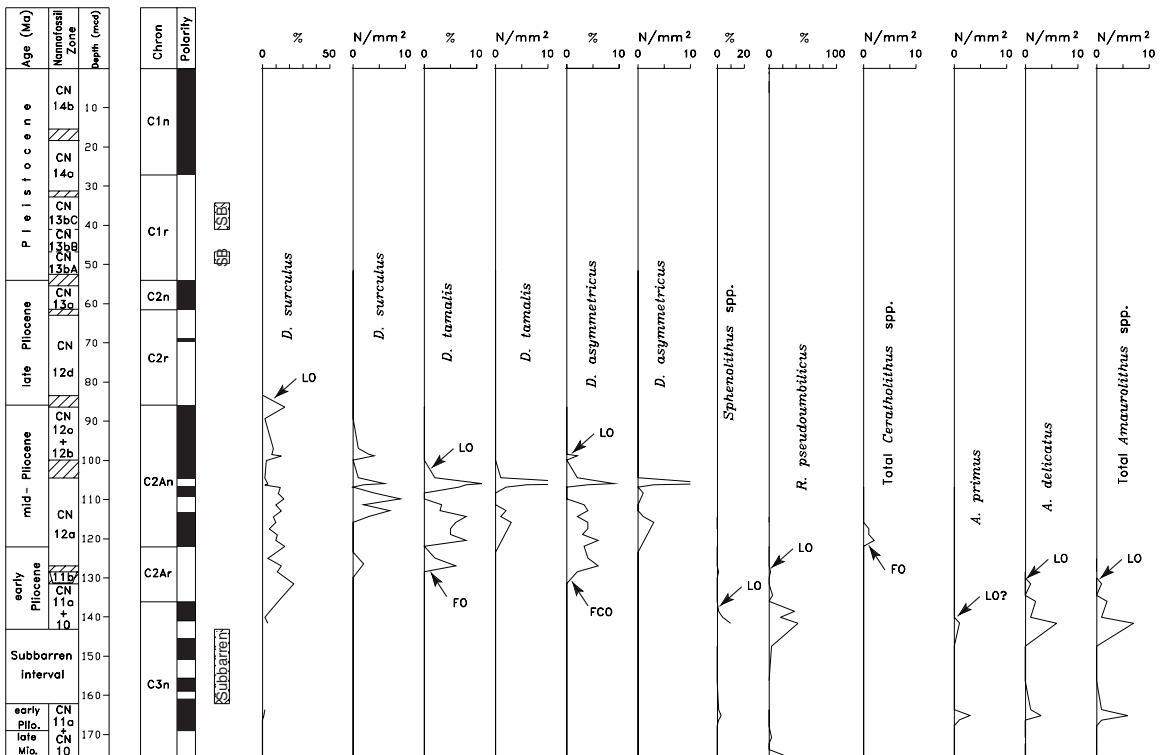


Figure 19. Abundance patterns of selected early Pliocene to Pleistocene calcareous nannofossils at Hole 1021B. See Figures 2 and 4 for symbol and abbreviation definitions.

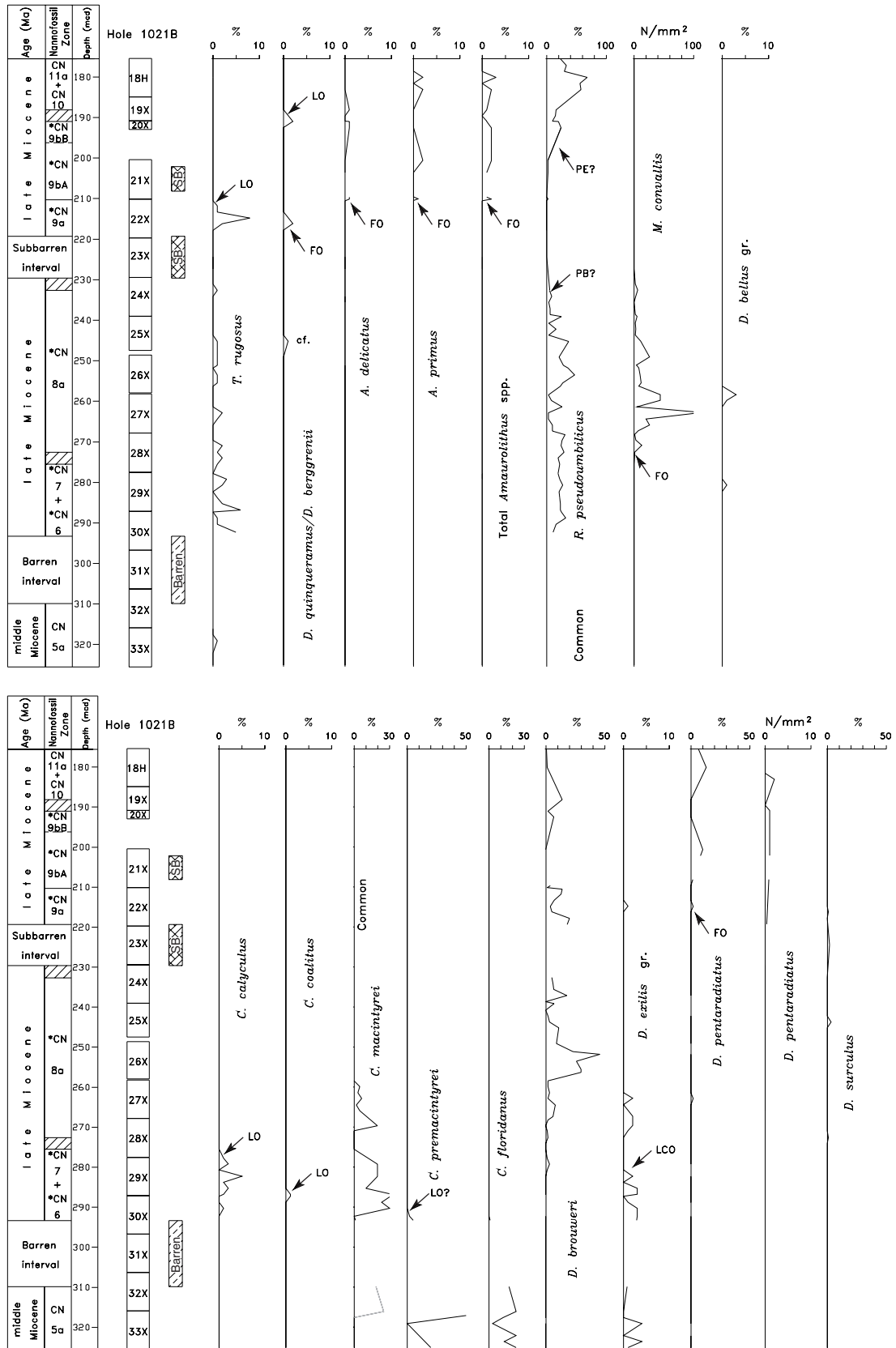


Figure 20. Abundance patterns of selected middle Miocene to late Miocene calcareous nanofossils at Hole 1021B. See Figures 2 and 4 for symbol and abbreviation definitions.

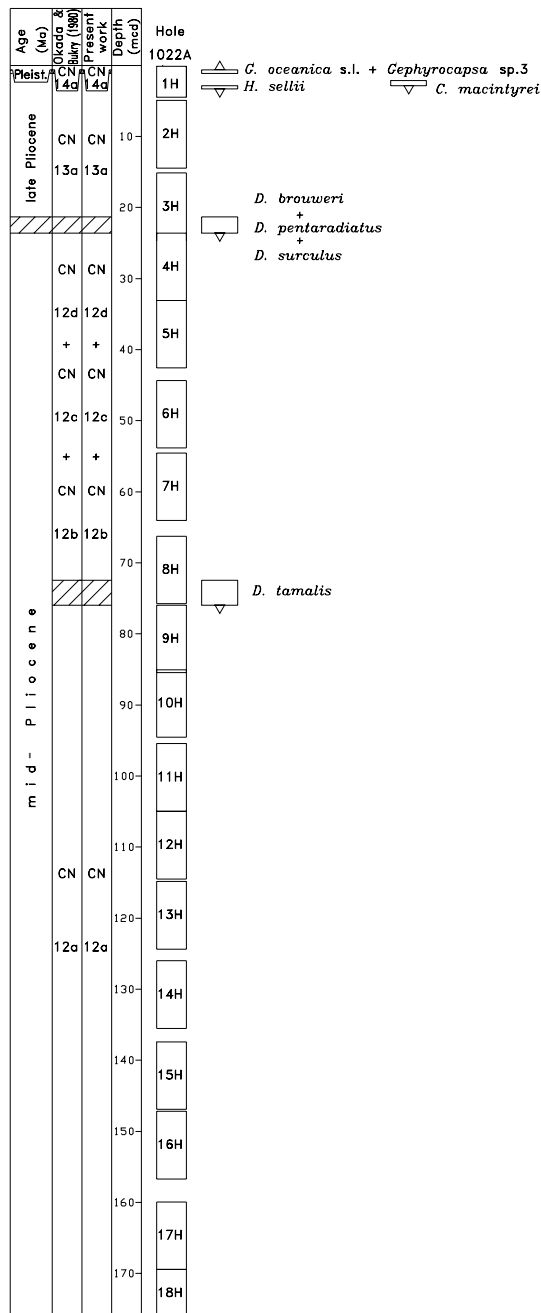


Figure 21. Chronostratigraphy and calcareous nannofossil biostratigraphy at Hole 1022A. See Figure 4 for symbol and abbreviation definitions.

Bukry (1973) suggested as a secondary criterion for defining the bottom of Zone CN10b the LO of *Triquetrorhabdulus rugosus*, a species evolutionarily related to the ceratoliths (Raffi et al., 1998). *T. rugosus*, *A. tricorniculatus*, and members of the genus *Ceratolithus* are virtually missing in the early Pliocene sediments of the California margin and, hence, the biostratigraphic intervals based on them are not recognizable in the area. *A. primus* is rare, whereas *Amaurolithus delicatus* is common and continuously present. The distribution pattern of *A. primus* has been established at low-latitude Site 1014 (Fig. 11) and mid-latitude Site 1021 (Fig. 19). The species occurs discontinuously, particularly at Site 1021. At this latter site *A. primus* apparently becomes extinct within the Cochiti (C3n.1n) Sub-

chron (Fig. 19), whereas previously it had been associated with the top of the Sidufjal (C3n.3n) Subchron in oceanic areas and with the Nunivak (C3n.2n) Subchron in the Mediterranean (Berggren, Hilgen, et al., 1995; Table 3). Because of these results, the LO of *A. primus* is considered a poorly reliable event in the California margin. The distribution pattern of *A. delicatus* has been established at Sites 1014 and 1021 (Figs. 11, 19), but the species is well represented also at the other sites. Its extinction is easily detected and occurs above the FCO of *D. asymmetricus* and close to the LO of *R. pseudoumbilicus*, in a stratigraphic position that is comparable to that observed in the Mediterranean area by Rio, Raffi, et al. (1990). At Site 1021, the LO of *A. delicatus* is associated with Chron C2Ar (upper Gilbert) with an interpolated age of  $3.962 \pm 0.065$  Ma (Fig. 25; Table 3). The inferred age is only indicative because of the low-resolution sampling available at this site (Table 1). The LO of *A. delicatus* seems to be consistently correlatable, at least in the California margin area, and is retained as a regionally reliable biohorizon.

#### Biohorizons Close to the Early/Mid-Pliocene Boundary

The early/mid-Pliocene boundary (corresponding to the Gilbert/Gauss transition) is characterized by a major turnover in the calcareous nannofossil assemblage. In particular, the final extinction of two major elements of the Neogene calcareous nannofossil assemblage occurred very close to the boundary. In fact, the last representatives of the genus *Sphenolithus* and of large reticulofenestrids (*Reticulofenestra pseudoumbilicus*) became extinct at 3.66 and at 3.82 Ma respectively (Shackleton et al., 1995). As already noted above, approximately in this time interval, the last member of the genus *Amaurolithus* (*A. delicatus*) became extinct, and the distribution pattern of *D. pentaradiatus* was affected by an absence interval detected both in the Mediterranean and in the California margin. In addition, in the latest part of the early Pliocene, the placolith *Pseudoemiliana lacunosa* made its first occurrence.

However, as already noted, in the California margin the genus *Sphenolithus* is often missing in the early Pliocene successions, except at low-latitude Site 1010 (Fig. 5) and mid-latitude Site 1021 (Fig. 19). At Site 1021 the LO of *Sphenolithus* spp. occurs much earlier than indicated in the literature, below the FCO of *D. asymmetricus* at the base of Chron C3n.1n (Fig. 18). At Site 1010 (Figs. 4, 5) a barren interval does not allow the observation of this extinction. In the California margin, the LO of *Sphenolithus* spp. is clearly a useless biohorizon.

*Reticulofenestra pseudoumbilicus* is common to abundant at all sites, but close to its final exit it may be missing for a short interval (Site 1021, Figs. 18, 19). The LO of *R. pseudoumbilicus* has been detected at Sites 1011 (Fig. 7), 1012 (Fig. 8), 1014 (Figs. 10, 11), 1016 (Fig. 12), 1020 (Figs. 16, 17), and 1021 (Figs. 18, 19). At all of these sites it occurs together or just above the LO of *A. delicatus*. The age-depth plot at Site 1021 suggests an age of  $3.83 \pm 0.03$  Ma (Fig. 25; Table 3), in good agreement with previous evaluations (Shackleton et al., 1995; Table 3). The LO of *R. pseudoumbilicus* seems to be a reliable and useful biohorizon in the California margin.

#### Other Early Pliocene Biohorizons

The FO of *Pseudoemiliana lacunosa* was proposed as a useful biohorizon in the late early Pliocene of the Mediterranean region (Raffi and Rio, 1979; Rio, Raffi, et al., 1990) and in the northern part of the California margin (Wise, 1973; Fig. 2). In the investigated area, *P. lacunosa* in its initial range is rare, small, and in poorly preserved material can be confused with small reticulofenestrids. The FCO of *P. lacunosa* is defined as the point at which its abundance reaches 1% in a counting of 50–100 reticulofenestrids. The distribution pattern of *P. lacunosa* has been established at Site 1014, where the FCO datum of the species occurs between the FCO of *D. asym-*

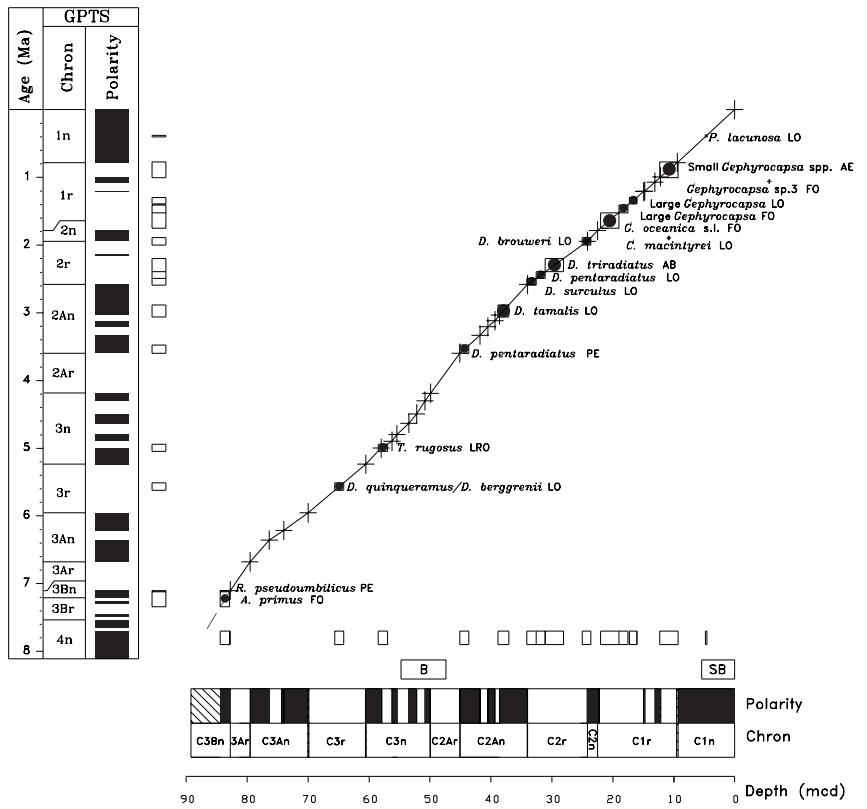


Figure 22. Age-depth plot of upper Miocene–Pleistocene sediments at Site 1010 based on magnetostratigraphic data of A. Hayashida et al. (unpubl. data). See Figures 2 and 4 for symbol and abbreviation definitions.

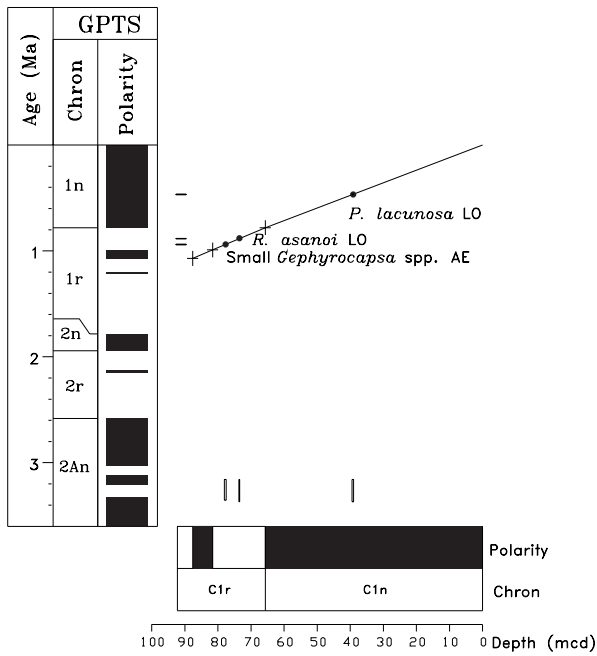


Figure 23. Age-depth plot of Pleistocene sediments at Site 1014 based on magnetostratigraphic data from Lyle, Koizumi, Richter, et al., 1997. See Figures 2 and 4 for symbol and abbreviation definitions.

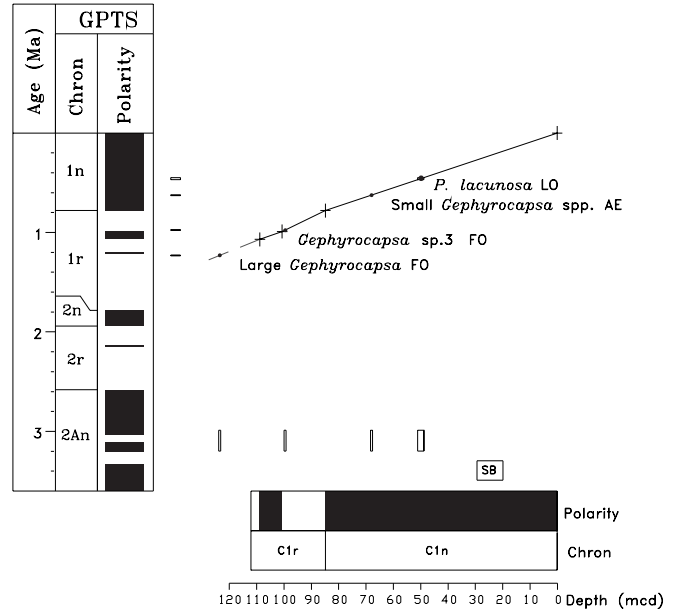


Figure 24. Age-depth plot of Pleistocene sediments at Hole 1020B based on magnetostratigraphic data from Lyle, Koizumi, Richter, et al., 1997. See Figures 2 and 4 for symbol and abbreviation definitions.

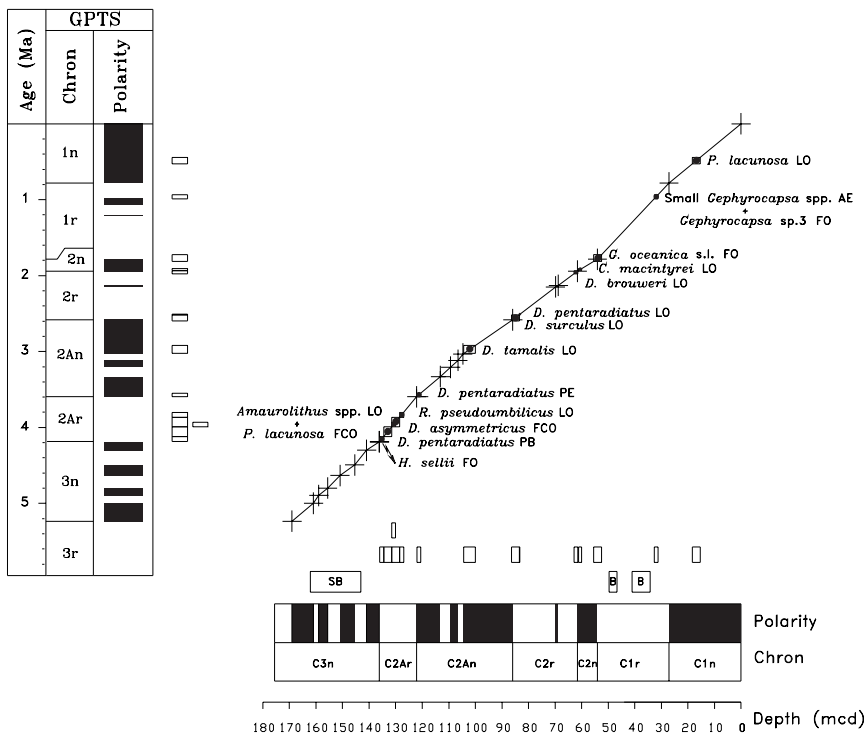


Figure 25. Age-depth plot of lower Pliocene–Pleistocene sediments at Hole 1021B based on magnetostratigraphic data from C. Richter (unpubl. data). See Figures 2 and 4 for symbol and abbreviation definitions.

*metricus* and the LO of *R. pseudoumbilicus* (Fig. 10) at a similar stratigraphic position as in the Mediterranean area (see Rio, Raffi, et al., 1990). However, this event has been considered moderately reliable because *P. lacunosa* is rare and difficult to recognize in its initial range.

The FO of *Helicosphaera sellii* was proposed as a useful event in the Mediterranean area by Rio, Raffi, et al. (1990). As already stated, helicoliths are rare in the California margin. The FO of *H. sellii* has been detected only at Site 1021 (Figs. 18, 19) where it occurs within Chron C2Ar, at an estimated age of  $4.15 \pm 0.03$  Ma (Fig. 25; Table 3), in a position comparable to that observed in the Mediterranean region (Table 3). However, the species is too rare and it occurs discontinuously for its FO datum to be considered as useful in the California margin.

#### Biostratigraphic Remarks

The previous discussion indicates that the middle and late Pliocene zones and subzones proposed by Okada and Bukry (1980) can all be recognized in the California margin area, except for Subzone CN12d at high-latitude sites (i.e., Sites 1020 and 1022) because of the early extinction of *D. brouweri* and *D. triradiatus*. The short Subzones CN12b and CN12c, defined by the extinction of *D. surculus* and *D. pentaradiatus* respectively (Fig. 2), have been recognized only at those sites sampled at high resolution (Site 1014; Fig. 10) or characterized by high accumulation rates (Sites 1011, 1012, 1018, and 1021; Figs. 7, 8, 14, and 18, respectively).

On the contrary, the recognition of most of the early Pliocene zones and subzones of Okada and Bukry (1980) has been difficult because of the scarcity of ceratoliths. Hence, for the biostratigraphic classification of the early Pleistocene sediments of the California margin, Zone CN10 and Subzone CN11a have been combined (Fig. 2).

#### Late Miocene

The late Miocene corresponds, by general agreement, to the Tortonian and Messinian Mediterranean stages. However, the position in time of the base of the historical Tortonian stratotype in the Rio Mazzapiedi-Castellania section (Piedmont Tertiary Basin, Northern Italy) is controversial (Rio, Cita, et al., 1997). No formal definition of the Tortonian stage (middle Miocene/late Miocene boundary) has been proposed to date. Therefore, this paper conforms to the most widespread usage by equating the base of the Tortonian to the first appearance of *Neogloboquadrina acostaensis*, occurring within Zone CN6 in the Mediterranean (Fornaciari et al., 1996) and in many oceanic areas (Berggren et al., 1995b). The bottom of Zone CN6 has been convincingly associated with the lower part of Chron C5n (Raffi et al., 1995; Schneider et al., 1997). Hence, the late Miocene is bounded by approximately the bottom of Chron C5n and the base of the Zanclean Stage at 5.33 Ma (Fig. 2). This usage is basically in agreement with Berggren et al. (1985), Berggren, Hilgen, et al. (1995), and Haq et al. (1987).

The late Miocene is entirely represented only at Site 1010, where it is 70 m thick, and at Site 1021, where it is ~100 m thick (Fig. 3). At Sites 1011 and 1014, only the upper part of the late Miocene is present (Fig. 3).

Late Miocene calcareous nannofossil assemblages are very characteristic with respect to those of the underlying middle Miocene. To remark this Bukry (1975b) introduced the “Sorolian Coccolith Stage,” largely based on the dominance of five-rayed discoasterids. Considering both standard zonations and the most recent literature, at least 20 biohorizons have been proposed for the biostratigraphic classification and correlation of the ~5.5-m.y.-long late Miocene time interval (Table 4; Fig. 2). The presence and distribution patterns of all the species defining the biohorizons reported in Table 4 have been checked. Some of the late Miocene biohorizons (the FOs of *Discoaster hamatus* [base

**Table 2. Summary of biostratigraphic use, biochronology, occurrence in Leg 167 material, and reliability of Pleistocene (0–1.80 Ma) calcareous nannofossil biohorizons.**

Code	Biohorizon	Previous use	Previous biochronology	Occurrence in sites	Reliability and biochronology in the study area
P8	<i>P. lacunosa</i> LO	Definition of the bottom of Zone NN20 and Subzone CN14b	Late MIS 12, at an age of 0.46 Ma (2)	1010, 1011, 1012, 1013, 1014, 1016, 1017, 1018, 1019, 1020, 1021B	Good; calibrated to middle part of C1n. Most probably synchronous with previous evaluation
P7	<i>R. asanoi</i> LO	Proposed first as useful event in the Pleistocene by (6) and proved useful on global scale (7)	MIS 22 (7), at an age of 0.88 Ma (9)	1014	Not sufficiently tested; at Site 1014 calibrated in middle part of C1r; age = 0.88 Ma
P6	<i>Gephyrocapsa</i> sp.3 FO = <i>Gephyrocapsa</i> spp. C-D FO (2) = medium <i>Gephyrocapsa</i> spp. re-entrance (4)	Proposed as useful event in the Mediterranean early Pleistocene (4) and proved useful on global scale although diachronous in different water masses (7, 8). Most probably corresponds to the <i>G. oceanica</i> FO of Bukry (1973), and hence, defines the base of CN14	Diachronous. MIS 27, at an age of 1.00 Ma (10); MIS 29 (eastern equatorial Pacific), lower part of MIS 25 (Atlantic, mid latitudes) (8)	1010, 1011, 1012, 1013, 1014, 1016, 1017, 1018, 1019, 1020, 1021, 1022	The species is rare and discontinuous; the first rare occurrence was detected at base of C1r.1r (Sites 1010 [0.885 ± 0.115 Ma], 1014 [0.940 ± 0.003 Ma], 1020 [0.975 ± 0.005 Ma], and 1021 [0.995 ± 0.015 Ma]) in agreement with age estimated in mid- to high-
P5	large <i>Gephyrocapsa</i> LO = <i>Gephyrocapsa</i> spp. A-B (2) LO	Proposed first as useful event in the Mediterranean early Pleistocene (4) and proved useful on global scale (8)	MIS 37, at an age of 1.24 Ma (8)	1010, 1012, 1014, 1017, 1018, 1020	Good and apparently synchronous with previous evaluations; calibrated to the upper part of C1r.2r (Sites 1010 (1.34 ± 0.05 Ma) and 1020 (1.232 ± 0.002 Ma)
P4	<i>H. sellii</i> LO	First proposed by (3) as useful early Pleistocene event, it has been shown to be time transgressive (5, 7, 8)	Diachronous. MIS 37/38 transition, at an age of 1.25 Ma; MIS 49 (eastern equatorial Pacific) (8)	1011, 1012, 1016, 1017, 1018, 1022	Not reliable; the species is rare and discontinuous
P3	large <i>Gephyrocapsa</i> FO = <i>Gephyrocapsa</i> spp. A-B > 5.5 (2) FO	Proposed first as useful event in the Mediterranean early Pleistocene (4) and proved useful on global scale, although diachronous in different water masses (7, 8)	Diachronous. MIS 55/56 transition, at an age of 1.58 Ma (11); MIS 48 (eastern equatorial Pacific) (8)	1010, 1012, 1013, 1014, 1017, 1018, 1020	Fairly good; calibrated to the lower part of C1r.2r at an age of 1.46 ± 0.06 Ma (Site 1010)
P2	<i>G. oceanica</i> s.l. FO = medium <i>Gephyrocapsa</i> FO (4) = <i>Gephyrocapsa</i> A-B FO (2)	First proposed by (1) as useful early Pleistocene event, proved useful on global scale and isochronous (7, 8)	MIS 59/60 transition, at an age of 1.69 Ma (8)	1010, 1011, 1012, 1013, 1014, 1016, 1018, 1020, 1021, 1022	Fairly good; calibrated to the lower part of C1r.2r (Sites 1010 [1.635 ± 0.115 Ma] and 1021 [1.765 ± 0.045 Ma])
P1	<i>C. macintyreii</i> LO	First proposed by (3) as earliest Pleistocene event, it has been show to be time transgressive (7, 8)	Diachronous. MIS 57/58 transition, at an age of 1.67 Ma; MIS 55 (western equatorial Atlantic) (8)	1010, 1011, 1012, 1013, 1014, 1016, 1020, 1021, 1022	Not reliable; it occurs consistently just below or with <i>G. oceanica</i> s.l. FO. Calibrated to the base of C2n (Site 1021 [1.915 ± 0.015 Ma]) or in the lower part of C1r.2r (Site 1010 [1.635 ± 0.115 Ma])

Notes: MIS = marine isotopic stage. FO = first occurrence, LO = last occurrence. Underline = site with magnetostratigraphy, bold = reference site. References: (1) = Boudreaux and Hay in Hay et al., 1967; (2) = Thierstein et al., 1977; (3) = Gartner, 1977; (4) = Rio, 1982; (5) = Backman and Shackleton, 1983; (6) = Takayma and Sato, 1987; (7) = Wei, 1993; (8) = Raffi et al., 1993; (9) = Bassinot et al., 1994; (10) = I. Raffi (unpubl. data); (11) = L.J. Lourens et al. (unpubl. data).

**Table 3. Summary of biostratigraphic use, biochronology, occurrence in Leg 167 material, and reliability of Pliocene (1.80–5.33 Ma) calcareous nannofossil biohorizons.**

Code	Biohorizon	Previous use	Previous biochronology	Occurrence in sites	Reliability and biochronology in the study area
PI16	<i>D. brouweri</i> <i>D. triradiatus</i> LOs	Definition of the bottom of Zones NN19 and CN13	MIS 71/72 transition (11), in the lowermost of Olduvai (C2n), at an age of 1.95/1.97 Ma (11)	1010, 1011B, 1012, 1013, 1014, 1016, 1018, 1020, 1021, 1022	Calibrated at the bottom of C2n at Sites 1010 (1.935 ± 0.055 Ma) and 1021 (1.955 ± 0.1 Ma). At Site 1020 (California current), it occurs together with <i>D. pentaradiatus</i> and <i>D. surculus</i> . Diachronous, reliable only regionally.
PI15	<i>D. triradiatus</i> AB	Evidenced by (5) as useful event	MIS 82 (11); in lowermost reversed Matuyama (C2r), at an age of 2.15 Ma (11)	1010, 1012, 1014	Poorly reliable; present in low-latitude sites and calibrated at Site 1010 in the upper part of C2r (2.29 ± 0.1 Ma). Missing in mid- to high-latitude sites.
PI14	<i>D. pentaradiatus</i> LO	Definition of the bottom of Zone NN18 and Subzone CN12d	Upper part MIS 100 (12); strongly diachronous (MIS 87-100) for (10); close to the Matuyama/Gauss boundary (C2r/C2An), at an age of 2.52 Ma (12)	1010, 1011, 1012, 1013, 1014, 1016, 1018, 1020, 1021, 1022	Fairly good, notwithstanding the species is rare and discontinuous; calibrated at the bottom of C2r.2r (Sites 1010 [2.44 ± 0.05 Ma] and 1021 [2.51 Ma]).
PI13	<i>D. surculus</i> LO	Definition of the bottom of Zone NN17 and Subzone CN12c	Apparently synchronous and associated with MIS 98-100 (10) in the lowermost Matuyama Chron (C2r.2r), at an age of 2.53 Ma (10) (12)	1010, 1011, 1012, 1013, 1014, 1016, 1018, 1020, 1021, 1022	Good and synchronous with previous evaluations. It occurs at Site 1010 in the lowermost C2r.2r (2.54 ± 0.05 Ma) and at Site 1021 (2.55 ± 0.04 Ma).
PI12	<i>D. tamalis</i> LO	Definition of the bottom of Subzone CN12b	Apparently synchronous over wide latitudes and associated with MIS G10/11 transition (12) in the mid part of Chron C2An.1n, at an age of 2.83 Ma (12)	1010, 1011, 1012, 1013, 1014, 1016, 1018, 1020, 1021, 1022	Fairly good, occurring in lower part of C2An.1n, at an age of 2.97 Ma, at Sites 1010 and 1021.
PI11	<i>Sphenolithus</i> spp. LO	Proposed as definition of the bottom of Subzone CN12aB (8)	Near the base of Gauss (C2An.3n) (13), at an age of 3.66 Ma (14)	1021B	The marker is rare to absent in its final range.
PI10	<i>D. pentaradiatus</i> PE	First proposed by (6) as useful subzonal boundary in the Mediterranean.	Close to the base of the Gauss Chron (C2An.3n) in the Mediterranean (15), at an age 3.61 of Ma (16)	1010, 1011, 1012, 1014, 1016, 1020, 1021	Useful in the area and occurring at Site 1010 at the base of C2An.3n (3.55 ± 0.05 Ma) and at Site 1021 (3.57 ± 0.02 Ma).
PI9	<i>R. pseudumbilicus</i> LO	Definition of the bottom of Subzone CN12a	In uppermost part of C2Ar (13), at an age of 3.82 Ma (14)	1011, 1012, 1014, 1016, 1020, 1021	Apparently good and synchronous occurring in the upper part of C2Ar at an age of 3.83 ± 0.03 Ma (Site 1021).
PI8	<i>A. delicatus</i> LO	Definition of the bottom of Subzone CN11a (2)		1011, 1012, 1014, 1016, 1020, 1021	Apparently good and synchronous, in the study area, occurring in the lower part of C2Ar at an age of 3.96 ± 0.03 Ma (Site 1021).
PI7	<i>D. pentaradiatus</i> PB	First evidenced by (3) as useful event in the Mediterranean.	In lower part of C2Ar in the Mediterranean (9), at an age of 3.93 Ma (16)	1011, 1014, 1016, 1020, 1021	Fairly good; calibrated within C2Ar at an age of 4.055 ± 0.065 Ma (Site 1021).
PI6	<i>P. lacunosa</i> FCO	Used as alternative event to recognize the base of Subzone CN12a (1, 7)		1011, 1014, 1016, 1020, 1021	Moderately reliable as FCO. Calibrated within C2Ar at an age of 3.96 ± 0.03 Ma (Site 1021).
PI5	<i>D. asymmetricus</i> FCO	Definition of the bottom of Subzone CN11b	Age 4.12 Ma (16), near the top of Cochiti (oceanic area); in upper Gilbert (Mediterranean) (13)	1011, 1014, 1016, 1020, 1021	Moderately reliable as FCO. Calibrated within C2Ar at an age of 3.925 ± 0.065 Ma (Site 1021).
PI4	<i>H. sellii</i> FO	Proposed as useful event in the Mediterranean (7)		1021B	Not reliable: the species is rare and discontinuous. Calibrated within C2Ar at an age of 4.15 ± 0.03 Ma (Site 1021).
PI3	<i>A. primus</i> LO	Definition of the bottom of Subzone CN11a	Near the top of Sidufjal (oceanic area); within Nunivak Subchron (Mediterranean) (13)	1011, 1014, 1016, 1021	Poorly reliable, most probably for taxonomic problems. Calibrated at Site 1021 at the base of C3n.1n.
PI2	<i>C. rugosus</i> FO	Definition of the bottom of Subzone CN10c	Within Thvera Subchron (C3n.4n), at an age of 5.089/5.23 Ma (12) (17)	1014, 1010, 1021B	Not reliable; the genus is underrepresented.
PI1	<i>T. rugosus</i> LO	Definition of the bottom of Subzone CN10b	At the base of Thvera (C3n.4n), at an age of 5.23 Ma (17)	1010, 1021	Poorly reliable; present at low-latitude Site 1010 and associated with C3r as last rare occurrence at an age of 4.995 ± 0.055 Ma, associated with Zone CN9a in high-latitude Site 1021B.

Notes: MIS = marine isotopic stage. FO = first occurrence, LO = last occurrence, FCO = first common and continuous occurrence. AB = acme beginning, PB = paraecme beginning, PE = paraecme end. Underline = site with magnetostratigraphy, bold = reference site. References: (1) = Wise, 1973; (2) = Bukry, 1981; (3) = Driever, 1981; (4) = Rio, 1982; (5) = Backman and Shackleton, 1983; (6) = Driever, 1988; (7) = Rio, Raffi, et al. 1990; (8) = Bukry, 1991; (9) = Rio et al., 1991; (10) = Wei, 1993; (11) = Raffi et al., 1993; (12) = Tiedeman et al., 1994; (13) = Berggren, Hilgen, et al., 1995; (14) = Shackleton et al., 1995; (15) = Cita et al., 1996; (16) = Lourens et al., 1996; (17) = Backman and Raffi, 1997.

**Table 4. Summary of biostratigraphic use, biochronology, occurrence in Leg 167 material, and reliability of late Miocene (5.33–11.20 Ma) calcareous nannofossil biohorizons.**

Code	Biohorizon	Previous use	Previous biochronology	Occurrence in sites	Reliability and biochronology in the study area
LM20	<i>C. acutus</i> FO	Definition of the bottom of Subzone CN10b	Within C3r, at an age of 5.37 Ma (7)	1010, 1011, 1014, 1016, 1021	Not reliable; the genus is underrepresented. Calibrated to C2Ar in Site 1010 and to the base of C2An.3n in Hole 1021B.
LM19	<i>D. quinquerramus</i> LO	Definition of the bottom of Subzone CN10a	Repeatedly calibrated in low to mid latitude to the mid C3r (4) at an age of 5.54 Ma (7)	1010, 1011, 1014, 1016, 1021	The marker is rare and discontinuous. At low-latitude Site 1010 it has been associated with mid C3r at an age of $5.55 \pm 0.05$ Ma, in agreement with previous evaluations.
LM18	<i>N. amplificus</i> LO	Proposed as definition of the bottom of Subzone CN9bC (5)	Associated with the top of C3An (4), at an age of 5.99 Ma (7)	Undetected	
LM17	<i>N. amplificus</i> FO	Proposed as definition of the bottom of Subzone CN9bB (5)	Associated with the base of C3An (4), at an age of 6.84 Ma (7)	Undetected	
LM16	<i>R. pseudoumbilicus</i> PE	Used as useful event in Subzone CN9b (4)	Associated with the lower part of C3Ar (4), at an age of 7.1 Ma (7)	1010, 1011, 1014, 1021?	Fairly reliable; calibrated to C3Ar at low-latitude Site 1010 at an age of $7.11 \pm 0.01$ Ma, in agreement with previous evaluations.
LM15	<i>A. primus</i> FO	Definition of the bottom of Subzone CN9b	Associated with C3Br.2r (4), at an age of 7.39 Ma (7)	1010, 1011, 1021	Apparently reliable; see text.
LM14	<i>M. convallis</i> LO	Event in Subzone CN9a (4)	Associated with C4n.2n (equatorial Pacific) (4), at an age of 7.8 Ma (6)	1010, 1011	Regionally fairly good
LM13	<i>D. berggrenii</i> FO	Definition of the bottom of Subzone CN9a	Associated with lowermost C4r (4), at an age of 8.28 Ma (7)	1010, 1011, 1021?	Poor reliable; the marker is rare and discontinuous in the mid latitude Site 1021B.
LM12	<i>D. loeblichii</i> FO	Definition of the bottom of Subzone CN9a	Associated with lower part of C4r (4), at an age of 8.43 Ma (5)		Not reliable; the marker is very rare and discontinuous.
LM11	<i>D. neorectus</i> FO	Definition of the bottom of Subzone CN9a		Undetected	
LM10	<i>R. pseudoumbilicus</i> PB	Definition of the bottom of Subzone CN8b	Associated with upper part of C4An (4), at an age of 8.78 Ma (7)	1010, 1011, 1021	Moderately reliable, even if the marker is near barren intervals.
LM9	<i>M. convallis</i> FO	Used as alternative event to define the bottom of Zone CN8 (1)	Associated with the top of C5n for (3) and with C4Ar.2r for (4), at an age of 9.3/9.5 Ma (6)	1010, 1021	Regionally fairly reliable
LM8	<i>D. hamatus</i> LO	Definition of the bottom of Zone CN8	Age 9.63 Ma (7), calibrated in low latitude to C4Ar.2r (4), in mid to high latitude in C4Ar.2 (2) and C5n/C4Ar (3)	1010	Poorly reliable; the marker is absent in the mid-latitude Site 1021B.
LM7	<i>C. calyculus</i> LO	Useful event near the top of Zone CN7	Associated with the bottom of C4Ar, at an age of 9.694 Ma (7)	1010, 1021	Fairly reliable
LM6	<i>C. coalitus</i> LO	Useful event near the top of Zone CN7	Associated with the top of C5n, at an age of 9.67 Ma (7)	1010, 1021	Moderately reliable; the marker is rare and discontinuous.
LM5	<i>D. hamatus</i> FO	Definition of the bottom of Zone CN7	Repeatedly calibrated in low to mid latitude to the mid Cn.2n (4) at an age of 10.47 Ma (7)	1010	Undetected
LM4	<i>C. calyculus</i> FO	Definition of the bottom of Subzone CN7b	Associated with C5n.2n (6), at an age of 10.7 Ma (7)	1010	Undetected
LM3	<i>C. miopelagicus</i> LCO	Useful event in Zone CN6 (4)	Associated with the base of C5n.2n (4) at an age of 10.941 Ma (7)	1010, 1021	Undetected
LM2	<i>D. bellus</i> FO	Useful event to approximate the bottom of Zone CN7	Associated with lower part of C5n.2n (4)	1010, 1021	Undetected
LM1	<i>C. coalitus</i> FO	Definition of the bottom of Zone CN6	Repeatedly calibrated in low latitude to lowermost C5n.2n (4) at an age of 10.79 Ma (7)	1010	Undetected

Notes: FO = first occurrence, LO = last occurrence, LCO = last common and continuous occurrence. PB = paracme beginning, PE = paracme end. Underline = site with magnetostratigraphy, bold = reference site. References: (1) = Rio, Fornaciari, et al., 1990; (2) = Olafsson, 1991, (3) = Gartner, 1992; (4) = Raffi et al., 1995; (5) = Raffi and Flores, 1995; (6) = Berggren, Kent, et al., 1995; (7) = Backman and Raffi, 1997.

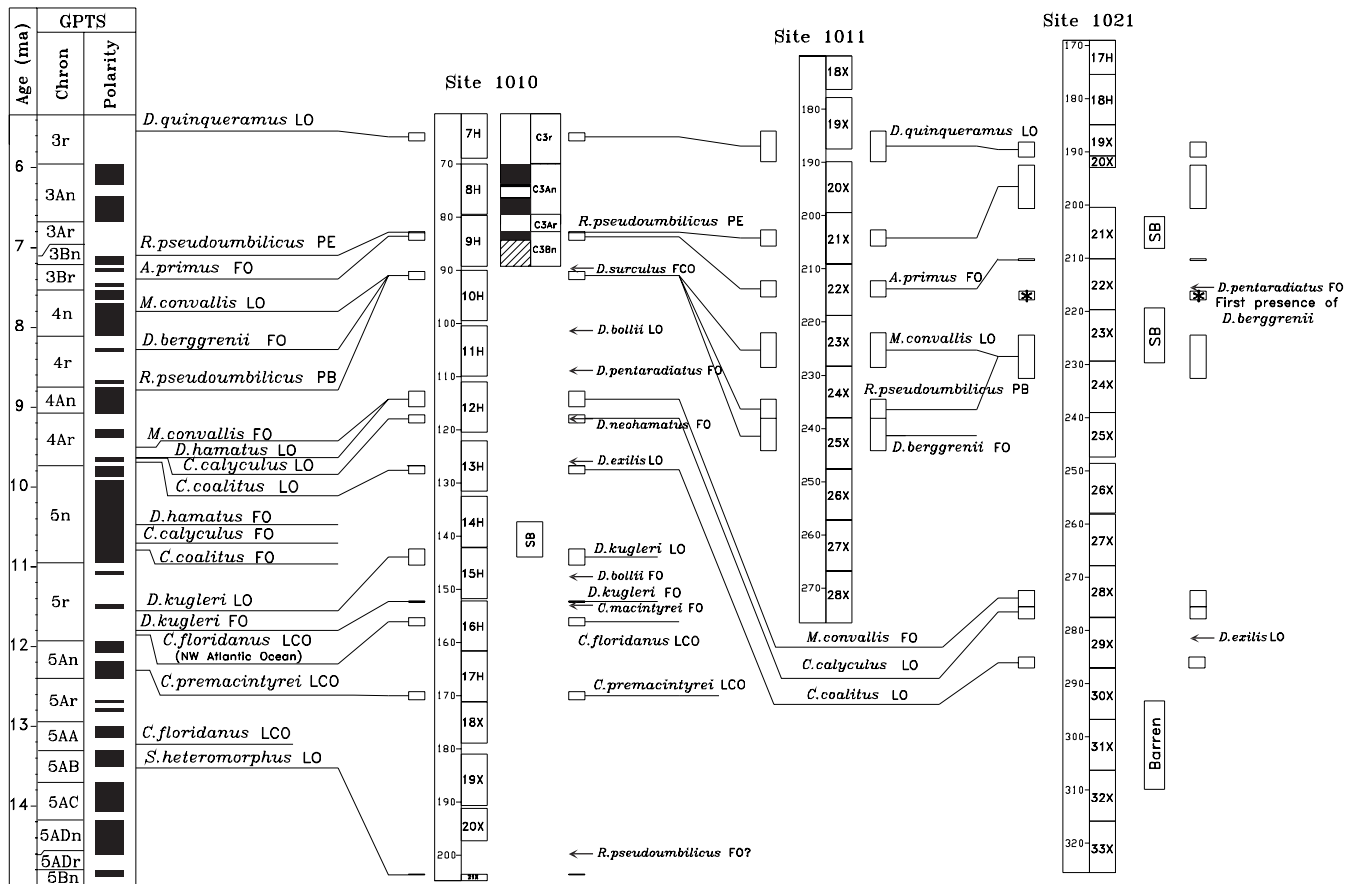


Figure 26. Summary of middle Miocene through late Miocene biostratigraphic correlation from three representative sites from Leg 167. Magnetic polarity time scale after Cande and Kent (1995). Magnetostratigraphies from A. Hayashida et al. (unpubl. data) and C. Richter (unpubl. data).

of CN7], *Catinaster calyculus*, *Catinaster coalitus* [base of CN6], *Discoaster bellus*, and the LCO of *Coccolithus miopelagicus*) fall in barren intervals at both Sites 1010 and 1021, and, hence, their reliability cannot be evaluated. Also, some biohorizons (FOs of *Discoaster loeblichii* and *Discoaster neorectus*, defining the base of Subzone CN8b) are based on species that are missing in the area. The remaining biohorizons are discussed below.

**Biohorizons Based on Discoasterids**

Discoasterids are generally rare to scarce in the late Miocene sediments of the California margin, even at low-latitude Site 1010, where, nevertheless, they are better represented (compare Sites 1010 [Figs. 5, 6] and 1021 [Figs. 19, 20]). This finding is not unexpected because the area was affected by high-productivity conditions that are unfavorable for discoasterids that thrive better in oligotrophic water masses (Chepstow-Lusty et al., 1989, 1991, 1992; Chepstow-Lusty and Chapman, 1995).

As already mentioned, some of the species used by Okada and Bukry (1980) in their zonation are missing or very rare. In particular, the standard zonation marker species *D. hamatus* (Figs. 4, 5), *D. berggrenii*, and *Discoaster quinquaramus* (Figs. 4, 5, 11, 18, 20) are too rare for allowing the recognition of the LO of *D. hamatus* (Zone CN8 base) and the FO of *D. berggrenii* (Zone CN9 base). However, it is worth mentioning that, when determined, their position is often comparable to that known in other oceanic areas (Fig. 26). In particular, note how the FO of *D. berggrenii* at Sites 1010 (Figs. 4, 5) and 1021 (Figs. 20, 21) is associated with the interval of absence of *R. pseudoumbilicus* as is seen in the equatorial Pacific Ocean (Raffi et

al., 1995). Likewise, the LO of *D. hamatus* at low-latitude Site 1010 (Figs. 4, 5) occurs close to the FO of *M. convallis* as suggested by Rio, Fornaciari, et al. (1990) for the tropical Indian Ocean.

The only discoasterid biohorizon used in the zonation of Okada and Bukry (1980) that could be retained as moderately useful in the studied area is the LO of *D. quinquaramus* (Zone CN10 base). This event has been detected at Sites 1010 (Figs. 4, 5), 1011 (Fig. 7), 1014 (Figs. 10, 11), and 1021 (Figs. 18, 20). At low-latitude Site 1010, this biohorizon is associated with the middle part of Chron 3r, at an interpolated age of  $5.55 \pm 0.05$  Ma (Fig. 22; Table 4), which compares well with previous evaluations (Gartner et al., 1984; Monechi, 1985; Bleil, 1985; Muza et al., 1987; Berggren, Kent, et al., 1995; Raffi et al., 1995; Backman and Raffi, 1997; Table 4). However, if the reliability of the LO of *D. quinquaramus* at low latitudes is confirmed by direct comparison with magnetostratigraphy, not very much can be said about the reliability of this biohorizon at middle latitudes, where the species is very rare. It can be noted, however, that it occurs in the same relative biostratigraphic position (ranking) observed in low-latitude areas (Fig. 26).

The distribution patterns of the following discoasterids, sometimes used for defining supplementary biohorizons or useful for recognizing biostratigraphic intervals, have been monitored: *Discoaster surculus* (Figs. 6, 20), *Discoaster pentaradiatus* (Figs. 6, 20), *Discoaster bollii* (Fig. 6), and *Discoaster neohamatus* (Fig. 6).

The FO of *Discoaster surculus* was used as a secondary marker for the base of Zone CN9 by Bukry (1975a) and the FCO of the species was considered a useful event within the lower part of Zone CN9 by Raffi et al. (1995). In the California margin area, *Discoaster surculus* is consistently represented only at low-latitude Site 1010,

where its FCO datum occurs in the same stratigraphic position proposed by Raffi et al. (1995; Fig. 26).

The FO of *D. pentaradiatus* was associated with Zone CN8 by Bukry (1973) and Raffi et al. (1995), although rare occurrences of the species were observed within Zone CN7 in the tropical Indian Ocean (Raffi et al., 1995). In the California margin *D. pentaradiatus* is rare and scattered in its initial range, and therefore its FO is difficult to pinpoint. At Site 1010 (low latitude; Fig. 6), this event is recorded in the lower part of Zone CN8, which is the same location as in the equatorial Pacific Ocean. However, at Site 1021 (middle latitude; Fig. 20) the first *D. pentaradiatus* has been detected only within the lower part of Subzone CN9a.

The LO of *D. bollii* was considered as occurring close to the LO of *D. hamatus* (CN7/CN8 boundary; Gartner, 1992; Raffi et al., 1995). In the California margin, *D. bollii* has been observed only at low-latitude Site 1010 (Fig. 6), where it becomes extinct in the same stratigraphic position indicated by previous authors.

The FO of *Discoaster neohamatus* was recorded within Zone CN7 (Bukry, 1973; Gartner, 1992) and was considered to be diachronous within this zonal interval (Raffi et al., 1995). In the California margin in agreement with Bukry (1981), the presence of *D. neohamatus* has been detected only at low-latitude Site 1010 (Fig. 6), where its FO datum occurs apparently in the same stratigraphic position (terminal part of Zone CN7) as observed in the equatorial Pacific Ocean by Raffi et al. (1995).

#### Biohorizons Based on *Catinaster* spp.

The species *Catinaster calyculus* and *Catinaster coalitus* are stratigraphically important in the lower part of the late Miocene (Fig. 2). Specifically, the FO of *C. coalitus* is the original definition of the bottom of Zone CN6. The FO of *C. calyculus* was used to define the bottom of Subzone CN7b (Fig. 2). In addition, Bukry (1973) suggested that the LOs of *C. calyculus* and *C. coalitus* occur above the LO of *D. hamatus* (Zone CN8 base). However, there are contrasting opinions among various authors about the distribution of *Catinaster* spp. probably because the species of the group seem to be affected by ecological factors that are not fully understood yet. In fact, Rio, Fornaciari, et al. (1990) found the FO of *C. calyculus* within Zone CN6. Raffi et al. (1995) observed that in both the equatorial Indian Ocean and the Pacific Ocean the LOs of *C. calyculus* and *C. coalitus* are in the lower and upper part of Zone CN7, respectively. In the California margin, the genus *Catinaster* is well represented both at low and middle latitudes (Figs. 6, 18, 20), but whereas *C. calyculus* is common, *C. coalitus* is few to rare.

As already mentioned, the FOs of *C. coalitus* and *C. calyculus* have not been detected because they occur in a barren interval at both Sites 1010 and 1021 (Figs. 6, 20). The LO of *C. calyculus* occurs close to the FO of *M. convallis*, whereas the LO of *C. coalitus* occurs in the middle part of Zone CN7 (Site 1010, Figs. 4, 6; Site 1021, Figs. 18, 20). These results are in agreement with the data of Raffi et al. (1995) and suggest that both events may be considered useful and provide good correlations between the low-latitude Site 1010 and mid-latitude Site 1021 (Fig. 26).

#### Biohorizons Based on *Ceratoliths*

The appearance and rapid evolution of horseshoe-shaped nannoliths (ceratoliths) in the upper part of the late Miocene provide biohorizons that allow us to finely subdivide this time interval. The zonation of Okada and Bukry (1980) utilized the FO of *Amaurolithus primus* as the boundary definition of the base of Subzone CN9b. Recently, Raffi and Flores (1995) subdivided Subzone CN9b of Okada and Bukry (1980) into three intervals on the base of the total range of *Nicklithus amplificus*. Ceratoliths are well represented in the area (Figs 5, 6, 10, 11, 18, 19, 20), but only the species *A. primus* and *A. delicatus* have been recognized. Specifically, *N. amplificus* is miss-

ing; therefore the subdivision of Subzone CN9b proposed by Raffi and Flores (1995) cannot be applied in the area.

*A. delicatus* is thought to appear slightly above the FO of *A. primus* (Gartner and Bukry, 1975; Rio, Fornaciari, et al., 1990; Hodell et al., 1994; Raffi and Flores, 1995; Raffi et al., 1995; Benson and Rakic-El Bied, 1996), and a high-resolution sampling together with a high sedimentation rate is needed to recognize this spacing. The simultaneous FOs of both species have been recognized at Sites 1010 (Fig. 6) and 1021 (Fig. 20). At Site 1010, the FOs of *A. primus* and *A. delicatus* are associated with Chron 3Br/3Br at an interpolated age of  $7.23 \pm 0.11$  Ma (Fig. 22). This result is in fairly good agreement with previous evaluations by Raffi et al. (1995) and Berggren, Kent, et al. (1995) who recorded the *A. primus* FO in Chron 3Br. Backman and Raffi (1997) estimated an age of 7.39 Ma on the base of astrocyctostratigraphy. The FO of *Amaurolithus* spp. in the California margin area has been considered a useful event.

#### Absence Interval (Paracme) of *Reticulofenestra pseudumbilicus*

In both the equatorial Indian Ocean and the Pacific Ocean many authors recorded an interval of almost total absence of *R. pseudumbilicus* (specimens  $>7 \mu\text{m}$ ) (Rio, Fornaciari, et al., 1990; Gartner, 1992; Takayama, 1993; Raffi and Flores, 1995; Backman and Raffi, 1997). In the California margin a similar interval of absence (paracme) has been detected in the same stratigraphic position. The end of this interval of absence (PE) is associated with the lower part of Chron 3Ar (Raffi et al., 1995) at an age of 7.1 Ma (Backman and Raffi, 1997; Table 4), whereas its beginning (PB) is calibrated within the upper part of Chron 4An (Raffi et al., 1995) at an age of 8.78 Ma (Backman and Raffi, 1997; Table 4). In the California margin these two biohorizons have been detected at Sites 1010 (Figs. 4, 6) and 1011 (Fig. 7). At Sites 1014 and 1021 only the PE of *R. pseudumbilicus* is present (Figs. 10, 11, 18, 20). At low latitudes (Site 1010) the PE of *R. pseudumbilicus* occurs within Chron 3Ar at an estimated age of  $7.11 \pm 0.01$  Ma (Fig. 22; Table 4), in agreement with previous evaluations. No magnetostratigraphic data were available to calibrate the PB of *R. pseudumbilicus*, which seems to occur close to a suspected hiatus at Site 1010 (Figs. 4, 6) and close to barren intervals at Site 1021 (Figs. 18, 20). This event is close to the *Minylitha convallis* LO and is below or associated with the *D. quinqueramus/berggrenii* FO (Site 1010, Figs. 4, 6; Site 1021, Figs. 18, 20). At Site 1011 (Fig. 7) the PB of *R. pseudumbilicus* is just above the *D. quinqueramus/berggrenii* FO, a discrepancy that can be explained by both the low sampling resolution (Table 1) and the discontinuous occurrence of *D. quinqueramus/berggrenii*. The PE is apparently reliable in the studied area, whereas it is not possible to make firm inference about the PB of this species. The PE and PB of *R. pseudumbilicus* have been used to define the base of Subzone CN9bB and the base of Zone \*CN8b (emended) respectively. In fact, despite the problems linked to the environmental characteristics of the study area, this event is more recognizable and correlatable even outside this region than the biohorizons utilized in the original definition of Okada and Bukry (1980; Fig. 2).

#### LO and FO of *Minylitha convallis*

Bukry (1973) noted the appearance of *M. convallis* within Subzone CN8a. In the studied area, *M. convallis* is common to abundant (Sites 1010, Fig. 6; 1021, Fig. 20) and in a few samples is dominant. The LO of *M. convallis* is associated with Chron 4n.2n in the equatorial Pacific Ocean (Raffi et al., 1995) at an age of 7.8 Ma (Berggren, Kent, et al., 1995), whereas at mid-latitudes Gartner (1992) detected this event in the upper part of Chron 4n. The FO of *M. convallis* occurs in Chron 4Ar.2r in the equatorial Pacific Ocean (Raffi et al., 1995) at an age of 9.3/9.5 Ma (Berggren, Kent, et al., 1995) close to the LOs of *Discoaster hamatus* and *Catinaster calyculus*. Gartner (1992) observed the FO of *M. convallis* in Chron C5n at mid-latitude

Site 608. During Leg 167, it was not possible to calibrate these biohorizons with the magnetostratigraphy. The LO of *M. convallis* has been recorded close to the *D. quinqueramus/berggrenii* FO (Sites 1010, Fig. 4; 1011, Fig. 7; and 1021, Fig. 18) in a stratigraphic position older than previous evaluations. The FO of *M. convallis* occurs above the *C. calyculus* LO (Site 1010, Fig. 4; Site 1011, Fig. 7; and Site 1021, Fig. 18), just above the LO of *D. hamatus* (Site 1010, Fig. 4). Regionally, these two events seem to be useful and fairly reliable.

### Biostratigraphic Remarks

The previous discussion shows how Subzone CN9b is the only biostratigraphic interval of the scheme of Okada and Bukry (1980) that is recognized with a moderate confidence in the California margin. All other biozones and subzones have been difficult to detect, even at the low-latitude Site 1010. The recognition of the recently proposed three-fold subdivision of Subzone CN9b by Raffi and Flores (1995) was also not possible because of the ecological exclusion of *N. amplificus* from the area. The correlation and, hence, the biostratigraphic classification of late Miocene sediments in this area are better achieved by utilizing the following biohorizons recently proposed in the literature:

- PE of *R. pseudoubilicus* (lower part of Subzone CN9b)
- LO of *M. convallis* (lower part of Subzone CN9a)
- PB of *R. pseudoubilicus* (upper part of Zone CN8)
- FO of *M. convallis* (Zone CN8/CN7 boundary)

Because of these results, the original definitions of the biostratigraphic intervals of Okada and Bukry (1980) have been "adjusted" (as marked by an asterisk [\*]) and are outlined below.

- \*CN6+CN7: from the FO of *Catinaster* spp. to the FO of *M. convallis*
- \*CN8a: from the FO of *M. convallis* to the PB of *R. pseudoubilicus*
- \*CN8b: from the PB of *R. pseudoubilicus* to the LO of *M. convallis*
- \*CN9a: from the LO of *M. convallis* to the FO of *Amaurolithus* spp.
- \*CN9bA: from the FO of *Amaurolithus* spp. to the PE of *R. pseudoubilicus*
- \*CN9bB: from the PE of *R. pseudoubilicus* to the LO of *D. quinqueramus*

The scheme proposed above is not intended to have any general value and must be considered as very preliminary for the California margin itself, because it is based only on a limited number of successions.

### Middle Miocene

The oldest sediments recovered at Sites 1010 and 1021 during Leg 167 are advanced middle Miocene in age. Specifically, the base of the Site 1010 succession belongs to the middle Miocene Zone CN4 (Langhian; Fig. 2), and the base of the succession recovered at Site 1021 belongs to Zone CN5 (Serravallian; Fig. 2). Both sites have been studied at low resolution and are affected by barren intervals (Fig. 3). In the fossiliferous intervals, the assemblages are in a moderate to good state of preservation. However, no magnetostratigraphy is available, and, hence, the evaluation of the biostratigraphic reliability of the relevant biohorizons is very tentative.

At low-latitude Site 1010 the scheme of Okada and Bukry (1980) has been easily recognized because the marker species (*S. heteromorphus* and *D. kugleri*) are well represented (Figs. 4, 6). It should be noted that *D. kugleri* is present as common and continuous in a short interval and its FO and LO probably correspond to the FCO and LCO

observed by Raffi et al. (1995) in the eastern equatorial Pacific Ocean.

Because both Zones CN4 and CN5 have a fairly long duration (Fig. 2), attempts have been made in the past to define additional biohorizons, most of which are listed in Table 5 (Bukry, 1973; Ellis, 1982; Gartner and Chow, 1985; Theodoridis, 1984; Olafsson, 1989, 1991; Fornaciari et al., 1990, 1993; Gartner, 1992; Fornaciari et al., 1996). These additional events include the LO of *Discoaster kugleri*, LO of *Discoaster exilis*, FO of *Discoaster bollii*, FO of *Calcidiscus macintyreii*, LCO of *Calcidiscus premacintyreii*, and LCO of *Cyclargolithus floridanus*.

The species defining these biohorizons are all well represented at low-latitude Site 1010 and all the biohorizons they define have been recognized in the same relative position (ranking) observed in previous studies (Table 5) except for the LO of *D. exilis*. The latter occurs apparently well within Zone CN7, whereas previous authors recorded it either in the upper part of Zone CN6 (Bukry, 1973; Rio, Fornaciari, et al., 1990; Raffi et al., 1995) or at the base of Zone CN7 (Raffi et al., 1995). It is to be noted that at mid-latitude Site 1021, *D. exilis* is less abundant and discontinuously distributed (Fig. 20). It is, therefore, clear that it is not possible to make firm inferences about the reliability of these biohorizons on the basis of the available single succession.

### SUMMARY AND CONCLUSIONS

In this paper the calcareous nannofossils biostratigraphy of middle Miocene to Pleistocene sediments recovered in the California margin during Leg 167 has been presented. The area covers a large latitudinal transect and is characterized by strongly variable paleobiogeographic conditions during this time interval that make it difficult to recognize most of the biostratigraphic intervals of the standard zonations of Martini (1971) and Okada and Bukry (1980), as pointed out before by Wise (1973) and Bukry (1981). To recover a biostratigraphic resolution and detailed intersite correlations, the regional reliability of 50 biohorizons were checked by considering their mode of occurrence, ranking, and spacing.

For the Pleistocene interval, the following six reliable biohorizons have been identified: LO of *P. lacunosa*, FO of *Gephyrocapsa* sp. 3, LO and FO of large *Gephyrocapsa*, FO of *G. oceanica* s.l., and LO of *R. asanoi*. The AE of small *Gephyrocapsa* spp. and the LOs of *H. sellii* and *C. macintyreii* do not seem to be reliable in the studied area. For the Pliocene interval, the following nine reliable biohorizons have been identified: LO of *D. pentaradiatus*, LO of *D. surculus*, LO of *D. tamalis*, LO and FCO of *D. asymmetricus*, PB and PE of *D. pentaradiatus*, LO of *R. pseudoubilicus*, and LO of *A. delicatus*. The LOs of *Discoaster brouweri* and *D. triradiatus* and the FCO of *P. lacunosa* seem to be moderately reliable. The AB of *Discoaster triradiatus*, the LO of *Sphenolithus* spp., the FO of *H. sellii*, the LO of *A. primus*, the FOs of *C. rugosus* and *C. acutus*, and the LO of *T. rugosus* do not seem to be reliable in the studied area.

At the transition between the early Pliocene (Zanclean) and mid-Pliocene (Piacenzian) a set of biohorizons were detected (*H. sellii* FO, *P. lacunosa* FCO, *D. pentaradiatus* PB, *A. delicatus* LO, and *D. pentaradiatus* PB) showing the same relative order and similar ages as those observed in the Mediterranean area. It therefore seems conceivable to infer similar paleoceanographic conditions between the distant California margin and the Mediterranean region during this time interval.

For the late Miocene interval, the following eight reliable biohorizons have been identified: LO of *D. quinqueramus*, PB and PE of *R. pseudoubilicus*, FO of *A. primus*, FO and LO of *M. convallis*, LO of *C. calyculus*, and FO of *Catinaster* spp. The following two biohorizons have been considered unreliable: FO of *D. berggrenii* and LO of *D. hamatus*. The following nine biohorizons are not detected in the study area: FO and LO of *N. amplificus*, FO of *D. loeblichii*, FO of

**Table 5. Summary of biostratigraphic use, biochronology, occurrence in Leg 167 material, and reliability of middle Miocene (11.20–13.52 Ma) calcareous nannofossil biohorizons.**

Code	Biohorizon	Previous use	Previous biochronology	Occurrence in sites	Reliability and biochronology in the study area
MM6	<i>D. kugleri</i> LO	Used as alternative event to define the bottom of Zone CN6	Associated with C5r.2n (6), at an age of 11.55 Ma (8)	1010	Not sufficiently tested; at Hole 1021B the marker is probably in a barren interval.
MM5	<i>D. kugleri</i> FO	Definition of the bottom of Subzone CN5b	Associated with lower part of C5r (6), at an age of 11.79 Ma (8)	1010	Not sufficiently tested; at Hole 1021B the marker is probably in a barren interval.
MM4	<i>C. macintyreii</i> >11 mm FO	Event within Subzone CN5b (2)	Associated with C5An.2n at Site 845 (6), at an age of 12.38 (7)	1010	Probably reliable; at Hole 1021B the marker is near a barren interval.
MM3	<i>C. floridanus</i> LO	Used as alternative event to define the bottom of Subzone CN5b	Age 13.24 Ma (7), associated with C5AAr for (7) and with the lower part of C5r for (3)	1010	Not sufficiently tested; the marker is present only at Site 1010, but apparently its stratigraphic position is similar to in the North Atlantic Ocean.
MM2	<i>C. premacintyreii</i> LO	Useful event to subdivide Zone CN5 (1, 5)	Age 12.22 Ma (7), associated with C5An.2n for (6) and C5An.1n for (5)	1010	Not sufficiently tested; the marker is present only at Site 1010.
MM1	<i>S. heteromorphus</i> LO	Definition of the bottom of Subzone CN5a	Associated with C5ABr (4) (6), at an age of 13.52 Ma (8)	1010	The marker is present only at Site 1010.

Notes: FO = first occurrence; LO = last occurrence. References: (1) = Theodoridis, 1984; (2) = Rio, Fornaciari, et al., 1990; (3) = Olafsson, 1991; (4) = Miller et al, 1991; (5) = Gartner, 1992; (6) = Raffi et al., 1995; (7) = Raffi and Flores, 1995; (8) = Backman and Raffi, 1997.

*D. neorectus*, FO of *D. hamatus*, FO of *C. calyculus*, LCO of *C. miopelagicus*, FO of *D. bellus*, and FO of *C. coalitus*.

Sediments of middle Miocene age have been recovered only at low-latitude Site 1010 and therefore the reliability of the six biohorizons identified (*D. kugleri* FO and LO, *C. macintyreii* FO, *C. floridanus* LCO, *C. premacintyreii* LO, and *S. heteromorphus* LO) cannot be fully evaluated.

As a result of this analysis, a set of biozones for the California margin has been proposed that has been correlated with the GCS and calibrated to the GPTS. This integrated time frame has been used for dating the successions recovered during Leg 167. The biozones proposed for the Pleistocene seem to have a global value and are proposed as an alternative to the standard zonation of Okada and Bukry (1980).

### TAXONOMIC NOTES

The taxonomic concepts are those adopted by Rio, Raffi, et al. (1990), Raffi et al. (1993), and Raffi and Flores (1995). A summary of the most important taxa concepts is reported below.

#### Gephyrocapsids

The taxonomic concepts used for this group are those adopted by Rio, Raffi, et al. (1990) and modified by Raffi et al. (1993). Within geophyrocapsids, three taxa have been considered on the basis of biometric taxonomic entities:

1. gephyrocapsids with sizes  $\leq 4 \mu\text{m}$  labeled "small" *Gephyrocapsa* spp.;
2. gephyrocapsids with sizes between 4 and 5.5  $\mu\text{m}$  with an open central area labeled *Gephyrocapsa oceanica* s.l.; and
3. gephyrocapsids with sizes  $\geq 5.5 \mu\text{m}$  labeled "large" *Gephyrocapsa* spp.

Moreover, two morphospecies have been distinguished: *Gephyrocapsa* sp. 3 following Rio (1982) and Rio, Raffi, et al. (1990) and *G. caribbeanica*, a morphotype with a closed central area.

#### Reticulofenestrads

Within the reticulofenestrads two groups have been considered: the *Reticulofenestra* spp., which includes small-sized ( $< 7 \mu\text{m}$ ) reticulofenestrads such as *Reticulofenestra minuta*, *R. haqii*, *R. minutula*, and *R. pseudoubilicus*, which, following the taxonomic concepts proposed by Raffi and Rio (1979) and Backman and Shackleton (1983), includes morphotypes  $> 7 \mu\text{m}$ .

#### Calcidiscus

Within the genus *Calcidiscus* three species have been distinguished following the taxonomic concepts expressed in Rio, Fornaciari, et al. (1990) and Fornaciari et al. (1990):

1. rounded *Calcidiscus* specimens with sizes  $\geq 11 \mu\text{m}$  labeled *Calcidiscus macintyreii*;
2. rounded *Calcidiscus* specimens with sizes  $\leq 11 \mu\text{m}$  labeled *Calcidiscus leptoporus*; and
3. elliptical *Calcidiscus* specimens labeled *Calcidiscus premacintyreii*.

#### Discoasterids

Discoasterids show a variable distribution and preservation pattern at different sites and stratigraphic intervals.

Pliocene species of *Discoaster* have been identified following Backman and Shackleton (1983).

The following late to middle Miocene five-rayed species of *Discoaster* have been recognized: *D. bellus* group, *D. quinquaramus/berggrenii*, *D. hamatus*, and *Discoaster* sp. 1 sensu Rio, Fornaciari, et al. (1990).

The *Discoaster bellus* group is characterized by five-rayed discoasterids with a small size (6–8  $\mu\text{m}$ ), a poorly developed central area, and by morphotypes with intergraded features between *D. bellus* and *D. hamatus* and between *D. bellus* and *D. berggrenii*. Five long rays with a spine extending and bending sharply near the tip characterize *D. hamatus*. In the California margin this species is present with specimens relatively smaller than average.

*Discoaster berggrenii* and *D. quinquaramus* are two distinct species with a distinct stratigraphic distribution. *D. berggrenii* appears and becomes extinct before *D. quinquaramus*, but because intergraded forms between the end members of these two species make their distinction difficult, they have been lumped together.

*Discoaster* sp. 1 is a small (6–8  $\mu\text{m}$ ) five-rayed *Discoaster* with a poorly developed central area and a very small knob evidenced by Rio, Fornaciari, et al. (1990) in the equatorial Indian Ocean that appears discontinuously within \*CN9a.

The main six-rayed species of *Discoaster* observed during Leg 167 in the late–middle Miocene interval are: *Discoaster variabilis*, *D. exilis*, *D. surculus*, *D. brouweri*, *D. intercalaris*, *D. neohamatus*, *D. micros*, *D. calcaris*, and *D. kugleri* sensu Rio, Fornaciari, et al. (1990).

*Discoaster brouweri*, *D. intercalaris*, *D. neohamatus*, *D. micros*, *D. calcaris*, and *D. kugleri* have been determined adhering strictly to the original descriptions. *D. variabilis* and *D. exilis* have been intended in *latu sensu*. A large taxonomic concept has been used for *D. exilis* that includes transitional forms between *D. variabilis* and *D. exilis*. Discoasterids possessing "trifurcated" tips are assigned to *D. surculus*.

#### Ceratolithids

This horseshoe-shaped group of calcareous nannofossils is a minor component of the assemblage during the late Miocene–early Pliocene. Among nonbirefringent ceratolithids (*Amaurolithus*), only *A. primus* and *A. delicatus* have been recognized.

*A. primus* has two morphotypes: a primitive form with a thick arc comparable to the holotype (Bukry and Percival, 1971) and a more delicate crescent-shaped form that occurs together with *A. delicatus*. During Leg 167, only the more evolved form of *A. primus* has been observed. Also intergraded morphotypes between *A. primus* and *A. delicatus* are present, which make it difficult to distinguish between the two species and consequently to detect the LO of *A. primus*. *Ceratolithus acutus*, *C. armatus*, *C. rugosus*, and *C. telesmus* have been found in low frequencies and with discontinuous distribution. Therefore it has not been possible to recognize the biohorizons marked by these ceratolithids. A rare and discontinuous transitional morphotype between genus *Amaurolithus* and genus *Ceratolithus* has been observed and labeled *Ceratolithus* sp. 1. This form appears as partially birefringent; namely, one arm is birefringent like *Ceratolithus* and the other arm is not birefringent like *Amaurolithus*. Probably this form could be the result of hybridization between species of the two genera.

### ACKNOWLEDGMENTS

Financial support for this study was provided by CNR grants to M.B. Cita, I. Premoli Silva, and D. Rio and by the "Centro di studio CNR per La Geodinamica Alpina." I am grateful to Jan Backman and Isabella Raffi for the careful revision of the manuscript. Special thanks go to Domenico Rio for the many useful suggestions, Maria Serena Poli for the first English revision of the manuscript, and Bruno Rampazzo for the technical support.

### REFERENCES

- Aguirre, E., and Pasini, G., 1985. The Pliocene-Pleistocene boundary. *Episodes*, 8:11–120.
- Aubry, M.-P., 1984. *Handbook of Cenozoic Calcareous Nannoplankton* (Book 1): *Ortholithae* (*Discoasters*): New York (Micropaleontology Press).
- , 1988. *Handbook of Calcareous Nannoplankton* (Book 2): *Ortholithae* (*Catinasters*, *Ceratoliths*, *Rhabdoliths*): New York (Micropaleontology Press).
- , 1989. *Handbook of Cenozoic Calcareous Nannoplankton* (Book 3): *Ortholithae* (*Pentaliths* and *Others*), *Heliolithae* (*Fasciculiths*, *Sphenoliths*, and *Others*): New York (Micropaleontology Press).
- , 1990. *Handbook of Cenozoic Calcareous Nannoplankton* (Book 4): *Heliolithae* (*Helicoliths*, *Criboliths*, *Lopadoliths*, and *Others*): New York (Micropaleontology Press).
- Backman, J., and Pestiaux, P., 1987. Pliocene *Discoaster* abundance variations, Deep Sea Drilling Project Site 606: biochronology and paleoenvironmental implications. In Ruddiman, W.F., Kidd, R.B., Thomas, E., et al., *Init. Repts. DSDP*, 94 (Pt. 2): Washington (U.S. Govt. Printing Office), 903–910.
- Backman, J., and Raffi, I., 1997. Calibration of Miocene nannofossil events to orbitally tuned cyclostratigraphies from Ceara Rise. In Shackleton, N.J., Curry, W.B., Richter, C., and Bralower, T.J. (Eds.), *Proc. ODP, Sci. Results*, 154: College Station, TX (Ocean Drilling Program), 83–99.

- Backman, J., and Shackleton, N.J., 1983. Quantitative biochronology of Pliocene and early Pleistocene calcareous nannofossils from the Atlantic, Indian and Pacific oceans. *Mar. Micropaleontol.*, 8:141–170.
- Bassinot, F.C., Labeyrie, L.D., Vincent, E., Quidelleur, X., Shackleton, N.J., and Lancelot, Y., 1994. The astronomical theory of climate and the age of the Brunhes-Matuyama magnetic reversal. *Earth Planet. Sci. Lett.*, 126:91–108.
- Benson, R.H., and Hodell, D.A., 1994. Comment on “A critical re-evaluation of the Miocene/Pliocene boundary as defined in the Mediterranean” by F.J. Hilgen and C.G. Langereis. *Earth Planet. Sci. Lett.*, 124:245–250.
- Benson, R.H., and Rakic-El Bied, K., 1996. The Bou Regreg Section, Morocco: proposed Global Boundary Stratotype Section and Point of the Pliocene. *Notes Mem. Ser. Geol. Maroc*, 383:51–150.
- Benson, R.H., Rakic-El Bied, K., Bonaduce, G., Hodell, D.A., Berggren, W.A., Aubry, M.-P., Napoleone, G., and Kent, D.V., 1991. A proposal for the Pliocene global boundary stratotype section and point: Bou Regreg section, Morocco. IX Congr. Reg. Comm. Medit. Neog. Stratigr. Barcelona, 57.
- Berggren, W.A., Hilgen, F.J., Langereis, C.G., Kent, D.V., Obradovich, J.D., Raffi, I., Raymo, M.E., and Shackleton, N.J., 1995. Late Neogene chronology: new perspectives in high-resolution stratigraphy. *Geol. Soc. Am. Bull.*, 107:1272–1287.
- Berggren, W.A., Kent, D.V., Swisher, C.C., III, and Aubry, M.-P., 1995. A revised Cenozoic geochronology and chronostratigraphy. In Berggren, W.A., Kent, D.V., Aubry, M.-P., and Hardenbol, J. (Eds.), *Geochronology, Time Scales and Global Stratigraphic Correlation*. Spec. Publ.—Soc. Econ. Paleontol. Mineral. (Soc. Sediment. Geol.), 54:129–212.
- Berggren, W.A., Kent, D.V., and Van Couvering, J.A., 1985. The Neogene, Part 2. Neogene geochronology and chronostratigraphy. In Snelling, N.J. (Ed.), *The Chronology of the Geological Record*. Geol. Soc. London Mem., 10:211–260.
- Berggren, W.A., and van Couvering, J.A., 1974. The Late Neogene: biostratigraphy, geochronology and paleoclimatology of the last 15 million years in marine and continental sequences. *Palaeogeogr., Palaeoclimatol., Palaeoecol.*, 16:1–216.
- Bleil, U., 1985. The magnetostratigraphy of northwest Pacific sediments, Deep Sea Drilling Project Leg 86. In Heath, G.R., Burckle, L.H., et al., *Init. Repts. DSDP*, 86: Washington (U.S. Govt. Printing Office), 441–458.
- Bonci, M.C., and Pirini Radrizzani, C., 1992. Presence of small *Gephyrocapsa* in late Miocene diatomaceous leves. (S. Agata Fossili Formation, Serravalle Scrivia, Alessandria, Italy). *Mem. Sci. Geol.*, 43:351–355.
- Bralower, T.J., Monechi, S., and Thierstein, H.R., 1989. Calcareous nannofossil zonation of the Jurassic-Cretaceous boundary interval and correlation with the geomagnetic polarity timescale. *Mar. Micropaleontol.*, 14:153–235.
- Bukry, D., 1973. Low-latitude coccolith biostratigraphic zonation. In Edgar, N.T., Saunders, J.B., et al., *Init. Repts. DSDP*, 15: Washington (U.S. Govt. Printing Office), 685–703.
- , 1975a. Coccolith and silicoflagellate stratigraphy, northwestern Pacific Ocean, Deep Sea Drilling Project Leg 32. In Larson, R.L., Moberly, R., et al., *Init. Repts. DSDP*, 32: Washington (U.S. Govt. Printing Office), 677–701.
- , 1975b. New Miocene to Holocene stages in the ocean basins based on calcareous nannoplankton zones. In Kulm, L.D., von Huene, R., et al. (Eds.), *Late Neogene Epoch Boundaries*: New York (Am. Mus. Nat. Hist., Micropaleontology Press), 162–166.
- , 1981. Pacific coast coccolith stratigraphy between Point Conception and Cabo Corrientes, Deep Sea Drilling Project Leg 63. In Yeats, R.S., Haq, B.U., et al., *Init. Repts. DSDP*, 63: Washington (U.S. Govt. Printing Office), 445–471.
- , 1991. Paleocological transect of western Pacific Ocean late Pliocene coccolith flora, Part I. Tropical Ontong-Java Plateau at ODP 806B. *Open-File Rep.—U.S. Geol. Surv.*, 91-552:1–35.
- Bukry, D., and Percival, S.F., 1971. New Tertiary calcareous nannofossils. *Tulane Stud. Geol. Paleontol.*, 8:123–146.
- Cande, S.C., and Kent, D.V., 1995. Revised calibration of the geomagnetic polarity timescale for the Late Cretaceous and Cenozoic. *J. Geophys. Res.*, 100:6093–6095.
- Castradori, D., Rio, D., Hilgen, F.J., and Lourens, L., 1998. The Global Standard Stratotype-section and Point (GSSP) of the Piacenzian Stage (Middle Pliocene). *Episodes*, 21:88–93.
- Channell, J.E.T., Rio, D., Sprovieri, R., and Glaçon, G., 1990. Biomagnetostratigraphic correlations from Leg 107 in the Tyrrhenian Sea. In Kastens, K.A., Mascle, J., et al., *Proc. ODP, Sci. Results*, 107: College Station, TX (Ocean Drilling Program), 669–682.
- Channell, J.E.T., Rio, D., and Thunell, R.C., 1988. Miocene/Pliocene boundary magnetostratigraphy at Capo Spartivento, Calabria, Italy. *Geology*, 16:1096–1099.
- Chepstow-Lusty, A., Backman, J., and Shackleton, N.J., 1989. Comparison of upper Pliocene *Discoaster* abundance variations from North Atlantic Sites 552, 607, 658, 659 and 662: further evidence for marine plankton responding to orbital forcing. In Ruddiman, W.F., Sarinthein, M., et al., *Proc. ODP, Sci. Results*, 108: College Station, TX (Ocean Drilling Program), 121–141.
- , 1991. Palaeoclimatic control of upper Pliocene *Discoaster* assemblages in the North Atlantic. *J. Micropaleontol.*, 9:133–143.
- Chepstow-Lusty, A., and Chapman, M., 1995. The decline and extinction of Upper Pliocene *Discoasters*: a comparison of two equatorial Pacific Ocean records. *J. Nannopl. Res.*, 17:15–19.
- Chepstow-Lusty, A., Shackleton, N.J., and Backman, J., 1992. Upper Pliocene *Discoaster* abundance from the Atlantic, Pacific, and Indian oceans: the significance of productivity pressure at low latitudes. *Mem. Sci. Geol.*, 44:357–373.
- Driever, B.W.M., 1981. A quantitative study of Pliocene associations of *Discoaster* from the Mediterranean. *Proc. K. Ned. Akad. Wet., Ser. B: Paleontol., Geol., Phys., Chem.*, 84:437–455.
- , 1988. Calcareous nannofossil biostratigraphy and paleoenvironmental interpretation of the Mediterranean Pliocene. *Utrecht Micropaleontol. Bull.*, 36:1–245.
- Ellis, C.H., 1979. Neogene Nannoplankton in Eastern Mediterranean. *Ann. Geol. Pays Hell.*, 1:391–401.
- Ellis, H.C., 1982. Calcareous nannoplankton biostratigraphy—Deep Sea Drilling Project Leg 60. In Hussong, D.M., Uyeda, S., et al., *Init. Repts. DSDP*, 60: Washington (U.S. Govt. Printing Office), 507–535.
- Ericson, D.B., Ewing, M., and Wollin, G., 1963. Plio-Pleistocene boundary in the deep-sea sediments. *Science*, 139:727–737.
- Fornaciari, E., Backman, J., and Rio, D., 1993. Quantitative distribution patterns of selected lower to middle Miocene calcareous nannofossils from the Ontong Java Plateau. In Berger, W.H., Kroenke, L.W., Mayer, L.A., et al., *Proc. ODP, Sci. Results*, 130: College Station, TX (Ocean Drilling Program), 245–256.
- Fornaciari, E., Di Stefano, A., Rio, D., and Negri, A., 1996. Middle Miocene quantitative calcareous nannofossil biostratigraphy in the Mediterranean region. *Micropaleontology*, 42:37–63.
- Fornaciari, E., Raffi, I., Rio, D., Villa, G., Backman, J., and Olafsson, G., 1990. Quantitative distribution patterns of Oligocene and Miocene calcareous nannofossils from the western equatorial Indian Ocean. In Duncan, R.A., Backman, J., Peterson, L.C., et al., *Proc. ODP, Sci. Results*, 115: College Station, TX (Ocean Drilling Program), 237–254.
- Gartner, S., 1977. Calcareous nannofossil biostratigraphy and revised zonation of the Pleistocene. *Mar. Micropaleontol.*, 2:1–25.
- , 1992. Miocene nannofossil chronology in the North Atlantic, DSDP Site 608. *Mar. Micropaleontol.*, 18:307–331.
- Gartner, S., and Bukry, D., 1975. Morphology and phylogeny of the coccolithophyceae family Ceratolithaceae. *J. Res. U.S. Geol. Surv.*, 3:451–465.
- Gartner, S., Chen, M.P., and Stanton, R.J., 1984. Late Neogene biostratigraphy and paleoceanography of the Northeastern Gulf of Mexico, and adjacent areas. *Mar. Micropaleontol.*, 8:17–50.
- Gartner, S., and Chow, J., 1985. Calcareous nannofossil biostratigraphy, Deep Sea Drilling Project Leg 85, eastern equatorial Pacific. In Mayer, L., Theyer, F., Thomas, E., et al., *Init. Repts. DSDP*, 85: Washington (U.S. Govt. Printing Office), 609–619.
- Gradstein, F.M., Agterberg, F.P., Brower, J.C., and Schwarzacher, W.S., 1985. *Quantitative Stratigraphy*: Dordrecht (Reidel).
- Haq, B.U., Hardenbol, J., and Vail, P.R., 1987. Chronology of fluctuating sea levels since the Triassic. *Science*, 235:1156–1167.
- Haq, B.U., and Van Eysinga, F., 1986. *Geological Timetable*: Amsterdam (Elsevier).
- Hay, W.W., Mohler, H.P., Roth, P.H., Schmidt, R.R., and Boudreaux, J.E., 1967. Calcareous nannoplankton zonation of the Cenozoic of the Gulf Coast and Caribbean-Antillean area and transoceanic correlation. *Trans. Gulf Coast Assoc. Geol. Soc.*, 17:428–480.
- Hilgen, F.J., and Langereis, C.G., 1988. The age of the Miocene-Pliocene boundary in the Capo Rossello area (Sicily). *Earth Planet. Sci. Lett.*, 91:214–222.
- Hills, S.J., and Thierstein, H.R., 1989. Plio-Pleistocene calcareous plankton biochronology. *Mar. Micropaleontol.*, 14:67–96.
- Hodell, D.A., Benson, R.H., Kent, D.V., Boersma, A., and Rakic-El Bied, K., 1994. Magnetostratigraphic, biostratigraphic, and stable isotope stratigraphy of an Upper Miocene drill core from the Salé Briqueterie (northwest-

- ern Morocco): a high-resolution chronology for the Messinian stage. *Paleoceanography*, 9:835–855.
- Loeblich, A.R., Jr., and Tappan, H., 1966. Annotated index and bibliography of the calcareous nannoplankton, I. *Phycologia*, 5:81–216.
- , 1968. Annotated index and bibliography of the calcareous nannoplankton, II. *J. Paleontol.*, 42:584–598.
- , 1969. Annotated index and bibliography of the calcareous nannoplankton, III. *J. Paleontol.*, 43:568–588.
- , 1970a. Annotated index and bibliography of the calcareous nannoplankton, IV. *J. Paleontol.*, 44:558–574.
- , 1970b. Annotated index and bibliography of the calcareous nannoplankton, V. *Phycologia*, 9:157–174.
- , 1971. Annotated index and bibliography of the calcareous nannoplankton, VI. *Phycologia*, 10:315–339.
- , 1973. Annotated index and bibliography of the calcareous nannoplankton, VII. *J. Paleontol.*, 47:715–759.
- Lourens, L.J., Antonarakou, A., Hilgen, F.J., Van Hoof, A.A.M., Vergnaud-Grazzini, C., and Zachariasse, W.J., 1996. Evaluation of the Plio-Pleistocene astronomical timescale. *Paleoceanography*, 11:391–413.
- Lyle, M., Koizumi, I., Richter, C., et al., 1997. *Proc. ODP, Init. Repts.*, 167: College Station, TX (Ocean Drilling Program).
- Martini, E., 1971. Standard Tertiary and Quaternary calcareous nannoplankton zonation. In Farinacci, A. (Ed.), *Proc. 2nd Int. Conf. Planktonic Microfossils Roma*: Rome (Ed. Tecnosci.), 2:739–785.
- Matsuoka, H., and Okada, H., 1989. Quantitative analysis of Quaternary nannoplankton in the subtropical northwestern Pacific Ocean. *Mar. Micropaleontol.*, 14:97–118.
- Monechi, S., 1985. Campanian to Pleistocene calcareous nannofossil stratigraphy from the northwest Pacific Ocean, Deep Sea Drilling Project Leg 86. In Heath, G.R., Burckle, L.H., et al., *Init. Repts. DSDP*, 86: Washington (U.S. Govt. Printing Office), 301–336.
- Müller, C., 1978. Neogene calcareous nannofossils from the Mediterranean—Leg 42A of the Deep Sea Drilling Project. In Hsü, K.J., Montadert, L., et al., *Init. Repts. DSDP*, 42 (Pt. 1): Washington (U.S. Govt. Printing Office), 727–751.
- Muza, J.P., Wise, S.W., Jr., and Mitchener Covington, J., 1987. Neogene calcareous nannofossils from Deep Sea Drilling Project Site 603, Lower Continental Rise, western North Atlantic: biostratigraphy and correlations with magnetic and seismic stratigraphy. In van Hinte, J.E., Wise, S.W., Jr., et al., *Init. Repts. DSDP*, 93 (Pt. 2): Washington (U.S. Govt. Printing Office), 593–616.
- Okada, H., and Bukry, D., 1980. Supplementary modification and introduction of code numbers to the low-latitude coccolith biostratigraphic zonation (Bukry, 1973; 1975). *Mar. Micropaleontol.*, 5:321–325.
- Olafsson, G., 1989. Quantitative calcareous nannofossil biostratigraphy of upper Oligocene to middle Miocene sediment from ODP Hole 667A and middle Miocene sediment from DSDP Site 574. In Ruddiman, W., Sarnthein, M., et al., *Proc. ODP, Sci. Results*, 108: College Station, TX (Ocean Drilling Program), 9–22.
- , 1991. Quantitative calcareous nannofossil biostratigraphy and biochronology of early through late Miocene sediments from DSDP Hole 608. *Medd. Stockholm Univ. Inst. Geol. Geochem.*, 285.
- Perch-Nielsen, K., 1985. Cenozoic calcareous nannofossils. In Bolli, H.M., Saunders, J.B., and Perch-Nielsen, K. (Eds.), *Plankton Stratigraphy*: Cambridge (Cambridge Univ. Press), 427–554.
- Pujos, A., 1987. Late Eocene to Pleistocene medium-sized and small-sized “reticulofenestrads.” *Proc. INA Vienna Meeting 1985, Abh. Geol. Bundesanst. (Austria)*, 39:239–277.
- Raffi, I., Backman, J., and Rio, D., 1998. Evolutionary trends of calcareous nannofossils in the Late Neogene. *Mar. Micropaleontol.*, 35:17–41.
- Raffi, I., Backman, J., Rio, D., and Shackleton, N.J., 1993. Plio-Pleistocene nannofossil biostratigraphy and calibration to oxygen isotopes stratigraphies from Deep Sea Drilling Project Site 607 and Ocean Drilling Program Site 677. *Paleoceanography*, 8:387–408.
- Raffi, I., and Flores, J.-A., 1995. Pleistocene through Miocene calcareous nannofossils from eastern equatorial Pacific Ocean. In Pisias, N.G., Mayer, L.A., Janecek, T.R., Palmer-Julson, A., and van Andel, T.H. (Eds.), *Proc. ODP, Sci. Results*, 138: College Station, TX (Ocean Drilling Program), 233–286.
- Raffi, I., and Rio, D., 1979. Calcareous nannofossil biostratigraphy of DSDP Site 132—Leg 13 (Tyrrhenian Sea-Western Mediterranean). *Riv. Ital. Paleontol. Stratigr.*, 85:127–172.
- Raffi, I., Rio, D., d’Atri, A., Fornaciari, E., and Rocchetti, S., 1995. Quantitative distribution patterns and biomagnetostratigraphy of middle and late Miocene calcareous nannofossils from equatorial Indian and Pacific oceans (Leg 115, 130, and 138). In Pisias, N.G., Mayer, L.A., Janecek, T.R., Palmer-Julson, A., and van Andel, T.H. (Eds.), *Proc. ODP, Sci. Results*, 138: College Station, TX (Ocean Drilling Program), 479–502.
- Rio, D., 1982. The fossil distribution of coccolithophore genus *Gephyrocapsa* Kamptner and related Plio-Pleistocene chronostratigraphic problems. In Prell, W.L., Gardner, J.V., et al., *Init. Repts. DSDP*, 68: Washington (U.S. Govt. Printing Office), 325–343.
- Rio, D., Cita, M.B., Iaccarino, S., Gelati, R., and Gnaccolini, M., 1997. Langhian, Serravallian, and Tortonian historical stratotypes. In Montanari, A., Odin, G.S., and Cocconi, R. (Eds.), *Miocene Stratigraphy: An Integrated Approach*: Amsterdam (Elsevier), 57–87.
- Rio, D., Fornaciari, E., and Raffi, I., 1990. Late Oligocene through early Pleistocene calcareous nannofossils from western equatorial Indian Ocean (Leg 115). In Duncan, R.A., Backman, J., Peterson, L.C., et al., *Proc. ODP, Sci. Results*, 115: College Station, TX (Ocean Drilling Program), 175–235.
- Rio, D., Raffi, I., Backman, J., 1997. Calcareous nannofossil biochronology and the Pliocene/Pleistocene boundary: the Neogene/Quaternary boundary. In Van Couvering, J.A. (Ed.), *The Pleistocene Boundary and the Beginning of the Quaternary: Final Report of the International Geological Correlation Program-Project 41, Neogene-Quaternary Boundary*: Cambridge (Cambridge Univ. Press), 63–78.
- Rio, D., Raffi, I., and Villa, G., 1990. Pliocene Pleistocene calcareous nannofossil distribution patterns in the Western Mediterranean. In Kastens, K.A., Mascle, J., et al., *Proc. ODP, Sci. Results*, 107: College Station, TX (Ocean Drilling Program), 513–533.
- Rio, D., Sprovieri, R., Castradori, D., and Di Stefano, E., 1998. The Gelasian Stage (upper Pliocene): a new unit of the global standard chronostratigraphic scale. *Episodes*, 21:82–87.
- Rio, D., Sprovieri, R., and Thunell, R., 1991. Pliocene–lower Pleistocene chronostratigraphy: a re-evaluation of Mediterranean type sections. *Geol. Soc. Am. Bull.*, 103:1049–1058.
- Ruggieri, G., Rio, D., and Sprovieri, R., 1984. Remarks on the chronostratigraphic classification of Lower Pleistocene. *Boll. Soc. Geol. Ital.*, 103:251–259.
- Ruggieri, G., and Sprovieri, R., 1977. Ricerche sul Siciliano di Palermo: Le argille del fiume Oreto. *Boll. Soc. Geol. Ital.*, 94:1613–1622.
- , 1979. Selinuntiano, nuovo superpiano per il Pleistocene inferiore. *Boll. Soc. Paleont. Ital.*, 96:797–802.
- Schneider, D.A., Backman, J., Chaisson, W.P., and Raffi, I., 1997. Miocene calibration for calcareous nannofossils from low-latitude Ocean Drilling Program sites and the Jamaican conundrum. *Geol. Soc. Am. Bull.*, 109:1073–1079.
- Shackleton, N.J., Baldauf, J.G., Flores, J.-A., Iwai, M., Moore, T.C., Jr., Raffi, I., and Vincent, E., 1995. Biostratigraphic summary for Leg 138. In Pisias, N.G., Mayer, L.A., Janecek, T.R., Palmer-Julson, A., and van Andel, T.H. (Eds.), *Proc. ODP, Sci. Results*, 138: College Station, TX (Ocean Drilling Program), 517–536.
- Suc, J.-P., Clauzon, G., and Gautier, F., 1997. The Miocene/Pliocene boundary: present and future. In Montanari, A., Odin, G.S., and Cocconi, R. (Eds.), *Miocene Stratigraphy: an Integrated Approach*: Amsterdam (Elsevier), 149–154.
- Takayama, T., 1970. The Pliocene-Pleistocene boundary in the Lamont Core V-21-98 and at Le Castella, Southern Italy. *J. Mar. Geol.*, 6:70–77.
- , 1993. Notes on Neogene calcareous nannofossil biostratigraphy of the Ontong Java Plateau and size variations of *Reticulofenestra* coccoliths. In Berger, W.H., Kroenke, L.W., Mayer, L.A., et al., *Proc. ODP, Sci. Results*, 130: College Station, TX (Ocean Drilling Program), 179–229.
- Takayama, T., and Sato, T., 1987. Coccolith biostratigraphy of the North Atlantic Ocean, Deep Sea Drilling Project Leg 94. In Ruddiman, W.F., Kidd, R.B., Thomas, E., et al., *Init. Repts. DSDP*, 94 (Pt. 2): Washington (U.S. Govt. Printing Office), 651–702.
- Theodoridis, S., 1984. Calcareous nannofossil biozonation of the Miocene and revision of the helicoliths and discoasters. *Utrecht Micropaleontol. Bull.*, 32:1–271.
- Thierstein, H.R., Geitzenauer, K., Molino, B., and Shackleton, N.J., 1977. Global synchronicity of late Quaternary coccolith datum levels: validation by oxygen isotopes. *Geology*, 5:400–404.
- Tiedemann, R., Sarnthein, M., and Shackleton, N.J., 1994. Astronomic timescale for the Pliocene Atlantic  $\delta^{18}\text{O}$  and dust flux records of Ocean Drilling Program Site 659. *Paleoceanography*, 9:619–638.
- Van Couvering, J.A., 1997. Preface: The new Pleistocene. In Van Couvering, J.A. (Ed.), *The Pleistocene Boundary and the Beginning of the Quaternary: Final Report of the International Geological Correlation Pro-*

- gramme Project 41, Neogene/Quaternary Boundary: Cambridge (Cambridge Univ. Press), xi–xvii.
- Van Eysinga, F., 1975. *Geological Timetable*: Amsterdam (Elsevier).
- Wei, W., 1993. Calibration of Upper Pliocene-Lower Pleistocene nannofossil events with oxygen isotope stratigraphy. *Paleoceanography*, 8:85–99.
- Wise, S.W., Jr., 1973. Calcareous nannofossils from cores recovered during Leg 18, Deep Sea Drilling Project: biostratigraphy and observations of diagenesis. In Kulm, L.D., von Huene, R., et al., *Init. Repts. DSDP*, 18: Washington (U.S. Govt. Printing Office), 569–615.
- Zijderveld, J.D.A., Zachariasse, W.J., Verhallen, P.J.J.M., and Hilgen, F.J., 1986. The age of the Miocene-Pliocene boundary. *Newsl. Stratigr.*, 16:169–181.

**Date of initial receipt: 9 October 1998**

**Date of acceptance: 17 June 1999**

**Ms 167SR-204**

## APPENDIX A

### Calcareous Nannofossils Considered in this Work\*

- Amaurolithus* Gartner and Bukry, 1975
- Amaurolithus delicatus* Gartner and Bukry, 1975
- Amaurolithus primus* (Bukry and Percival, 1971) Gartner and Bukry, 1975
- Amaurolithus tricorniculatus* (Gartner, 1967) Gartner and Bukry, 1975
- Calcidiscus leptoporus* (Murray and Blackman, 1898) Loeblich and Tappan, 1978
- Calcidiscus macintyreii* (Bukry and Bramlette, 1969) Loeblich and Tappan, 1978
- Calcidiscus premacintyreii* Theodoridis, 1984
- Catinaster calyculus* Martini and Bramlette, 1963
- Catinaster coalitus* Martini and Bramlette, 1965
- Ceratolithus* Kamptner, 1950
- Ceratolithus acutus* Gartner and Bukry, 1974
- Ceratolithus armatus* Müller, 1974
- Ceratolithus cristatus* Kamptner, 1968
- Ceratolithus rugosus* Bukry and Bramlette, 1968
- Ceratolithus telesmus* Norris, 1965
- Ceratolithus* sp. 1
- Coccolithus miopelagicus* Bukry, 1971
- Coccolithus pelagicus* (Wallich, 1877) Schiller, 1930
- Cyclicargolithus floridanus* (Roth and Hay in Hay et al., 1967) Bukry, 1971
- Dictyococcites* Black, 1967
- Discoaster asymmetricus* Gartner, 1969
- Discoaster bellus* Bukry and Percival, 1971
- Discoaster berggrenii* Bukry, 1971
- Discoaster bollii* Martini and Bramlette, 1963
- Discoaster brouweri* Tan (1927) emend. Bramlette and Riedel, 1954
- Discoaster calcaris* Gartner, 1967
- Discoaster exilis* Martini and Bramlette, 1963
- Discoaster hamatus* Martini and Bramlette, 1963
- Discoaster intercalaris* Bukry, 1971
- Discoaster kugleri* Martini and Bramlette, 1963
- Discoaster loeblichii* Bukry, 1971
- Discoaster micros* Theodoridis, 1984
- Discoaster neohamatus* Bukry and Bramlette, 1969
- Discoaster neorectus* Bukry, 1971
- Discoaster pentaradiatus* Tan (1927) emend. Bramlette and Riedel, 1954
- Discoaster quinqueramus* Gartner, 1969
- Discoaster surculus* Martini and Bramlette, 1963
- Discoaster tamalis* Kamptner, 1967
- Discoaster triradiatus* Tan, 1927
- Discoaster variabilis* Martini and Bramlette, 1963
- Discoaster* sp. 1 Rio et al., 1990
- Emiliania huxleyi* (Lohmann, 1902) Hay and Mohler in Hay et al., 1967
- Gephyrocapsa caribbeanica* Boudreaux and Hay, 1969
- Gephyrocapsa oceanica* Kamptner, 1943
- Gephyrocapsa* A-B Matsuoka and Okada, 1990
- Gephyrocapsa* C Matsuoka and Okada, 1990
- Gephyrocapsa* D Matsuoka and Okada, 1990
- Gephyrocapsa large* Raffi et al., 1993
- Gephyrocapsa medium* Raffi et al., 1993
- Gephyrocapsa small* Raffi et al., 1993
- Gephyrocapsa* sp. 3 Rio, 1982
- Helicosphaera carteri* (Wallich, 1877) Kamptner, 1954
- Helicosphaera sellii* Bukry and Bramlette, 1969
- Minylitha convallis* Bukry, 1973
- Nicklithus amplificus* (Bukry and Percival, 1971) Raffi et al., 1998
- Pseudoemiliania lacunosa* (Kamptner, 1963) Gartner, 1969
- Reticulofenestra* Hay, Mohler and Wade, 1966
- Reticulofenestra asanoi* Sato and Takayama, 1992
- Reticulofenestra haqii* Backman, 1978
- Reticulofenestra minuta* Roth, 1970
- Reticulofenestra minutula* (Gartner, 1967) Haq and Berggren, 1978
- Reticulofenestra pseudoumbilicus* (Gartner, 1967) Gartner, 1969
- Sphenolithus* Deflandre in Grassé, 1952
- Sphenolithus heteromorphus* Deflandre, 1953
- Triquetrorhabdulus rugosus* Bramlette and Wilcoxon, 1967
- Triquetrorhabdulus serratus* (Bramlette and Wilcoxon, 1967) Olafsson, 1989

\* = Listed in alphabetic order of generic epithets.

## APPENDIX B

## Leg 167 Calcareous Nannofossil Biohorizons

Appendix B Table 1. Summary of positions of calcareous nannofossil biohorizons, Site 1010.

Event	Core, section, interval (cm)	Depth (mcd)
	167-1010B-	
<i>Pseudoemiliania lacunosa</i> LO	1H-CC to 2H-1, 23	4.58-4.81
small <i>Gephyrocapsa</i> spp. AE	2H-4, 23 to 2H-6, 23	9.31-12.31
<i>Gephyrocapsa</i> sp. 3 FO	2H-4, 23 to 2H-6, 23	9.31-12.31
large <i>Gephyrocapsa</i> LO	2H-CC to 1010C-2H-CC	16.04-17.30
	167-1010C-	
large <i>Gephyrocapsa</i> FO	3H, 1, 22 to 3H-2, 23	17.52-19.03
<i>Gephyrocapsa oceanica</i> s.l. FO	3H-2, 23 to 3H-4, 22	19.03-22.03
<i>Calcidiscus macintyreii</i> LO	3H-2, 23 to 3H-4, 22	19.03-22.03
<i>Discoaster brouweri</i> LO	3H-5, 28 to 3H-6, 22	23.58-25.02
<i>Discoaster triradiatus</i> AB	4H-1, 22 to 4H-2, 23	28.08-31.09
<i>Discoaster pentaradiatus</i> LO	4H-3, 23 to 4H-4, 23	31.09-32.59
<i>Discoaster surculus</i> LO	4H-4, 23 to 4H-5, 23	32.59-34.04
<i>Discoaster tamalis</i> LO	4H-7, 22 to 4H-CC	37.08-38.86
<i>Discoaster asymmetricus</i> LO	4H-7, 22 to 4H-CC	37.08-38.86
<i>Discoaster pentaradiatus</i> PE	5H-4, 26 to 5H-5, 23	43.62-45.09
<i>Triquetrorhabdulus rugosus</i> LRO	7H-4, 21 to 7H-5, 21	64.14-65.64
<i>Discoaster quinqueramus/berggrenii</i> LO	7H-4, 21 to 7H-5, 21	64.14-65.64
<i>Reticulofenestra pseudoumbilicus</i> PE	9H-3, 06 to 9H-3, 19	82.79-82.92
<i>Amaurolithus primus</i> FO	9H-3, 19 to 9H-4, 19	82.92-84.42
<i>Amaurolithus delicatus</i> FO	9H-3, 19 to 9H-4, 19	82.92-84.42
<i>Discoaster surculus</i> FCO	9H-7, 19 to 10H-1, 23	88.92-90.26
<i>Discoaster quinqueramus/berggrenii</i> FO	10H-1, 23 to 10H-2, 27	90.26-91.8
<i>Minylitha convallis</i> LO	10H-1, 23 to 10H-2, 27	90.26-91.8
<i>Reticulofenestra pseudoumbilicus</i> PB	10H-1, 23 to 10H-2, 27	90.26-91.8
<i>Discoaster bollii</i> LO	11H-1, 22 to 11H-2, 22	100.65-102.15
<i>Discoaster pentaradiatus</i> FO	11H-6, 22 to 11H-7, 22	108.15-109.65
<i>Minylitha convallis</i> FO	12H-2, 22 to 12H-4, 22	112.73-115.73
<i>Discoaster hamatus</i> LO	12H-2, 22 to 12H-4, 22	112.73-115.73
<i>Discoaster neohamatus</i> FO	12H-5, 22 to 12H-6, 22	117.23-118.73
<i>Catinaster calyculus</i> LO	12H-5, 22 to 12H-6, 22	117.23-118.73
<i>Discoaster exilis</i> LO	13H-3, 22 to 13H-4, 22	125.29-126.79
<i>Catinaster coalitus</i> LO	13H-4, 22 to 13H-5, 22	126.79-128.29
<i>Discoaster kugleri</i> LO	15H-1, 22 to 15H-3, 22	142.43-145.43
<i>Discoaster bollii</i> FO	15H-4, 22 to 15H-5, 22	146.93-148.43
<i>Discoaster kugleri</i> FO	15H-CC to 16H-1, 22	152.14-152.36
<i>Calcidiscus macintyreii</i> FO	16H-1, 22 to 16H-2, 22	152.36-153.86
<i>Cyclicargolithus floridanus</i> LCO	16H-3, 22 to 16H-4, 22	155.36-156.86
<i>Calcidiscus premacintyreii</i> LO	17H-6, 22 to 17H-7, 23	169.28-170.79
<i>Reticulofenestra pseudoumbilicus</i> FCO	20X-3, 76 to 20X-CC	194.99-203.56
<i>Sphenolithus heteromorphus</i> LO	21X-1, 02 to 21X-1, 16	203.58-203.72

Notes: FO = first occurrence, LO = last occurrence, LRO = last rare occurrence, FCO = first common occurrence, LCO = last common occurrence. AB = acme beginning, AE = acme end, PB = paracme beginning, PE = paracme end.

Appendix B Table 2. Summary of positions of calcareous nannofossil biohorizons, Hole 1011B.

Event	Core, section, interval (cm)	Depth (mcd)
	167-1011B-	
<i>Pseudoemiliania lacunosa</i> LO	2H-CC to 3H-2, 17	21.14-22.81
small <i>Gephyrocapsa</i> spp. AE	3H-6, 17 to 4H-3, 22	28.81-34.66
<i>Gephyrocapsa</i> sp. 3 FO	3H-6, 17 to 4H-3, 22	28.81-34.66
<i>Helicosphaera sellii</i> LO	6H-1, 22 to 6H-3, 21	51.90-54.89
<i>Gephyrocapsa oceanica</i> s.l. FO	6H-5, 21 to 7H-1, 95	57.89-63.37
<i>Calcidiscus macintyreii</i> LO	6H-5, 21 to 7H-1, 95	57.89-63.37
<i>Discoaster brouweri</i> LO	7H-5, 100 to 7H-CC	69.42-71.72
<i>Discoaster pentaradiatus</i> LO	10H-1, 22 to 10H-3, 22	91.54-94.54
<i>Discoaster surculus</i> LO	11H-1, 75 to 11H-2, 76	101.69-103.20
<i>Discoaster tamalis</i> LO	11H-5, 76 to 11H-6, 76	107.70-109.20
<i>Discoaster pentaradiatus</i> PE	13H-1, 21 to 13H-3, 22	122.07-125.08
<i>Reticulofenestra pseudoumbilicus</i> LO	15H-CC to 15H-3, 22	146.06-148.84
<i>Amaurolithus delicatus</i> LO	15H-CC to 15H-3, 22	146.06-148.84
<i>Discoaster asymmetricus</i> FCO	16X-1, 22 to 16X-5, 22	149.06-155.06
<i>Pseudoemiliania lacunosa</i> FCO	16X-1, 22 to 16X-5, 22	149.06-155.06
<i>Discoaster pentaradiatus</i> PB	16X-1, 22 to 16X-5, 22	149.06-155.06
<i>Amaurolithus primus</i> LO	17X-1, 22 to 17X-5, 22	157.28-163.28
<i>Ceratolithus</i> spp. FO	17X-1, 22 to 17X-5, 22	157.28-163.28
<i>Discoaster quinqueramus/berggrenii</i> LO	19X-5, 22 to 19X-CC	184.04-189.94
<i>Reticulofenestra pseudoumbilicus</i> PE	21X-3, 22 to 21X-5, 22	202.06-205.66
<i>Amaurolithus primus</i> FO	22X-3, 22 to 22X-5, 22	212.26-215.26
<i>Minylitha convallis</i> LO	23X-3, 22 to 24X-1, 22	221.96-228.56
<i>Discoaster quinqueramus/berggrenii</i> FO	25X-1, 14 to 25X-5, 22	238.08-244.16
<i>Reticulofenestra pseudoumbilicus</i> PB	25X-1, 14 to 24X-5, 22	238.08-234.56

Notes: FO = first occurrence, LO = last occurrence, FCO = first common occurrence. AE = acme end, PB = paracme beginning, PE = paracme end.

**Appendix B Table 3. Summary of positions of calcareous nannofossil biohorizons, Hole 1012A.**

Event	Core, section, interval (cm)	Depth (mcd)
	167-1012A-	
<i>Pseudoemiliana lacunosa</i> LO	5H-1, 22 to 5H-3, 19	35.59-38.56
<i>Gephyrocapsa</i> sp. 3 FO	8H-3, 22 to 8H-5, 22	68.77-71.77
small <i>Gephyrocapsa</i> spp. AE	8H-3, 22 to 8H-5, 22	68.77-71.77
<i>Helicosphaera sellii</i> LO	10H-5, 22 to 10H-CC	92.47-95.75
large <i>Gephyrocapsa</i> LO	10H-3, 22 to 10H-5, 22	89.47-92.47
large <i>Gephyrocapsa</i> LO	11H-CC to 12H-1, 22	105.57-105.79
<i>Gephyrocapsa oceanica</i> s.l. FO	12H-6, 114 to 12H-7, 45	114.21-115.02
<i>Calcidiscus macintyreii</i> LO	12H-CC to 13H-1, 21	115.07-115.28
<i>Discoaster brouweri</i> LO	14X-3, 21 to 14X-3, 21	129.44-132.44
<i>Discoaster triradiatus</i> AB	16X-3, 22 to 16X-5, 22	149.63-152.63
<i>Discoaster pentaradiatus</i> LO	18X-CC to 18X-5, 22	171.83-175.21
<i>Discoaster surculus</i> LO	20X-3, 22 to 20X-5, 22	181.53-184.53
<i>Discoaster tamalis</i> LO	22X-5, 22 to 22X-CC	202.63-206.01
<i>Discoaster pentaradiatus</i> PE	25X-5, 22 to 25X-CC	231.33-233.91
<i>Pseudoemiliana lacunosa</i> FCO	?27X-3, 22 to 27X-5, 21	247.63-250.63
<i>Reticulofenestra pseudumbilicus</i> LO	29X-4, 22 to 29X-CC	266.33-272.59
<i>Amaurolithus delicatus</i> LO	29X-4, 22 to 29X-CC	266.33-272.59

Notes: FO = first occurrence, LO = last occurrence, FCO = first common occurrence. AB = acme beginning, AE = acme end, PE = paracme end. ? = doubtful position of biohorizon.

**Appendix B Table 4. Summary of positions of calcareous nannofossil biohorizons, Hole 1013A.**

Event	Core, section, interval (cm)	Depth (mcd)
	167-1013A-	
<i>Pseudoemiliana lacunosa</i> LO	2H-6,07 to 3H-1, 23	12.58-14.56
<i>Gephyrocapsa</i> sp. 3 FO	7H-5, 20 to 7H-CC	59.75-63.53
small <i>Gephyrocapsa</i> spp. AE	7H-5, 20 to 7H-CC	59.75-63.53
large <i>Gephyrocapsa</i> FO	9H-CC to 10H-1, 22	84.3-84.52
<i>Gephyrocapsa oceanica</i> s.l. FO	10H-CC to 11H-CC	92.97-104.81
<i>Calcidiscus macintyreii</i> LO	10H-CC to 11H-CC	92.97-104.81
<i>Discoaster brouweri</i> LO	12X-1, 22 to 12X-2, 22	105.03-106.53
<i>Discoaster pentaradiatus</i> LO	14X-5, 22 to 14X-CC	130.63-133.61
<i>Discoaster surculus</i> LO	14X-5, 22 to 14X-CC	130.63-133.61
<i>Discoaster tamalis</i> LO	15X-3, 22 to 15X-5, 22	136.83-139.83

Notes: FO = first occurrence, LO = last occurrence. AE = acme end.

**Appendix B Table 5. Summary of positions of calcareous nannofossil biohorizons, Site 1014.**

Event	Core, section, interval (cm)	Depth (mcd)
	167-	
<i>Pseudoemiliana lacunosa</i> LO	1014B-5H-5, 14 to 5H-5, 64	38.96-39.46
<i>Reticulofenestra ansanoi</i> LO	1014A-9X-5, 139 to 9X-6, 14	73.42-73.67
small <i>Gephyrocapsa</i> spp. AE	1014B-9H-5, 14 to 9H-5, 39	77.50-78.00
large <i>Gephyrocapsa</i> LO	1014D-11X-2, 139 to 11X-3, 14	95.50-96.15
large <i>Gephyrocapsa</i> FO	?1014D-13X-3, 114 to 13X-4, 14	113.87-113.97
<i>Gephyrocapsa oceanica</i> s.l. FO	1014A-15X-4, 139 to 15X-5, 14	122.95-123.2
<i>Calcidiscus macintyreii</i> LO	1014B-14X-4, 114 to 1014A-15X-2, 139	119.75-119.95
<i>Discoaster brouweri</i> LO	1014A-19X-1, 114 to 19X-2, 14	157.67-158.17
<i>Discoaster triradiatus</i> AB	1014A-20X-5, 64 to 20X-5, 114	172.08-172.58
<i>Discoaster pentaradiatus</i> LO	1014A-23X-2, 14 to 23X-2, 64	194.86-195.36
<i>Discoaster surculus</i> LO	1014A-23X-6, 64 to 24X-1, 14	200.73-201.94
<i>Discoaster tamalis</i> LO	1014A-30X-5, 14 to 30X-5, 39	249.64-249.89
<i>Discoaster asymmetricus</i> LO	1014A-31X-3, 14 to 31X-3, 64	252.00-252.50
<i>Discoaster pentaradiatus</i> PE	1014A-38X-1, 14 to 38X-1, 64	317.64-318.14
<i>Ceratolithus</i> spp. FO	1014A-44X-4, 114 to 44X-5, 39	379.54-380.29
<i>Reticulofenestra pseudumbilicus</i> LO	1014A-39X-5, 39 to 39X-5, 116	332.02-332.79
<i>Amaurolithus delicatus</i> LO	1014A-40X-4, 39 to 40X-4, 114	340.56-341.31
<i>Discoaster tamalis</i> FO	1014A-41X-4, 39 to 41X-4, 114	350.94-351.69
<i>Discoaster pentaradiatus</i> PB	1014A-41X-5, 39 to 41X-5, 88	352.44-352.93
<i>Pseudoemiliana lacunosa</i> FCO	1014A-41X-5, 88 to 42X-1, 38	352.93-356.38
<i>Discoaster asymmetricus</i> FCO	1014A-42X-1, 112 to 42X-2, 38	357.12-357.88
<i>Amaurolithus primus</i> LO	1014A-44X-4, 39 to 44X-4, 114	378.79-379.54
<i>Discoaster quinqueramus/berggrenii</i> LO	1014A-46X-5, 40 to 46X-5, 111	399.81-400.52
<i>Reticulofenestra pseudumbilicus</i> PE	?1014A-50X-1, 39 to 50X-1, 112	433.19-433.92

Notes: FO = first occurrence; LO = last occurrence, FCO = first common occurrence. AB = acme beginning, AE = acme end, PB = paracme beginning, PE = paracme end. ? = doubtful position of biohorizon.

**Appendix B Table 6. Summary of positions of calcareous nannofossil biohorizons, Hole 1016A.**

Event	Core, section, interval (cm)	Depth (mcd)
	167-1016A-	
<i>Pseudoemiliana lacunosa</i> LO	3H-5, 22 to 3H-5, 118	24.52-25.48
<i>Gephyrocapsa</i> sp. 3 FO	?3H-7, 40 to 3H-CC	27.7-28.20
small <i>Gephyrocapsa</i> spp. AE	?4H-5, 18 to 5H-2, 17	34.38-40.29
<i>Helicosphaera sellii</i> LO	6H-5, 22 to 6H-CC	54.56-58.34
<i>Gephyrocapsa oenica</i> s.l. FO	?7H-2, 22 to 8H-2, 23	60.06-70.87
<i>Calcidiscus macintyreii</i> LO	8H-2, 23 to 8H-CC	70.87-79.10
<i>Discoaster brouweri</i> LO	9H-5, 22 to 9H-CC	85.32-90.22
<i>Discoaster pentaradiatus</i> LO	12X-2, 21 to 12X-5, 22	107.79-112.30
<i>Discoaster surculus</i> LO	12X-2, 21 to 12X-5, 22	107.79-112.30
<i>Discoaster tamalis</i> LO	14X-2, 21 to 14X-5, 23	129.75-134.26
<i>Discoaster pentaradiatus</i> PE	17X-4, 41 to 17X-5, 22	168.36-169.67
<i>Reticulofenestra pseudoumbilicus</i> LO	18X-2, 22 to 18X-2, 45	174.77-175.00
<i>Amaurolithus delicatus</i> LO	18X-2, 22 to 18X-2, 45	174.77-175.00
<i>Discoaster pentaradiatus</i> PB	18X-3, 45 to 18X-4, 44	176.5-177.99
<i>Discoaster asymmetricus</i> FCO	18X-5, 45 to 18X-6, 50	179.5-181.05
<i>Pseudoemiliana lacunosa</i> FCO	18X-5, 45 to 18X-6, 50	179.5-181.05
<i>Ceratolithus</i> spp. FO	18X-6, 50 to 18X-7, 42	181.05-182.92
<i>Amaurolithus primus</i> LO	19X-1, 63 to 19X-2, 21	185.43-186.51
<i>Discoaster quinqueramus/berggrenii</i> LO	30X-2, 20 to 30X-5, 23	299.60-304.13

Notes: FO = first occurrence, LO = last occurrence, FCO = first common occurrence. AE = acme end, PB = paracme beginning, PE = paracme end. ? = doubtful position of biohorizon.

**Appendix B Table 7. Summary of positions of calcareous nannofossil biohorizons, Hole 1017A.**

Event	Core, section, interval (cm)	Depth (mcd)
	167-1017A-	
<i>Pseudoemiliana lacunosa</i> LO	10H-CC to 11H-3, 19	102.80-105.99
small <i>Gephyrocapsa</i> spp. AE	11H-CC to 12H-5, 18	113.96-120.14
<i>Gephyrocapsa</i> sp. 3 FO	17X-3, 15 to 17X-5, 15	158.92-161.92
large <i>Gephyrocapsa</i> LO	19X-CC to 20X-3, 19	184.95-188.14
<i>Helicosphaera sellii</i> LO	20X-3, 19 to 20X-5, 19	188.14-191.14
large <i>Gephyrocapsa</i> FO	20X-5, 19 to 21X-3, 19	191.14-195.51

Notes: FO = first occurrence, LO = last occurrence. AE = acme end.

**Appendix B Table 8. Summary of positions of calcareous nannofossil biohorizons, Hole 1018A.**

Event	Core, section, interval (cm)	Depth (mcd)
	167-1018A-	
<i>Pseudoemiliana lacunosa</i> LO	10H-3, 19 to 10H-CC	93.03-100.52
<i>Gephyrocapsa</i> sp. 3 FO	12X-CC to 13X-5, 19	122.32-125.51
small <i>Gephyrocapsa</i> spp. AE	11X-CC to 12X-5, 18	109.90-116.08
large <i>Gephyrocapsa</i> LO	17X-CC to 18X-5, 19	174.63-180.50
<i>Helicosphaera sellii</i> LO	17X-CC to 18X-5, 19	174.63-180.50
large <i>Gephyrocapsa</i> FO	19X-5, 19 to 19X-3, 19	190.10-196.26
<i>Gephyrocapsa oceanica</i> s.l. FO	22X-CC to 23X-3, 19	223.37-226.56
<i>Discoaster brouweri</i> LO	29X-CC to 30X-3, 19	291.89-295.08
<i>Discoaster pentaradiatus</i> LO	34X-5, 17 to 34X-CC	336.56-339.99
<i>Discoaster surculus</i> LO	34X-CC to 35X-3, 18	339.99-343.17
<i>Discoaster tamalis</i> LO	38X-5, 19 to 38X-CC	375.28-378.69

Notes: FO = first occurrence, LO = last occurrence. AE = acme end.

**Appendix B Table 9. Summary of positions of calcareous nannofossil biohorizons, Hole 1019C.**

Event	Core, section, interval (cm)	Depth (mcd)
	167-1019C-	
<i>Pseudoemiliana lacunosa</i> LO	6H-3, 18 to 6H-5, 19	50.99-53.99
small <i>Gephyrocapsa</i> spp. AE	10X-CC to 11X-5, 18	97.04-103.22
<i>Gephyrocapsa</i> sp. 3 FO	22X-3, 18 to 22X-5, 18	206.18-209.18

Notes: FO = first occurrence, LO = last occurrence. AE = acme end.

Appendix B Table 10. Summary of positions of calcareous nannofossil biohorizons, Hole 1020B.

Event	Core, section, interval (cm)	Depth (mcd)
	167-1020B-	
<i>Pseudoemiliana lacunosa</i> LO	5H-7, 39 to 6H-1, 39	48.85-51.11
small <i>Gephyrocapsa</i> spp. AE	7H-5, 39 to 7H-5, 115	67.61-68.37
<i>Gephyrocapsa</i> sp. 3 FO	10H-3, 39 to 10H-3, 114	99.24-99.99
large <i>Gephyrocapsa</i> LO	12H-6, 39 to 10H-6, 114	123.13-123.88
large <i>Gephyrocapsa</i> FO	15H-1, 114 to 15H-2, 114	147.42-148.92
<i>Gephyrocapsa oceanica</i> s.l. FO	16H-7, 39 to 16H-CC	165.10-166.10
<i>Calcidiscus macintyreii</i> LO	18H-1, 39 to 18H-3, 39	177.30-180.30
<i>Discoaster brouweri</i> LO	23X-6, 114 to 25X-1, 42	238.37-246.49
<i>Discoaster pentaradiatus</i> LO	23X-6, 114 to 25X-1, 42	238.37-246.49
<i>Discoaster surculus</i> LO	23X-6, 114 to 25X-1, 42	238.37-246.49
<i>Discoaster tamalis</i> LO	25X-7, 39 to 26X-1, 39	255.46-256.06
<i>Discoaster asymmetricus</i> LO	25X-7, 39 to 26X-1, 39	255.46-256.06
<i>Discoaster pentaradiatus</i> PE	27X-1, 42 to 27X-1, 114	265.79-266.51
<i>Reticulofenestra pseudoumbilicus</i> LO	28X-7, 39 to 29X-CC	284.36-293.77
<i>Amaurolithus</i> spp. LO	28X-7, 39 to 29X-CC	284.36-293.77

Notes: FO = first occurrence, LO = last occurrence, FCO = first common occurrence. AE = acme end, PE = paracme end.

Appendix B Table 11. Summary of positions of calcareous nannofossil biohorizons, Hole 1021B.

Event	Hole, core, section, interval (cm)	Depth (mcd)
	167-1021B-	
<i>Pseudoemiliana lacunosa</i> LO	2H-5, 23 to 2H-7, 23	15.41-18.41
<i>Gephyrocapsa</i> sp. 3 FO	4H-2, 23 to 4H-3, 23	31.23-32.73
small <i>Gephyrocapsa</i> spp. AE	4H-2, 23 to 4H-3, 23	31.23-32.73
<i>Gephyrocapsa oceanica</i> s.l. FO	6H-2, 22 to 6H-4, 22	52.48-55.48
<i>Calcidiscus macintyreii</i> LO	6H-7, 21 to 6H-CC	59.97-61.19
<i>Discoaster brouweri</i> LO	7H-1, 22 to 7H-2, 22	61.41-62.91
<i>Discoaster pentaradiatus</i> LO	8H-CC to 9H-1, 23	83.21-83.44
<i>Discoaster surculus</i> LO	9H-1, 23 to 9H-3, 23	83.44-86.44
<i>Discoaster asymmetricus</i> LO	10H-2, 20 to 10H-2, 60	98.45-98.85
<i>Discoaster tamalis</i> LO	10H-3, 20 to 10H-6, 20	99.95-104.45
<i>Discoaster pentaradiatus</i> PE	12H-3, 20 to 12H-4, 20	120.51-122.0
<i>Ceratolithus</i> spp. FO	12H-5, 20 to 12H-6, 20	123.51-125.01
<i>Sphenolithus</i> spp. LO	?13H-7, 21 to 14H-3, 21	136.01-138.64
<i>Discoaster tamalis</i> FO	13H-1, 22 to 13H-2, 22	127.01-128.51
<i>Reticulofenestra pseudoumbilicus</i> LO	13H-1, 22 to 13H-2, 22	127.01-128.51
<i>Amaurolithus delicatus</i> LO	13H-3, 22 to 13H-4, 22	130.01-131.51
<i>Discoaster asymmetricus</i> FCO	13H-2, 22 to 13H-4, 22	128.51-131.51
<i>Pseudoemiliana lacunosa</i> FCO	13H-3, 22 to 13H-4, 22	130.01-131.51
<i>Helicosphaera sellii</i> FO	?13H-6, 22 to 13H-7, 22	134.51-136.01
<i>Discoaster pentaradiatus</i> PB	13H-4, 22 to 13H-6, 22	131.51-134.51
<i>Amaurolithus primus</i> LO	14H-4, 18 to 14H-5, 18	140.11-141.60
<i>Discoaster quinqueramus/berggrenii</i> LO	19X-3, 22 to 20X-1, 23	188.13-191.04
<i>Reticulofenestra pseudoumbilicus</i> PE	?20X-2, 23 to 21X-1, 23	192.54-200.64
<i>Triquetrorhabdulus rugosus</i> LO	22X-1, 37 to 22X-2, 22	210.48-211.83
<i>Amaurolithus</i> spp. FO	21X-CC to 22X-1, 37	210.11-210.48
<i>Discoaster pentaradiatus</i> FO	22X-4, 19 to 22X-5, 12	214.80-216.23
<i>Discoaster quinqueramus/berggrenii</i> FO	?22X-5, 12 to 26X-6, 19	216.23-217.80
<i>Reticulofenestra pseudoumbilicus</i> PB	23X-4, 22 to 24X-3, 23	224.43-232.64
<i>Minylitha convallis</i> FO	28X-4, 24 to 28X-6, 23	272.55-275.54
<i>Catinaster</i> spp. LO	28X-6, 23 to 29X-1, 17	275.54-277.78
<i>Discoaster exilis</i> LCO	29X-3, 06 to 29X-4, 20	280.67-282.31
<i>Catinaster</i> spp. FO	?30X-3, 16 to 30X-4, 67	290.27-292.28

Notes: FO = first occurrence, LO = last occurrence, FCO = first common occurrence, LCO = last common occurrence. AE = acme end, PB = paracme beginning, PE = paracme end. ? = doubtful position of biohorizon.

Appendix B Table 12. Summary of positions of calcareous nannofossil biohorizons, Hole 1022A.

Event	Core, section, interval (cm)	Depth (mcd)
	167-1022A-	
<i>Gephyrocapsa</i> sp. 3 FO	1H-1, 50 to 1H-1, 100	0.62-1.12
<i>Gephyrocapsa oceanica</i> s.l. FO	1H-1, 50 to 1H-1, 100	0.62-1.12
<i>Calcidiscus macintyreii</i> LO	1H-2, 125 to 1H-2, 125	2.12-2.87
<i>Helicosphaera sellii</i> LO	1H-2, 125 to 1H-3, 21	2.87-3.33
<i>Discoaster brouweri</i> LO	3H-5, 19 to 3H-CC	21.35-23.61
<i>Discoaster pentaradiatus</i> LO	3H-5, 19 to 3H-CC	21.35-23.61
<i>Discoaster surculus</i> LO	3H-5, 19 to 3H-CC	21.35-23.61
<i>Discoaster tamalis</i> LO	8H-5, 21 to 8H-CC	72.47-75.97

Note: FO = first occurrence, LO = last occurrence.

## APPENDIX C

## Calcareous Nannofossil Zonal Schemes

The results of the present study and data from the most recent literature (Wei, 1993; Raffi et al., 1993; Rio, Raffi, et al., 1997) suggest the proposal of a new zonation for the Pleistocene and that the late Miocene zonation of Okada and Bukry (1980) needs to be adapted to be applied to the California Margin paleobiogeographic setting where many low-latitude marker species are missing or rare.

## Pleistocene new zonal scheme

For the early and middle Pleistocene the following zones are proposed. Note that the alphanumeric code of Okada and Bukry (1980) has been maintained. The proposed biostratigraphic intervals have been ranked at zone level because they are virtually global. In addition, the nomenclature of the zones on the basis of the generally adopted taxonomy of Perch-Nielsen (1985) has been adjusted.

CN13a - *Dictyococcites productus* Zone

**Definition:** Interval between the LO of *Discoaster brouweri* and the FO of *Gephyrocapsa oceanica* s.l.

**Occurrence:** This zone has been recognized at most Leg 167 sites and can be recognized globally as demonstrated by the works of Gartner (1977); Rio (1982); Rio, Raffi, et al. (1990); Wei (1993); Raffi et al. (1993); and so on.

**Remarks:** The zone was introduced by Raffi and Rio (1979) and emended by Rio, Raffi, et al. (1990) for the Mediterranean area. It corresponds most probably to the *Emiliania annula* Subzone of Bukry (1973) and to the *Coccolithus dornicoides* Zone of Wise (1973).

CN13bA *Gephyrocapsa caribbeanica* Zone

**Definition:** Interval between the FO of *G. oceanica* s.l. and the FO of large *Gephyrocapsa* spp.

**Occurrence:** This zone has been recognized at Sites 1010, 1012, 1013, 1014, 1017 (*pars*), 1018, and 1020 and can be recognized globally as demonstrated by the works of Rio (1982); Rio, Raffi, et al. (1990); Wei (1993); Raffi et al. (1993); and so on.

**Remarks:** In the original definition of Bukry (1973), the bottom of the zone was defined by the FO of *G. caribbeanica*, and the top was defined by the FO of *G. oceanica*. Most probably, *G. caribbeanica* of Bukry (1973) corresponds to *G. oceanica* of Gartner (1977) and to *G. oceanica* s.l. of Rio (1982), and the *G. oceanica* of Bukry (1973) corresponds to *Gephyrocapsa* sp. 3, as intended here following Rio (1982). Hence, the proposed zone corresponds to the lower part of the original Subzone CN13b of Bukry (1973; see Fig. 2).

The LO of *C. macintyreii* occurs in the lowermost part of the zone.

CN13bB Large *Gephyrocapsa* Zone

**Definition:** Interval corresponding to the total range of large *Gephyrocapsa* spp.

**Occurrence:** This zone has been recognized in Sites 1010, 1012, 1014, 1017, 1018, and 1020 and can be recognized globally as demonstrated by the various studies of Rio (1982); Rio, Raffi, et al. (1990); Wei (1993); Raffi et al. (1993); and so on.

**Remarks:** The zone was first introduced by Rio, Raffi, et al. (1990) for the Mediterranean area. In many areas *H. sellii* becomes extinct at the top of the zone.

CN13bC small *Gephyrocapsa* Zone

**Definition:** Interval between the LO of large *Gephyrocapsa* spp. and the FO of *Gephyrocapsa* sp. 3

**Occurrence:** This zone has been recognized at Sites 1010, 1012, 1014, 1017, 1018, 1019 (*pars*), and 1020 and can be recognized globally as demonstrated by the works of Gartner (1977); Rio (1982); Rio, Raffi, et al. (1990); Wei (1993); Raffi et al. (1993); etc.

**Remarks:** The zone was first defined by Rio, Raffi, et al. (1990) in the Mediterranean area. It corresponds substantially to the small *Gephyrocapsa* spp. Zone of Gartner (1977), which was defined on the basis of the LO of *H. sellii* (bottom) and the acme end of small *Gephyrocapsa* spp. (top), two biohorizons of more limited applicability than those utilized here.

This zone corresponds to the upper part of Subzone CN13b of Okada and Bukry (1980).

CN14a *Pseudoemiliania lacunosa* Zone

**Definition:** Interval between the FO of *Gephyrocapsa* sp. 3 and the LO of *Pseudoemiliania lacunosa*

**Occurrence:** This zone has been recognized at all Leg 167 sites and can be recognized globally as demonstrated by the works of Gartner (1977); Rio (1982); Rio, Raffi, et al. (1990); Wei (1993); Raffi et al. (1993); and so on.

**Remarks:** The zone as defined here was introduced by Raffi and Rio (1979) and emended by Rio, Raffi, et al. (1990) for the Mediterranean area. It corresponds substantially to the *P. lacunosa* Zone of Gartner (1977), which was defined on the basis of the acme end of small *Gephyrocapsa* spp. (bottom) and the LO of *P. lacunosa* (top), and to the *Emiliania ovata* Subzone (CN14a) of Okada and Bukry (1980), which was defined on the basis of the FO of *G. oceanica* at the bottom and the LO of *E. ovata* (*P. lacunosa* of this work) at the top.

## Adopted California Margin Miocene Zones

The original late Miocene zones of Okada and Bukry (1980) have been emended (emendation is denoted by the asterisk [\*]) as follows:

\*CN6–CN7 *Catinaster coalitus*–*Discoaster hamatus* combined Zones

**Definition:** Interval between the FO of *Catinaster* spp. and the FO *Minylitha convallis*.

**Occurrence:** This zone has been recognized at Sites 1010 and 1021.

**Remarks:** The CN6 and CN7 zones of Okada and Bukry (1980) are combined and their definitions emended because the FO of *C. coalitus* (base of Zone CN6), the FO of *D. hamatus* (base of Zone CN7), and the LO of *D. hamatus* (base of Zone CN8) are unreliable datums in the California Margin.

\*CN8a *Discoaster bellus* Zone

**Definition:** Interval of common occurrence of *Minylitha convallis* below the PB of *R. pseudoubilicus*

**Occurrence:** This zone has been recognized at Sites, 1010, 1011 (*pars*), and 1021.

**Remarks:** The original definition of Subzone CN8a of Okada and Bukry (1980) is emended because the LO of *D. hamatus* (base of Zone CN8a) and the FOs of *D. loeblichii* and *D. neorectus* (base of Zone CN8b) are not reliable in the California Margin.

\*CN8b *Discoaster neorectus* Zone

**Definition:** Interval between the PB of *R. pseudoubilicus* and the LO of *Minylitha convallis*

**Occurrence:** This zone has been recognized at Site 1011

**Remarks:** The original definition of Subzone CN8b of Okada and Bukry (1980) is emended because the FOs of *D. loeblichii* and *D. neorectus* (base of Zone CN8b) and the FO of *D. berggrenii* (base of Zone CN9) are not reliable in the California Margin. Note that the nominal species of the zone is missing in the area and that the FO of *M. convallis* seems to approximate the FO of *D. berggrenii* in the area.

\*CN9a *Discoaster berggrenii* Subzone

**Definition:** Interval between the LO of *Minylitha convallis* and the FO of *Amaurolithus primus*.

**Occurrence:** This subzone has been recognized at Site 1010, 1011 and 1021 (*pars*).

**Remarks:** See Zone CN8b.

CN9bA *Amaurolithus primus* Subzone

**Definition:** Interval between the FO of *A. primus* and the PE of *R. pseudoubilicus*.

**Occurrence:** This subzone has been recognized at Sites 1010, 1011, and 1021.

**Remarks:** This new biostratigraphic interval is introduced for improving the biostratigraphic resolution in the California Margin. The biohorizons defining the biostratigraphic intervals (FO of *A. primus* and the PE of *R.*

E. FORNACIARI

*pseudoumbilicus*) are recognized also outside the California Margin and probably the proposed subzone is widely recognizable.

CN9bB *Calcidiscus leptoporus* Subzone

**Definition:** Interval between the PE of *R. pseudoumbilicus* and the LO of *D. quinquerramus*.

**Occurrence:** This subzone has been recognized at Sites 1010, 1011 and 1021.

**Remarks:** See Subzone CN9bA.